Closure Report

File Number :	EMR/2017/005383
Project Title :	Computational Investigation on the membrane-induced self-assembly and aggregation of -Synuclein
Principal Investigator :	Dr. Mattaparthi Venkatasatish Kumar
	Tezpur University
	Distt. sonitpur p.b.no.72 napaam, tezpur, Tezpur, Assam-784011
Total Sanctioned Amount :	44,78,375 (INR)
Total Released Amount :	41,60,000 (INR)
Start Date of the Project:	04 Dec, 2018
Date of completion:	03 Dec, 2021 (36 months)

Approved Objectives :

• To obtain the structural and dynamic insights of membrane bound -synuclein at the atomistic level resolution using molecular dynamics simulations
• To study the impact of -synuclein diseased point mutations present on the N-terminal of -synuclein on the lipid membrane binding
• To develop therapeutic strategies that disrupts the -synuclein protein-lipid interactions

Deviation made from original objectives (If Any) :

Not applicable

Ph.D. Produced/ Likely to be Produced   : 1

Technical Personnel Trained   : 0

Total Expenditure :   42,51,575 (INR)

Concise Research Accomplishment :

a) Developed a novel method to identify the conformers of -synuclein with druggability feature in it. b) Developed a novel method to identify conformational shifts of -Syn near the site of mutation. c) Devised a novel method to construct protein-lipid bilayer (DOPE: DOPS: DOPC) system to study the effect of variants, post-translational modifications, C-terminal truncations, and peptidomimetic inhibitors on the -Syn protein lipid interactions. Other achievements related to this project a. Published 3 research articles in the international journal b. The outcome of this project work has been presented in the form of Poster presentation on the topic "Effect of pY39 Post-translational modification on the interactions between - Synuclein and Lipid membrane" in the event of 12th India-Japan Science and Technology Conclave International Conference on Frontier Areas of Science and Technology (ICFAST 2022) held at University of Hyderabad, India during 9th-10th September, 2022 c. The outcome of this project work (Computational investigation on conformational ensembles of A30G -Synuclein in its membrane bound state and in free solution that causes familial PD) has been presented in the form of an oral presentation at the National Seminar on "Excitements in Biological Research" held in the Department of Molecular Biology and Biotechnology conducted by the Students Science Council, Tezpur university, India, on March 6, 2023. The student was awarded first place for the same. d.The outcome of this project work (Impact of phosphorylation at Ser87 on the -Synuclein aggregation and synuclein-membrane interactions: an in silico study) has been presented in the form of an oral presentation at the National Seminar on "Research at the Interface of Chemical, Biological, and Material Sciences" held in the Department of Chemical Sciences conducted by the Students Science Council, Tezpur University, India, on March 10, 2023. For the same the student was awarded second place.
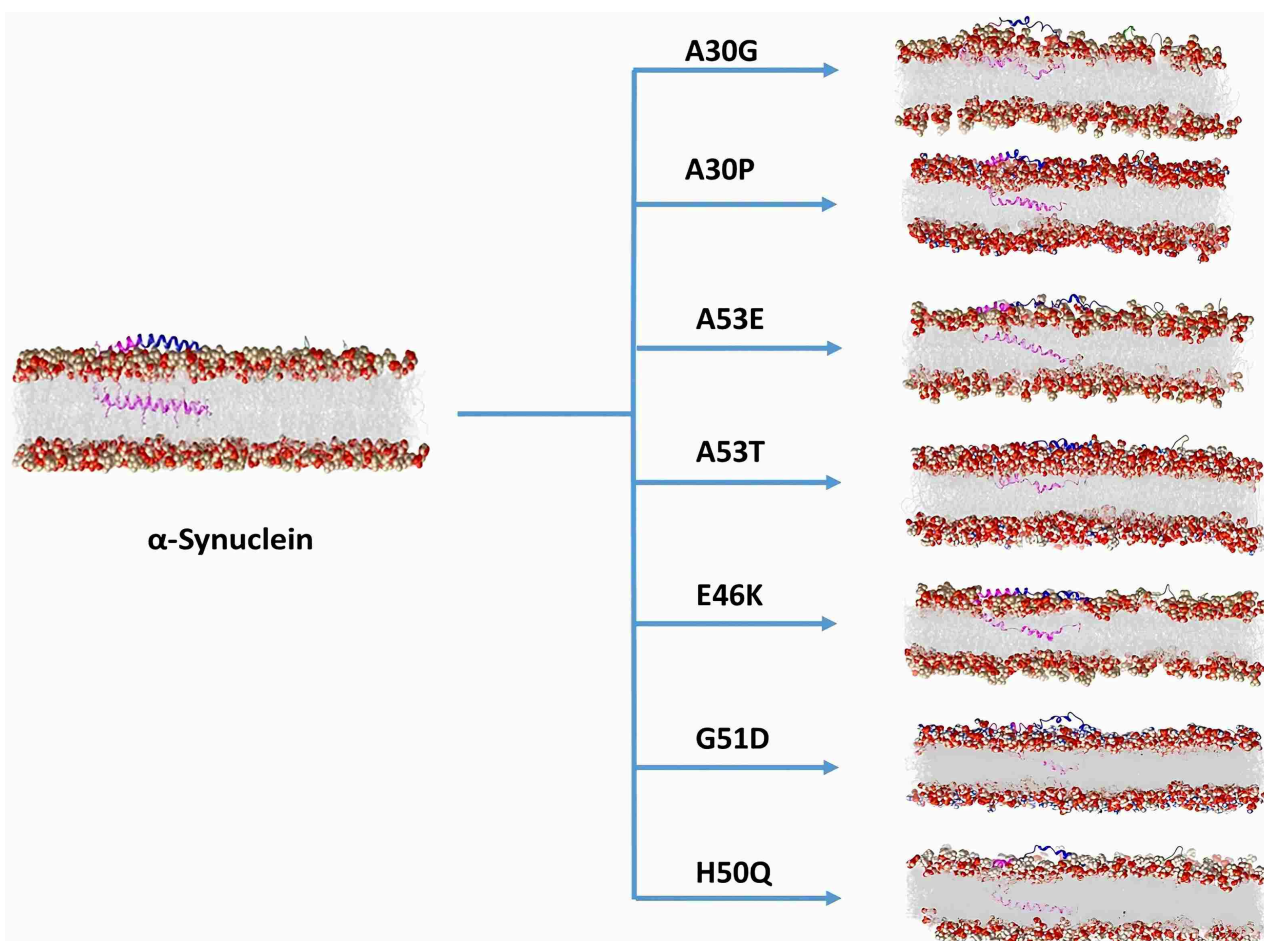
Closure Details
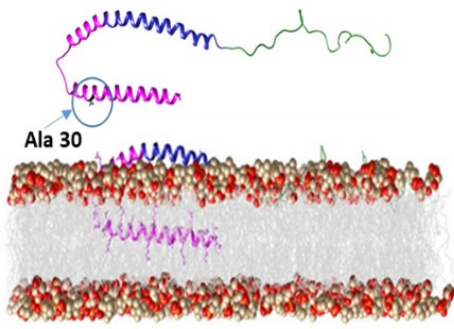
Experimental/ Theoretical Investigation carried out

(a)Screening of druggable conformers of -synuclein using Molecular dynamics simulation. In order to develop therapeutic strategies to overcome -synuclein aggregation, we have identified the druggable conformers of -synuclein in the absence of membrane from its molecular dynamics simulation trajectory. In this study, we have identified the most probable druggable conformers from molecular dynamics simulation on -synuclein based on the structural parameters: radius of gyration (Rg), solvent accessible surface area and the standard secondary structure content. To identify the most probable druggable conformers, the conformers present in the MD simulation trajectory were grouped in three clusters based on the Rg values (Lower, Moderate and Higher). The conformers in the clusters were analysed using the online server tool CASTp (Computed Atlas of Surface Topography of proteins) that detects, measures and provides a detailed characterization of the binding pockets on the surface of the proteins as well as the voids in the interior of proteins. (b) Construction of crowding medium on -synuclein In this experiment, cubic simulation boxes were filled with different proportions of water-ethanol mixtures using Packmol. In all these cases, the -synuclein protein molecule was placed at the center of the simulation box using Leap module of AmberTools 14 program. The volume occupied by ethanol was set up to about 0%, 5%, 10%, 20%, 50% and 100% of total volume. The system was subjected to one stage minimization to ensure the stability of the structure. The integration time step was set to 1 fs. Heating was gradually performed to bring the temperature of the system to 300 K over a time of 10 ps. To ensure the equilibration of the system, pressure, density, temperature, root mean square deviation (RMSD), potential energy, kinetic energy and total energy of the initial structure of -synuclein were plotted. The trajectories were collected and visualized by VMD package after intervals of 10 ns for a total MD run of 50 ns and analysed using cpptraj program from AMBER tools. (c) Preparation of wild type and variants of -Synuclein (A30P, A30G, A53E, A53T, E46K, G51D and H50Q) The initial structure of -Syn variants for the MD simulation study was obtained by modifying the 3D structure of human micelle-bound WT -Syn (PDB ID: 1XQ8). The 3D structure of WT -Syn was retrieved from the Protein Data Bank. The Rotamer tool of the University of California, San Francisco CHIMERA software was used to construct A30P, A30G, A53T, A53E, E46K, G51D and H50Q -Syn, where Alanine was replaced with Proline and Glycine at position 30; Alanine replaced by Threonine and Glutamate at position 53; Glutamate is replaced by lysine at position 46; Glycine is replaced by Aspartic acid at position 51 and Histidine is replaced by glutamine at position 50 in the WT -Syn. The variants of -Syn were then uploaded to initiate the construction of membrane bilayer using CHARMM GUI server. (d) Preparation of (i) phosphorylated and (ii) C-terminal truncated -Synuclein to study its effect on disrupting -Syn protein-lipid interaction (i) The initial micelle bound 3-D structure of the WT (PDB ID: 1XQ8) of -synuclein (-Syn) was retrieved from the Research Collaboratory for Structural Bioinformatics (RCSB) database. Subsequently the phosphate group is added at position 39, 87 and 129 of -Syn respectively to study the post-translational modifications at the corresponding locations in the -Syn and (ii) To study the effect of C-terminal truncation on the inhibition of -Syn aggregation, the truncated -Syn (residues 100-140 and 109-140) were constructed using Xleap module of AMBER 18 software and observed in Chimera. The phosphorylated -Syn (pY39, S87 and S129) and C-terminal truncated -Syn were then uploaded to initiate the construction of membrane bilayer using CHARMM GUI server. (e) Preparation and optimization of -Synuclein-peptidomimetic inhibitor (NPT100-18A and NPT200-11) complexes to study the effect of inhibitor in disrupting -Syn protein-lipid interaction The docking of -Synuclein + peptidomimetic inhibitors (NPT100-18A and NPT200-11) were performed using CB Dock2 server. The best structure obtained from the docking was used as the initial complex structure. Density functional theory calculations were performed for geometry optimization of the two inhibitors considered in this study without any constraint (NPT100-11 and NPT200-11). Frequency calculations were carried at the same level of theory in order to characterize the correct stationary ground state and for all of them obtained minima with real vibrational frequencies. All calculations were carried out with Gaussian 16 version C.01 suit of program. The xyz conformation of NPT100-18A and NPT200-11 structure was then changed to PDB format using Open Babel server. Using CB-Dock2 server, the docking of inhibitor molecule and -Syn was performed. The docked complex were uploaded to initiate the construction of membrane bilayer using CHARMM GUI server. The membrane bound docked complex was then subjected to antechamber to generate the frcmod file. The topology and co-ordinate file was then obtained using xleap module of AMBER18 software. (f) Molecular Dynamics Simulation Setup CHARMM general force field is used to read the hetero chain residue and the initial orientation of the protein with respect to the lipid/water interface was predicted using the PPM server. This composition of lipid bilayer was selected because it excellently mimics the synaptic vesicles. Membrane bilayer consisting of DOPE, DOPS, and DOPC in a ratio of 5:3:2 and model it with lipid17 force field parameters. The MD simulation was performed by using the AMBER 18 simulation package with force field ff99SBildn. To solvate the protein, a rectangular box with a minimum distance of 10Å to the edges of the box was employed. The TIP4PEW water model was used. To neutralize the system, the required number of counter ions were added. The calculations were done at a temperature of 300 K and a pressure of 1 bar. The minimization and equilibration of the system were performed during 100 ps and 1 ns, respectively. Following the equilibration step, the production runs were carried out for 100 ns with NTP ensemble. The time step for MD simulations was calculated to be 2 fs. The trajectories and coordinates were obtained for further analysis
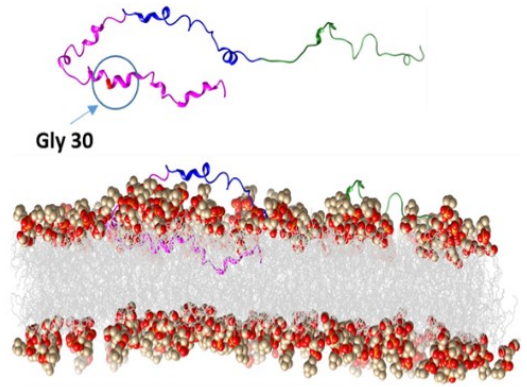
Detailed Analysis of result

(a) In order to address the objective 3 (To develop therapeutic strategies that disrupts the -synuclein protein-lipid interactions), we have investigated the druggable conformers of -synuclein by performing molecular dynamic simulations. We have identified the probable druggable conformers of -synuclein from the simulation trajectory based on the parameters: radius of gyration (Rg), solvent accessible surface area and the standard secondary structure content. As per the observations, the conformers with higher compactness, lower solvent accessible surface area, and moderate standard secondary structure content were observed to exhibit well defined binding pockets. Binding pockets in the screened conformers of -synuclein having lower (L1-L5), moderate radius of gyration (Rg) (M1-M5) and higher Rg (H1-H5) values have been predicted with the help of CASTp server. From the Rg, SASA and number of binding pockets, it can be inferred that the conformers having lesser SASA values to have more binding pockets. We have also calculated the percentage of individual secondary structure content across the screened conformers using YASARA software. It can be inferred that the conformers (L4, M5 and H3), showed higher percentage of -helical secondary structure content as compared to the other conformers in the corresponding groups. Therefore, it can be concluded from the above observations that in addition to Rg and SASA, the percentage of the standard secondary structure content, especially, helical portion of the protein to play a significant role in influencing the occurrence of number of binding pockets that inherently serves -synuclein as an input in designing drug like molecules. (b) In addressing the objective 1 (To obtain the structural and dynamic insights of membrane bound -synuclein at the atomistic level resolution using molecular dynamics simulations), we have investigated the consequences of crowding medium (ethanol) on the conformational dynamics of - synuclein. In this work, the effect of molecular crowding on the conformational dynamics of -synuclein without lipid membrane was studied before going for membrane bound -synuclein. The conformational changes and fluctuations in -synuclein were found to decrease gradually with an increase in the concentration of ethanol, the crowding agent. We observed most of the region in -synuclein to be in -helical conformation with increasing concentration of ethanol. We also calculated the percentage of individual secondary structure content in -synuclein across all conformers using YASARA software that were sampled during the production job of trajectories. We observed that -synuclein in 100% ethanol contains a higher amount of -helix than the other systems. So, these observations support that higher helical conformation in -synuclein which is predominant in case of 100% ethanol, to be actually responsible for preventing fibrillation process as this structural characteristic feature would induce a similar conformation that restricts fibrillation as proposed earlier. We also noticed the solvent accessible surface area of -synuclein protein to decrease and the 3-D structure to become less compact at higher concentration of ethanol, which explains its decreasing tendency towards aggregation. We also determined the Diffusion coefficient of -synuclein in the crowding environment and it was found to be dependent on concentration of the ethanol, the crowding agent. With an increase in concentration of ethanol, the value of diffusion coefficient decreases initially but again increases at higher concentrations due to the change in dielectric medium, intermolecular interactions and structural changes in -synuclein. The intermolecular interactions between the solvent water molecules and -synuclein protein were found to decrease with an increase in concentration of ethanol. Our results show that along with excluded volume effect, the co-solute properties of crowded intracellular environment need to be considered to understand -synuclein dynamics in cells. (c) In addressing the objective 1 (To obtain the structural and dynamic insights of membrane bound -synuclein at the atomistic level resolution using molecular dynamics simulations), we have carried molecular dynamics simulation of Wild type -Syn bound to membrane. From the MD simulation trajectory analysis of membrane bound wild type -Syn, it was observed that the Helix-N embedded deeper than the turn region beneath the lipid head group phosphates. While average depth of the helix-C in all the cases, lies below the bilayer centre (Z=0). The alpha helical content of WT -Syn was found to be around 19.3%. Therefore, it can be concluded that the N-helix region of the WT -Syn is buried immediately below the lipid head group/water interface, allowing the hydrophobic face of the protein to interact with the lipid membrane hydrophobic core and the hydrophilic face to connect with the lipid's polar region and water. (d)To address the objective 2 (To study the impact of -synuclein diseased point mutations present on the N-terminal of -synuclein on the lipid membrane binding), A30P, A30G, A53E, A53T, E46K, G51D and H50Q -Syn mutation were carried out and studied their conformational dynamics. From our observation (Figure 1), the alpha helical content of G51D (20.1%) and H50Q (21.1%) were found to be highest while other mutants were found to be similar indicating that substitution had an effect on the flexibility of the protein variants throughout the simulations. From the MD trajectory analysis, the structure of A30P, A30G, A53E, A53T, E46K, G51D and H50Q -Syn were noticed to undergo rapid change in conformations and to have higher backbone flexibility near the site of mutation. In particular, the helicity of membrane-bound A30G -Syn (Figure 2) was found to be more pronounced in the N-helix (3–37) and turn (38–44) regions, but helicity was shown to be significantly disrupted in the elevated regions above the lipid bilayer surface. We also found that -Syn rather than attaching evenly to membrane as a single entity, the different regions of -Syn demonstrated diverse interaction modes. The key structural characteristics of A30G -Syn addressed in this study may be helpful in understanding its function. (e)To address the objective 3 (To develop therapeutic strategies that disrupts the -synuclein protein-lipid interactions), we have studied (a) post translational modifications (PTMs) that includes phosphorylation at different locations (pY39, Ser87 and Ser129) in the -Syn protein, (b) the effect of C-terminal truncation (residues 100-140 and 109-140) of -Syn on its aggregation propensity and (c) the effect of peptidomimetic inhibitors (NPT200-11 and NPT100-18A) in disrupting the protein-lipid interactions using molecular dynamics simulations. The phosphorylation of -Syn at

Serine residue 87 and 129, were observed to lower the membrane protein interaction as well the aggregation propensity. On the contrary, phosphorylation at 39 showed high degree of fluctuation (Figure 3) at N-terminal that results in disruption of helix-2 binding region and thereby affecting membrane protein interaction but the -Syn may probably initiate aggregation with other available monomer on dissociating from the membrane. (f) Evidences of truncated C-terminal domain (CTD) in the brain of PD patients were reported to be higher. From our study (Figure 4), it was found that CTD -Syn exhibited more extended -helical conformation resulting in stronger interaction with membrane. Importantly, higher cytotoxicity with lower membrane disruption capacity was observed in CTD -Syn. The number of long range interactions between the N-terminal and C-terminal domains of -Syn were noticed to decrease by the C-terminal truncation. Many studies have been reported that truncated CTD of -Syn inhibits shielding of N-terminal from intermolecular interaction, promoting cytotoxicity and aggregation of -Syn by maintaining moderate -Syn-membrane interactions. Our study concludes that prevention of CTD truncation is a potent strategy to prevent the progression of PD and synucleinopathies. (g) The impact of peptidomimetic inhibitors (NPT100-18A and NPT200-11) on -Synuclein protein-lipid interaction were determined using Molecular dynamics (MD) simulations. NPT100-18a and NPT200-11 are two peptidomimetics that were developed recently and highlighted to inhibit -Syn oligomerization by interfering with membrane function. NPT100-18a, a cyclic peptidomimetic analogue to the 96KKDQLGK102 sequence of -Syn that most usually binds to another -Syn molecule during oligomerisation, was obtained and optimized using DFT calculations. Our findings put forward the potential binding position of these two drugs NPT100-18A and NPT200-11 on -Syn and also on the -Syn and lipid membrane interactions. The NPT200-11 compound have active centres that are believed to mimic the C-terminal domain and subsequently prevent the aggregation by hindering the interaction between the -Syn and lipid membrane. In both the cases of inhibitor complexes (Figure 5), the N-terminal and central domain regions were totally embedded in the lipid membrane. Therefore, the NAC region may not be available for inter-molecular hydrophobic interaction with the NAC region of other free alpha synuclein monomer to undergo self-assembly. We thus, conclude that inhibitor NPT200-11 on binding to the C-terminal of membrane bound -Syn showed decreasing effect on aggregation propensity that leads to targeting the interaction between -Syn and lipid membrane.
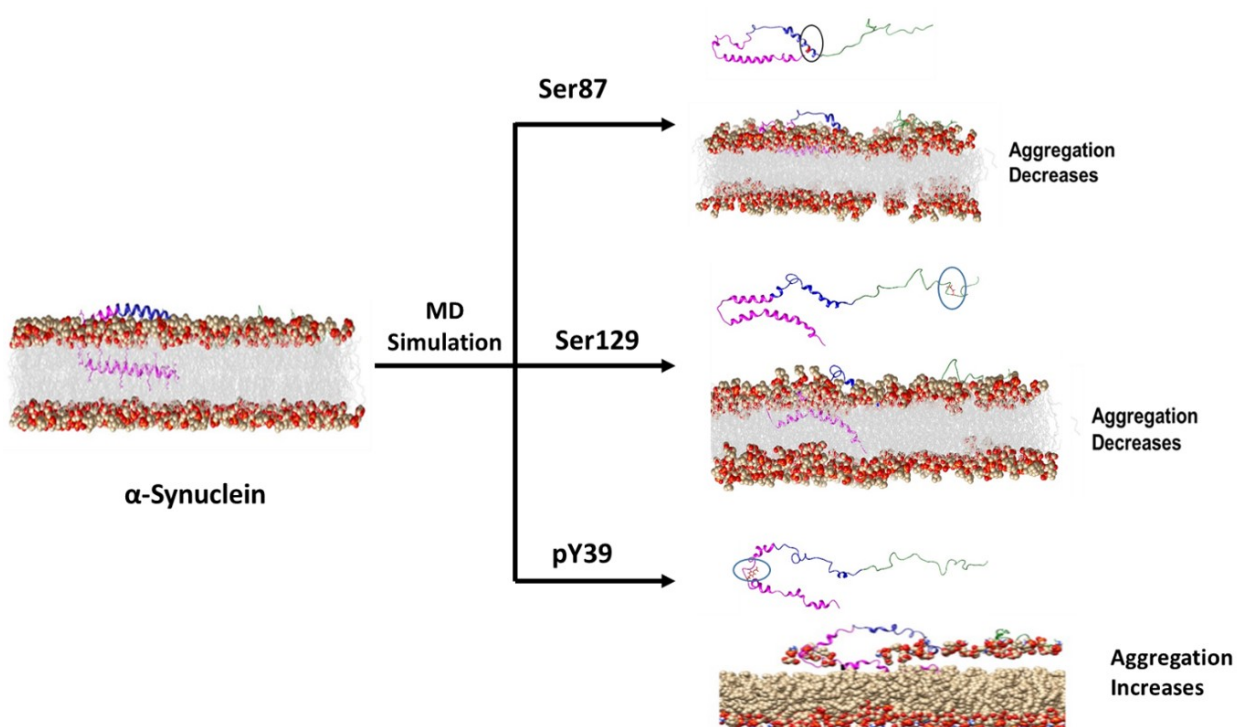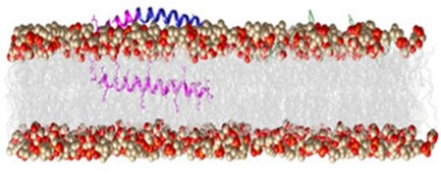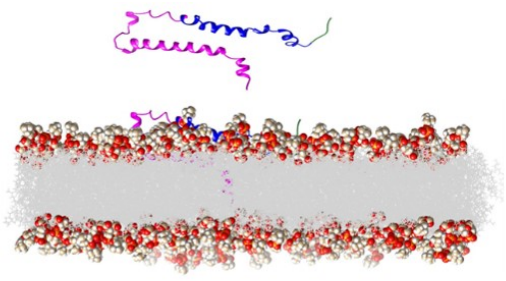
α-Synuclein

A30G
mutation

Ala 30

Gly 30

α-Synuclein

MD Simulation

Ser87

Aggregation
Decreases

Ser129

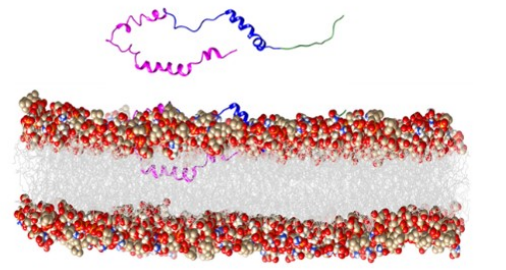Aggregation
Decreases

pY39

Aggregation
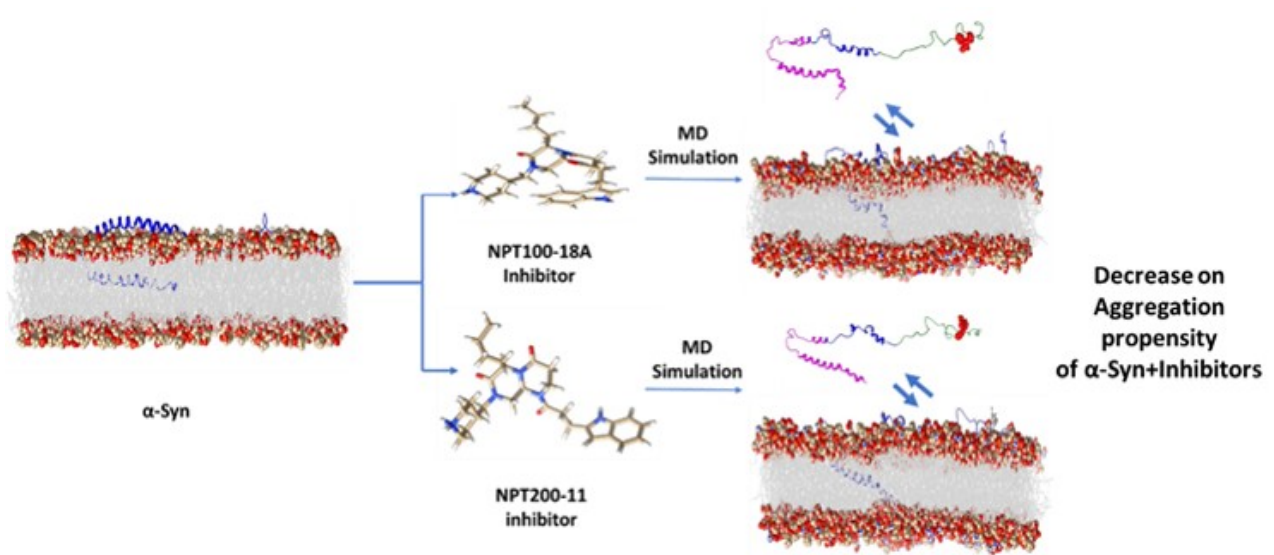Increases

α-Synuclein

MD
simulation

Truncated CTD (residue 100-140)

Truncated CTD (residue 109-140)

Conclusions

(a) We found the -synuclein conformers with lower solvent accessible surface area and higher secondary structure content of -helical to have well defined and suitable binding pockets for druggability. (b) We observed the -synuclein protein to experience stronger crowding effects with an increase in concentration of ethanol, the crowding agent. The findings that we obtained from this simulation study would serve as valuable guides for expected crowding effects on conformational dynamics of - synuclein. (c) From the MD trajectory analysis, the structure of Wild type and variants (A30P, A30G, A53E, A53T, E46K, G51D and H50Q) of -Syn were noticed to undergo rapid change in conformations and to have higher backbone flexibility near the site of mutation. (d) In particular, the helicity of membrane-bound A30G -Syn was found to be more pronounced in the N-helix (3–37) and turn (38–44) regions, but helicity was shown to be significantly disrupted in the elevated regions above the lipid bilayer surface. (e) We found that the different regions (N-terminal, NAC and C-terminal regions) of -Syn demonstrated diverse interaction modes rather than attaching evenly to membranes as a single entity. (f) The post translational modification of -Syn such as phosphorylation at pY39 plays an important role in enhancing aggregation propensity of -Syn but Ser87 and Ser129 PTMs decreased aggregation of -Syn. Phosphorylation of -Syn impacts membrane protein interaction. (g) The number of long range interactions between the N-terminal and C-terminal domains of -Syn were noticed to decrease by the C-terminal truncation. (h) The peptidomimetic inhibitors (NPT100-18A and NPT200-11) on binding to C-terminal region of membrane bound -Syn showed decreasing effect on aggregation propensity by disrupting protein-lipid interactions.

Scope of future work

In this study, the conformational dynamics of wild type and variants of -Syn protein bound to membrane were studied along with the methods to disrupt the protein-membrane interactions. Also methods to inhibit -Syn self-assembly and aggregation have been discussed. But the interaction of membrane bound -Syn with the unbound free monomer of -Syn protein needs to be studied in future to understand the self-assembly mechanism.

List of Publications (only from SCI indexed journals) :

Title of the Paper	List of Authors	Journal Details	Month & Year	Volume	Status	DOI No	Impact Factor
Screening of druggable conformers of -synuclein using molecular dynamics simulation	Dorothy Das , Mridusmita Kakati, Aroon Gracy, Airy Sanjeev, Swarna Mayee Patra and Venkata Satish Kumar Mattaparthi	Biointerface Research in Applied Chemistry (International)	Mar-2020	10 (5338-5347)	Published	https://doi.org/10.33263/BRIAC103.338347	0.86
Conformational Dynamics of A30G - Synuclein that causes familial Parkinson disease	Dorothy Das and Venkata Satish Kumar Mattaparthi	Journal of Biomolecular Structure and Dynamics (International)	Feb-2023	1 (1-13)	Published	http://dx.doi.org/10.1080/07391102.2023.2193997	5.23

List of Papers Published in Conference Proceedings, Popular Journals :

Title of the Paper	List of Authors	Journal Details	Month & Year	Volume	Status	DOI No	Impact Factor
Effect of ethanol as molecular crowding agent on the conformational dynamics of -synuclein.	Mridusmita Kakati, Dorothy Das, Pundarikaksha Das, Airy Sanjeev and Venkata Satish Kumar Mattaparthi.	Letters in Applied NanoBioScience (International)	Jan-2020	9 (779-783)	Published	https://doi.org/10.33263/LIANBS91.779783	0.60

List of Patents filed/ to be filed :

Patent Title	Authors	Patent Type	Country/Agency Name	Patent Status	Applicant No.
Not Available					

Equipment Details :

Equipment Name	Cost (INR)	Procured	Make & Model	Utilization %	Amount Spent (INR)	Date of Procurement
High performance Computing Cluster (Master Node)	6,47,325	Yes	HPE Proliant DL380 Gen10	20	6,03,025	19 Sep, 202
16 port KVM Switch	36,750	Yes	Netrack NR-CV-51601	10	34,883	19 Sep, 202
Cluster Management (Commercial/ Open source) Installation & configuration of Hardware,OS & Cluster M	52,500	Yes	Cluster management installation	10	9,933	19 Sep, 202
1 U Console with 19" LCD monitor	63,000	Yes	Netrack	10	58,863	19 Sep, 202
Compute Node	17,89,200	Yes	HPE Apollo 2800r Gen10	20	17,81,648	19 Sep, 202
36 U Rack	47,250	Yes	36U Rack TATA TRYNOX	10	47,187	19 Sep, 202
10 Gigabit Switch	1,62,750	Yes	HPE Office connect 1950 12XGT 4SFP+switch	20	1,43,010	19 Sep, 202

**Plans for utilizing the equipment facilities in future:**

The High performance computing cluster can be used for multiple purpose to study the molecular modelling and simulation of any complex biomolecules, membrane dynamics and drug designing, We are planning to study the dynamics of intrinsically disordered proteins and also to study protein aggregation mechanisms.

FINAL REPORT

OBJECTIVE 1: To obtain the structural and dynamic insights of membrane bound α-synuclein at the atomistic level resolution using molecular dynamics simulations

To investigate the druggable conformers of α-synuclein by performing molecular dynamic simulations. We have identified the probable druggable conformers of α-synuclein from the simulation trajectory based on the parameters: radius of gyration (R_g), solvent accessible surface area and the standard secondary structure content. As per the observations, the conformers with higher compactness, lower solvent accessible surface area, and moderate standard secondary structure content were observed to exhibit well defined binding pockets. Binding pockets in the screened conformers of α-synuclein having lower (L1-L5), moderate radius of gyration (R_g) (M1-M5) and higher R_g (H1-H5) values have been predicted with the help of CASTp server (**Figure 2**). **Table 1** summarizes the R_g, SASA and the number of binding pockets of the corresponding screened conformers of α-Synuclein. From the Table 1, it can be inferred that the conformers having lesser SASA values to have more binding pockets.

We have also calculated the percentage of individual secondary structure content across the screened conformers using YASARA software. The results were summarized in the **Table 2**. From **Table 2,** it can be inferred that the conformers (L4, M5 and H3), showed higher percentage of α-helical secondary structure content as compared to the other conformers in the corresponding groups. Therefore, it can be concluded from the above observations that in addition to R_g and SASA, the percentage of the standard secondary structure content, especially, α helical portion of the protein to play a significant role in influencing the occurrence of number of binding pockets that inherently serves α-synuclein as an input in designing drug like molecules.

A.

B.

C.

H1 H2 H3 H4 H5
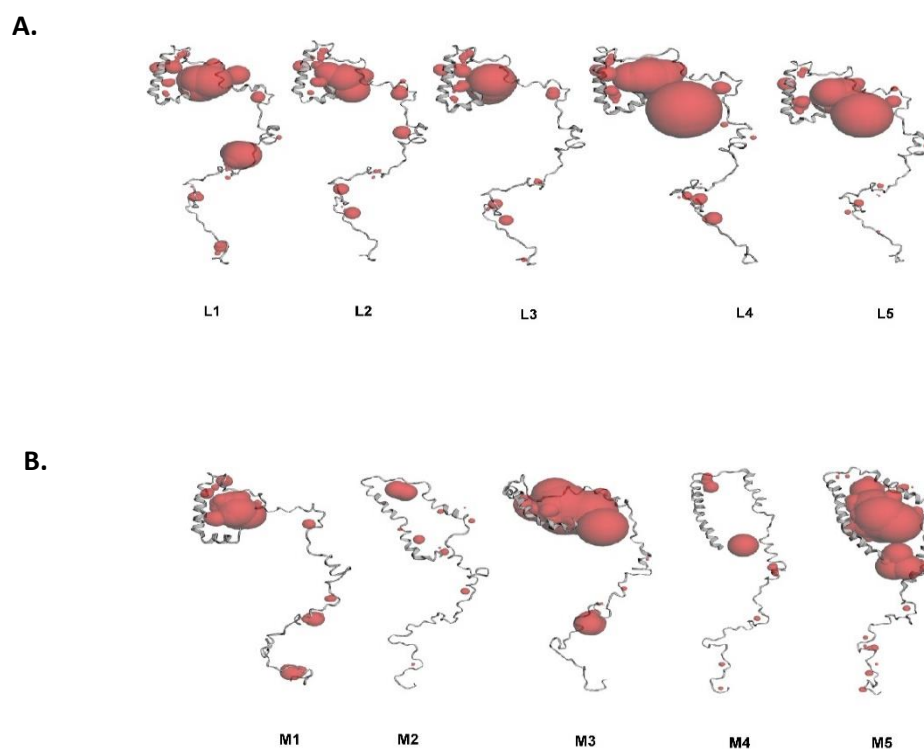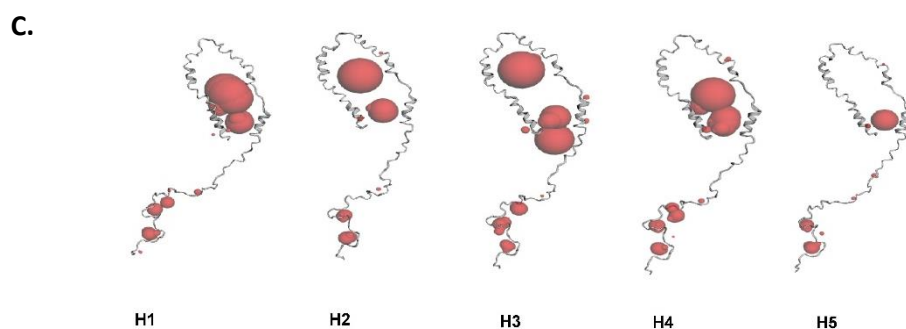
Figure 2. Binding pocket analysis for the conformers of α-synuclein having **(A)** lower R_g values **(B)** moderate R_g values **(C)** higher R_g values.

Table 1. Rg, SASA and Number of binding pockets for the screened conformers of α-synuclein having lower, middle and higher Rg values.

CONFORMERS	Rg VALUES (Å)	SASA VALUES (Å^2)	NUMBER OF BINDING POCKETS
L1	41.582	13692.33	15
L2	41.588	13748.63	17
L3	41.597	13728.49	11
L4	41.599	13791.03	19
L5	41.603	13798.73	16
M1	42.997	13973.61	9
M2	43.999	13804.06	10
M3	44.998	13862.44	11
M4	45.973	14255.19	7
M5	46.041	14655.89	15
H1	47.895	14494.96	11
H2	47.868	14477.31	7
H3	47.868	14341.28	11
H4	47.864	14377.58	9
H5	47.855	14415.70	8

Table 2. Secondary structure content and the Number of Binding Pockets for the conformers of α-Syn having lower, middle and higher Rg values

CONFORMERS	SECONDARY STRUCTURES				NUMBER OF BINDING POCKETS
	HELIX (%)	SHEETS (%)	TURNS (%)	COILS (%)	
L1	21.4	0.0	14.3	64.3	15
L2	22.1	0.0	14.3	60.0	17
L3	17.9	0.0	22.9	59.3	11
L4	22.9	0.0	14.3	62.9	19
L5	17.9	0.0	14.3	65.0	16
M1	19.3	0.0	20.0	60.7	9
M2	20.7	0.0	22.9	52.9	10
M3	20.7	0.0	20.0	59.3	11
M4	26.4	0.0	11.4	59.3	7
M5	40.0	0.0	11.4	48.6	15
H1	12.9	0.0	31.4	55.7	11
H2	11.4	0.0	40.0	48.6	7
H3	21.4	0.0	25.7	52.9	11
H4	15.7	0.0	34.3	50.0	9
H5	12.1	0.0	25.7	59.3	8

In addressing the **objective 1** of our project, we have also investigated the consequences of crowding medium (ethanol) on the conformational dynamics of α- synuclein. In this work, the effect of molecular crowding on the conformational dynamics of α-synuclein without lipid membrane was studied before going for membrane bound α-synuclein. The conformational changes and fluctuations in α-synuclein were found to decrease gradually with an increase in the concentration of ethanol, the crowding agent. In Figure 3, we can see the snapshots of α-synuclein at 0%, 5%, 10%, 20%, 50% and 100% concentration of ethanol. We observed most of the region in α-synuclein to be in α-helical conformation with increasing concentration of ethanol.
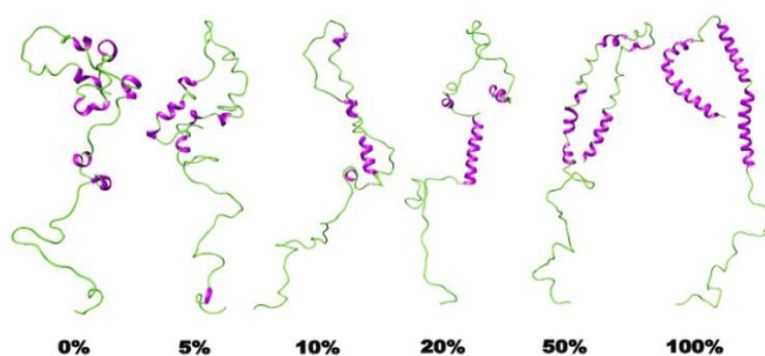
0%   5%   10%   20%   50%   100%

Figure 3. Snapshots of α-synuclein conformers in presence of 0%, 5%, 10%, 20%, 50% and 100% ethanol during the time course of simulation.

We also calculated the percentage of individual secondary structure content in α-synuclein across all conformers using YASARA software that were sampled during the production job of trajectories and the results were summarized in Table 3. From Table 3, we observed that α-synuclein in 100% ethanol contains a higher amount of α-helix than the other systems. So, these observations support that higher helical

conformation in α-synuclein which is predominant in case of 100% ethanol, to be actually responsible for preventing fibrillation process as this structural characteristic feature would induce a similar conformation that restricts fibrillation as proposed earlier.

Table 3. Secondary structure content of α-synuclein in 0%, 5%, 10%, 20%, 50% and 100% ethanol.

Concentration of Ethanol	α-Helix	Sheet	Turn	Coil	3_{10} helix	Π-helix
0%	4.3%	0.0%	34.3%	61.4%	0.0%	0.0%
5%	8.6%	0.0%	37.1%	54.3%	0.0%	0.0%
10%	5.0%	1.4%	30.0%	60.0%	3.6%	0.0%
20%	22.1%	0.0%	8.6%	63.6%	5.7%	0.0%
50%	20.0%	2.1%	30.0%	47.9%	0.0%	0.0%
100%	55.0%	0.0%	5.7%	39.3%	0.0%	0.0%

We also noticed the solvent accessible surface area of α-synuclein protein to decrease and the 3-D structure to become less compact at higher concentration of ethanol, which explains its decreasing tendency towards aggregation. We also determined the Diffusion coefficient of α-synuclein in the crowding environment and it was found to be dependent on concentration of the ethanol, the crowding agent (**Table 4**). With an increase in concentration of ethanol, the value of diffusion coefficient decreases initially but again increases at higher concentrations due to the change in dielectric medium, intermolecular interactions and structural changes in α-synuclein. The intermolecular interactions between the solvent water molecules and α-synuclein protein were found to decrease with an increase in concentration of ethanol. Our results show that along with excluded volume effect, the co-solute properties of crowded intracellular environment need to be considered to understand α-synuclein dynamics in cells.

Table 4. Diffusion Coefficient values of α-synuclein in different concentrations of ethanol.

Concentrations of Ethanol	Diffusion Coefficient ($\times 10^{-10}$ cm^2/s)
0% Ethanol	0.5829
5% Ethanol	0.3703
10% Ethanol	0.2516
20% Ethanol	0.2148
50% Ethanol	0.2699
100% Ethanol	0.4446

Construction of lipid Bilayer using CHARMM GUI

The initial orientation of the α-Synuclein protein structure with respect to the lipid bilayer plane was determined for MD simulations using CHARMM GUI server (Monje and Klauda 2015). Before initiating MD simulation, OPM database was used to provide PDB coordinates of

membrane proteins in the optimal spatial arrangements with respect to core of the lipid bilayer which are predicted by minimizing its solvation free energy in membrane and by positioning each protein in an adjustable thickness of the membrane (Lomize et.al. 2006). After submitting the PDB co–ordinates of the membrane protein and determining the orientation, the membrane protein was inserted into an explicit lipid bilayer system. From review of literature, various protocols were reported to build a reasonable initial structure of a protein–membrane complex (Sunhwan et.al. 2007; Christian et.al. 2007; Matti 2014; Mohammad 2014; Phillip 2015). But, only CHARMM-GUI Membrane Builder is widely used for system building in homogenous or mixed bilayers with more than 180 lipid bilayer types available (Sunhwan et.al. 2009; Emilia et.al. 2014). It also provides well-validated equilibration and production inputs for many MD program packages including AMBER software package (Jumin et.al. 2016).

In STEP 1, CHARMM-GUI user includes internal residue format PROTEIN (1-140) (**Figure 1 (a.)**) protein instead of PDB chain id. STEP1 reads and initiate a manipulation of the model chain from the PDB file. The Terminal Group patching is selected to determine the end terminals of the chain. During the manipulation step our Alpha synuclein protein model used different protonation state of His residue at selected site; because only at neutral or low pH MD simulation were performed. In the process, CHARMM occasionally add hydrogens at regular intervals but our system selected to preserve the hydrogens as it included specific hydrogens for protonation state. To check the job progress or to retrieve previous submitted job, it is important to save the JOB ID using Job retriever.

STEP 2 helps in orientation of the α-synuclein protein with respect to the DOPE: DOPS: DOPC membrane bilayer in 5:3:2 ratio (Giuliana et.al. 2016). A lipid bilayer positioned normally along the Z plane with center at Z=0. The transmembrane domain of the complex model was assigned to pre-orientation by aligning the principal axis along the Z plane, where center at Z=0 and it is not necessary to change the orientation of the Complex model. The generated file of "step2_orient.pdb" was downloaded to visualise if the protein to make sure that the α-Synuclein protein is properly positioned in the lipid bilayer.

STEP 3 initiates in building a heterogeneous bilayer system. Selection of Heterogeneous membrane is performed due its compatibility. The water thickness of the membrane is selected to be 17.5Å to add minimum water height on upper and lower leaflet of the system. Number of lipid component option is selected with XY dimension ratio to be 1, we have selected the number of lipids. To fill the ratio values into the specified input boxes click on the "show the system info" to calculate the number of lipid molecule required to build the hetrogenous lipid bilayer. The calculated content will be visualized on the right side table (**Table 1**). Each upper and lower leaflets of lipid molecule envelopes a certain area per lipid. In the system information, protein X

and Y content was estimated to be 32.01 and 91.98. The average area of the complex system was calculated to be 36296.16 area per system. Calculation of the system information was performed as to ensure the system size should not be large enough to hold the protein otherwise the membrane building process will be aborted **Fig. 1(b)**.
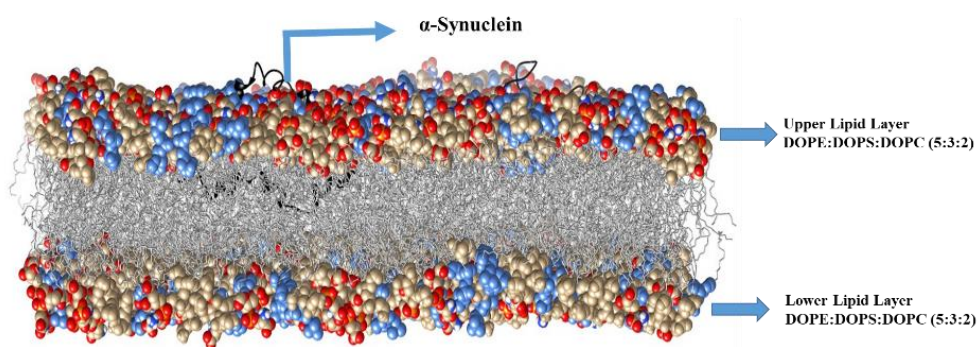
Fig. 4. Graphical illustration of membrane bound A30G α-Syn built using CHARMM GUI server. For better visuals, ions and water box was not included. The snapshots are generated using UCSF CHIMERA 1.14.

Table5. Ratio and Number of lipids in protein membrane system.

LIPID COMPOSITION	RATIO	UPPER LEAFLET	LOWER LEAFLET
DOPE	5	270	260
DOPS	3	162	156
DOPC	2	108	104

STEP 4 includes Membrane Builder that uses the so-called "replacement" method that first packs lipid-like pseudo atoms and then replaces them with lipid molecules one at a time by randomly selecting a lipid molecule from a lipid structural library. The replacement in STEP 4 takes long time due to careful checks of lipid bilayer building to avoid unphysical structures, such as penetration of acyl chains into ring structures in sterols, aromatic residues, and carbohydrates. This is the reason why water box generation and ion placement are done separately in STEP 4. We added 0.15 M KCl in the system, mimicking the cellular environment, with the Monte Carlo method for ion placing and it is used to calculate the trajectories of protein molecules on the surfaces and in the liquid transport medium. In our system potassium (K+) ions and chloride (Cl-) ions are selected and calculated to neutralize the charge in the system. The significant characteristics of the lipid bilayer system is their impermeability to ions due to their low dielectric

environment during the hydrophobic N-terminal region. During the simulation, the tail groups of hydrophobic lipid bilayer were observed to be fluctuating significantly and form random conformation. The head groups of lipid bilayer formed an interaction with the water molecules of the system through Hydrogen bonds.

In the 5th step, assembly pdb file is generated that includes lipid bilayer, protein, water molecule and ions. Water molecules overlapping with α-Synuclein protein, ions and lipids were removed during the assembly. Then, we select "Next Step" for "AMBER" in "Input Generation Options" and select the NPT ensemble at T = 303.15K in "Equilibration Options". At this temperature, DOPE: DOPC: DOPS bilayers show liquid phase rather than gel phase (T = 271K). Note that input generation takes long time to prepare all restraints for protein positions, chiral centers, cis double bonds of acyl tails, and sugar chair conformations; these restraints are used for the optimized equilibration inputs to prevent any unwanted structural changes in lipids and embedded proteins, so that production simulations can probe physically realistic behaviors of biomolecules. After selection of the final 6th step, we added missing hydrogen atoms and heavy atoms, leap module of AMBER was applied using the Amber force field (ff99SBildn) (Joao et.al. 2015) parameters. For neutralizing the charge of the system, appropriate number of K^+ ions were added. The TIP4PEW water model was used with the lipid 17 force field and all simulations were performed using the AMBER software package we can download a set of input files for minimization, equilibration, and production runs for AMBER at the final step of the membrane builder.

Using CHARMM-GUI server, we have constructed lipid bilayer comprising of DOPE: DOPS: DOPC in 5:3:2 ratio and this lipid composition is selected because it excellently mimics the synaptic membrane. A step-wise building protocol was emphasized that include 6 step for the construction of protein-membrane bilayer complex and each step is designated to specific user parameters through a web browser and generate the executable CHARMM input files. On the first step, Membrane only system was selected to build a lipid bilayer by uploading the PDB file (1XQ8) obtained from PDB data bank. Orientation of the protein and protonation state of the protein are carried out based on the system requirement. In the next step, in membrane with protein complex water thickness of the membrane is selected (17.5Å) or otherwise without protein Hydration number is required. Selection of Heterogeneous membrane is performed due its compatibility. Number of lipid component option is selected with XY dimension ratio to be 1, we have selected the number of lipids and water molecules to be added in the system. Each upper and lower leaflets of lipid molecule envelopes a certain area per lipid. Calculation of the system information was performed as the system size should be large enough to hold the protein otherwise the membrane building process will be aborted. In the next steps, we add 0.15 M KCl in the system,

mimicking the cellular environment, with the Monte Carlo method for ion placing and it is used to calculate the trajectories of protein molecules on the surfaces and in the liquid transport medium. In our system potassium (K+) ions and chloride (Cl-) ions are selected and calculated to neutralize the charge in the system. During the simulation, the tail groups of hydrophobic lipid bilayer were observed to be fluctuating significantly and form random conformation. The head groups of lipid bilayer formed an interaction with the water molecules of the system through Hydrogen bonds. In the 5th step, assembly pdb file is generated that includes lipid bilayer, protein, water molecule and ions. The significant characteristics of the lipid bilayer system is their impermeability to ions due to their low dielectric environment during the hydrophobic N-terminal region. Then, we select "Next Step" for "AMBER" in "Input Generation Options" and select the NPT ensemble at T = 303.15K in "Equilibration Options". At this temperature, DOPE: DOPC: DOPS bilayers show liquid phase rather than gel phase (T = 271K). After selection of the final 6th step, we can download a set of input files for minimization, equilibration, and production runs for AMBER at the final step of the membrane builder.

Simulation setup and initial co-ordinates and topology parameters of Membrane bound wild type α-synuclein

The generated CHARMM GUI membrane-protein system is converted to AMBER simulated system using charmm2lipid.py script. The topology and co-ordinate files required for MD simulation were generated by LEaP module. We then conducted explicit MD simulations on A30G mutant α-Synuclein as its initial structures using AMBER 18 software package. From the literature, force field have been used in many of the studies to characterize the structural features of intrinsically disordered proteins. Molecular dynamics simulation of DOPE: DOPS: DOPC membrane with α-synuclein was minimized using the steepest descent method for 1000ps, followed by 1ns of NVT equilibration with the time step and NPT equilibration. After minimization, the system was gradually heated from 0 to 300 K for a time-period of 50 ps to 100ps with constraints on membrane, and thereby maintained in the isothermal-isobaric ensemble (NPT). Temperature of 300K and 1atm of pressure was controlled to maintain the temperature of the system. Subsequently using Berendsen weak coupling method (0.5ps time constant for heat bath coupling and 0.2 ps pressure relaxation time), MD for constant pressure-temperature conditions (NPT) with temperature regulation was achieved. For treating the long range electrostatic interactions, Particle Mesh Ewald (PME) method was used with the default parameter. Using cubic periodic boundary conditions, all the simulations were carried out in the NPT ensemble.

Simulation setup and initial co-ordinates and topology parameters of α-synuclein in free monomer state

MD simulation study of wild type α-synuclein was carried out using standard protocol that included two step minimization, heating dynamics, equilibration step and production dynamics run for a time period of 100ns. Energy minimized systems were used for initial steps of MD simulation. After minimization, the system was gradually heated from 0 to 300 K for a time-period of 50 ps to 100ps with constraints on membrane, and thereby maintained in the isothermal-isobaric ensemble (NPT). Temperature of 300K and 1atm of pressure was controlled to maintain the temperature of the system. Subsequently using Berendsen weak coupling method (0.5ps time constant for heat bath coupling and 0.2 ps pressure relaxation time), MD for constant pressure-temperature conditions (NPT) with temperature regulation was achieved. For treating the long range electrostatic interactions, Particle Mesh Ewald (PME) method was used with the default parameter. Using cubic periodic boundary conditions, all the simulations were carried out in the NPT ensemble. The MD production of 100ns time period were run for the equilibrated structures of both the systems using the Particle Mesh Ewald (PME) algorithm. The pdb files of each production run were generated and the snapshots of each system after completion of 10ns were recorded for further analysis.

Analysis of trajectory

The analysis of structural properties (Root mean square deviation (RMSD), Root mean square surface area analysis (RMSF), secondary structure development were carried out using cpptraj module of AMBER software package. For the visualization of 3D structure of the molecules, we used UCSF Chimera, VMD. To generate the graphs, xmgrace plotting tool was used. The secondary structure analysis for wild in presence of membrane as well was carried out using the Kabsch and Sander algorithm incorporated in their DSSP (Dictionary of Secondary Structure for Protein) program [54]. The intermolecular hydrogen bond analysis were employed for membrane bound wild type α-synuclein based on membrane bilayer and protein as potential acceptors (HA) and donors (HD) of the hydrogen atoms.

Membrane Analysis

Electron Density Analysis

Electron density determines the measure of the probable position of an electron at a specified location. The electron density analysis calculates the time averaged z-direction of electrons of simulation setup, which can be analysed with good precision as all the atomic co-ordinates are known from the simulation. A typical electron density profile across the membrane, includes the

following characteristics: a minimum in the middle of the bilayer (near the CH3 groups), two maxima (peaks) at the position of the head groups (phosphate groups), and a local minimum in the water layer. In the electron density profile, the hydrophobic thickness is defined as the distance between the peaks of the electron density profile and changes may occur when a molecule is inserted into or interacts with the membrane.

Average Area per Lipid in Upper and lower leaflet of the bilayer

Average area per lipid analysis is one of the main parameters in evaluating the equilibrium of membrane setup. The average area per lipid allows the determination of a measure for tuning the force fields and other parameters for membrane systems. The analysis is considered to be a quantitative evaluation of membrane prior using for molecular simulation. The depth of each component of α-synuclein in the lipid bilayer describes the spontaneous diffusion of each molecules at atomistic resolution and their chemical component within a lipid bilayer. The variation in free energy value for N helix was observed an average of 12 Å embedded beneath the phosphate headgroup of the lipid layer central bilayer of bulk water phase towards the membrane lipid headgroups could be attributed to the increase in density.
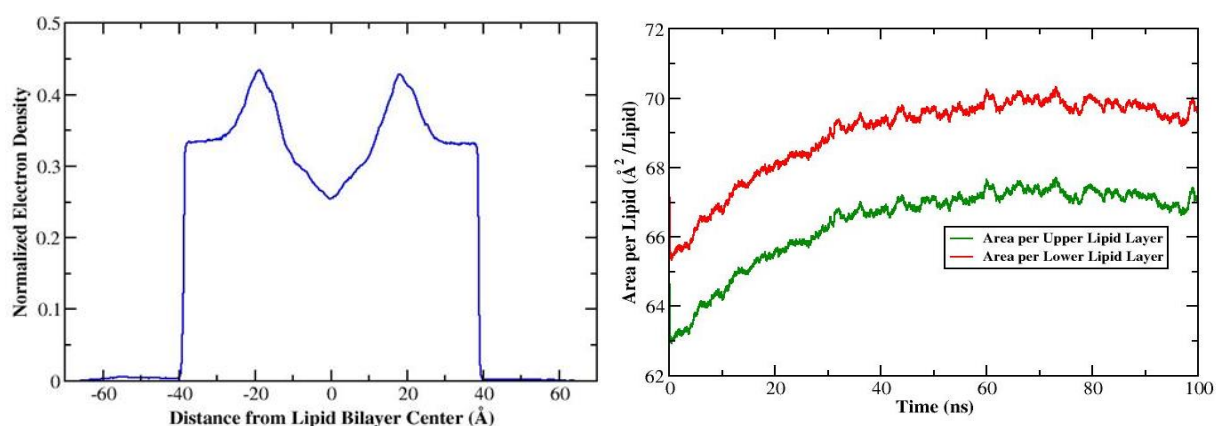
Fig. 5. a). Electron Density profile Analysis b). Area per Lipid Layer Analysis of membrane bound wild type α-synuclein during a simulation time period of 100ns
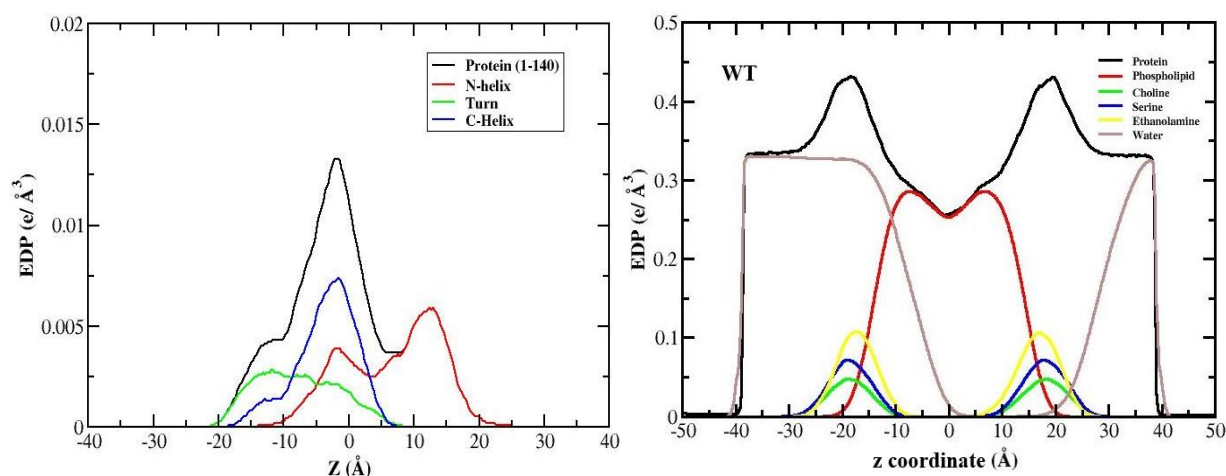
Fig. 6. a). Electron density profile of N helix, Turn and C helix of wild type α-syn b). Electron density profile of different lipid profile of wild type α-synuclein
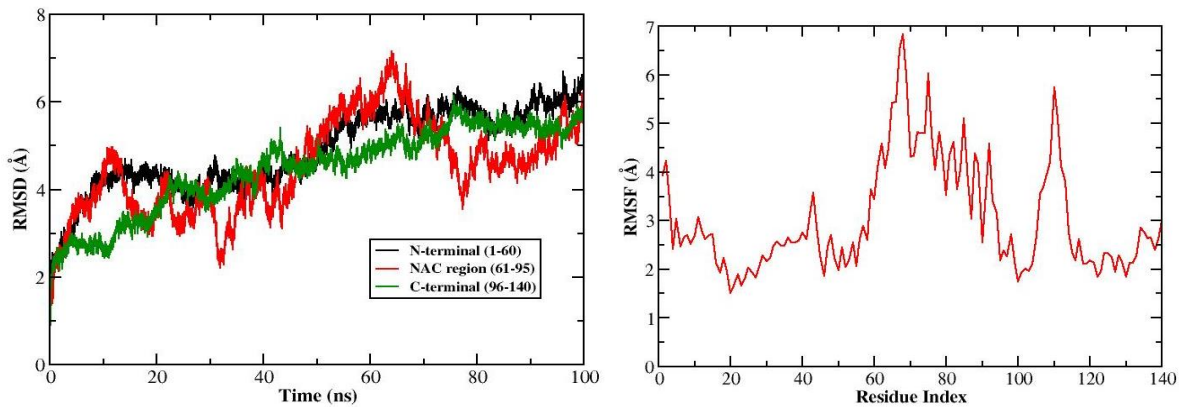
Fig. 7. a). Root Mean Square Deviation Analysis of membrane bound wild type α- synuclein during simulation period. b). Root Mean Square Fluctuation Analysis wild type α-synuclein during simulation period of 100 ns
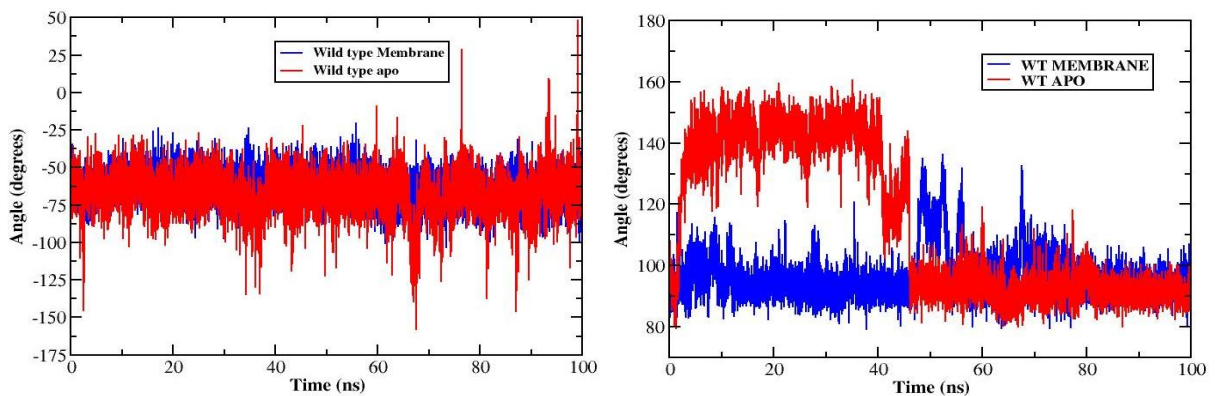
Fig. 8. a). Helical bending at position Glycine 68. The color scheme is as follows: wild type α-synuclein in lipid-bound state (blue) b). The conformations of each residues of the mutant chain in its bound state that demonstrate unfolding leading to unbinding at residue 26 of the wild type α-synuclein.
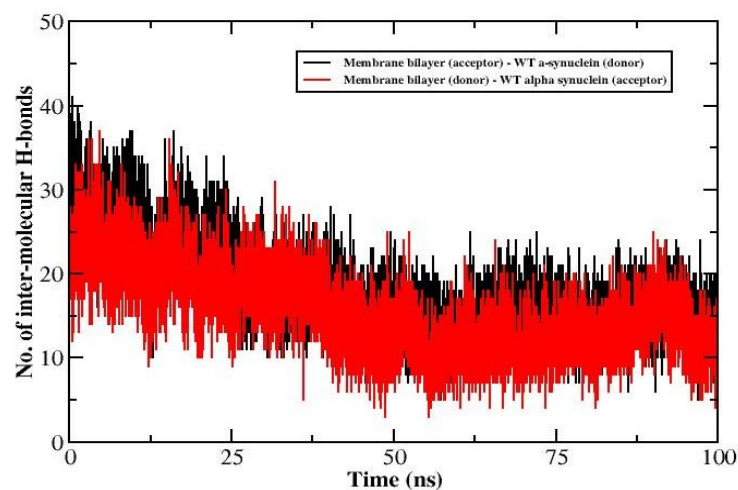
Fig. 9. The number of intermolecular hydrogen bonds between wild type α-synuclein in lipid bound state during MD simulation of 100ns
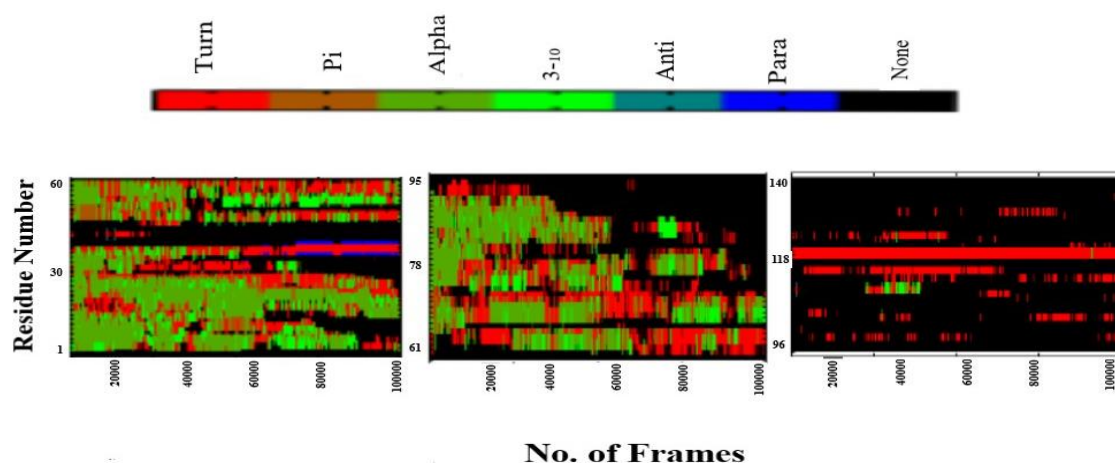
Fig. 10. Secondary structural analysis of membrane bound wild type α-synuclein is calculated by Kabsch and Sander Algorithm using dssp software. The color index depicts different conformational changes of each residue of wild type α-synuclein during simulation period of 100ns

Table 6. Secondary Structural Analysis of wild type α-synuclein during the simulation time period of 100 ns using YASARA software

Wild type α- synuclein	TURN	SHEET	Pi	ALPHA	3-10	COIL
Percentage (%)	19.3	2.5	0	20.7	0	57.5
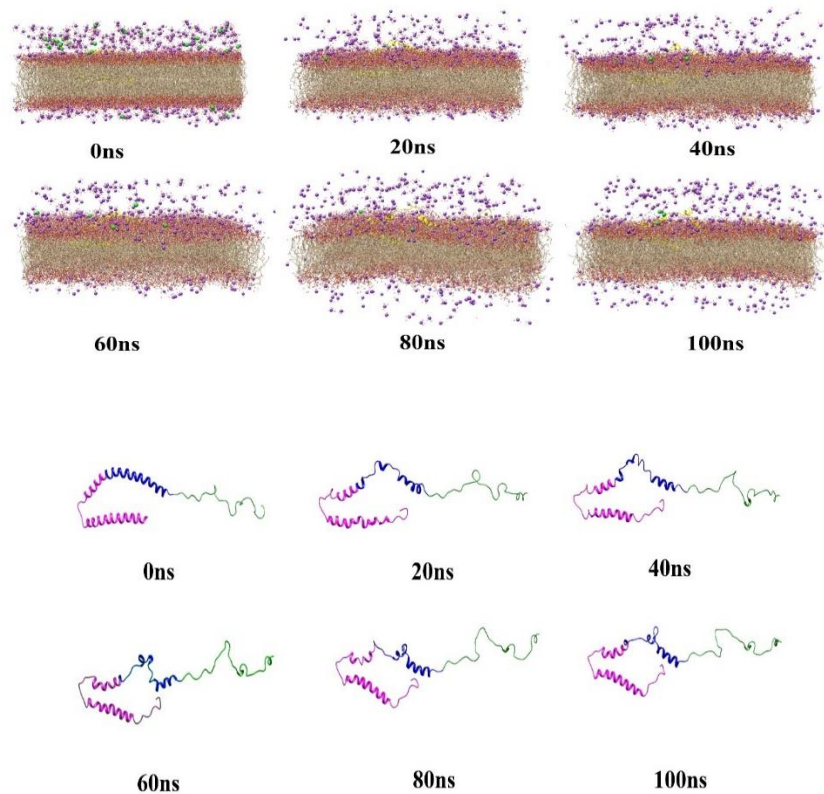
Fig. 11. Snapshots of Membrane bound wild type α- synuclein at different intervals of simulation time

Objective 2: To study the impact of α-synuclein diseased point mutations present on the N-terminal of α-synuclein on the lipid membrane binding

Effects of α- synuclein mutant (A30G, A30P, A53T, A53E, E47K, H50Q, and G51D) bound to lipid membrane DOPE: DOPC: DOPS using MD simulation methods

1.1 Molecular Dynamic Analysis of A30G α- synuclein mutant bound to lipid membrane DOPE: DOPC: DOPS

An electron density corresponds to the probability of the electrons being present at a specific location. In this profile, it exhibits a global minimum in the middle of the bilayer (near the terminal CH3 groups of the acyl chains), two maxima corresponding to the positions of the head groups (phosphate groups) in each leaflet, and a local minimum reflecting the water layer outside the membrane. From the profile it can be inferred that the time-averaged positions of electrons (Fig

9). Area per Lipid analysis determines the degree of quality of a lipid Force field. Area per lipid analysis determines the degree of binding to other membrane properties, acyl chain ordering, compressibility, and molecular packaging. From the Area per lipid profile of mutant A30G α-synuclein and wild type α-synuclein, it showed an equilibrium of insertion of the protein into the lipid profile (Figure 9.b.). Snapshots of A30G mutant bound to lipid membrane (DOPE: DOPS: DOPC) during simulation time period of 100ns as shown in Fig. 15.

RMSD analysis

From the MD analysis of RMSD (root mean square deviation), DOPE:DOPS:DOPC lipid membrane bound H50Q mutant was observed showed higher oscillation (1-7 Å) as compared to DOPE:DOPS:DOPC lipid membrane bound mutant **Fig. 11.a**. Also, indicated higher fluctuation rates that inhibit the stability of the system.

RMSF Analysis

The RMSF (root mean square fluctuation) plots demonstrate flexibility of individual residues during simulation period of 100ns. The observed RMSF values showed that residue fluctuations were less (1–5.5 Å) during simulation time period of 100ns.

Helical bend Analysis

Helical bending can determine two factors i.e. the equiliberated fluctuations that causes the binding and shaping of the helices to a rigid membrane bilayer and the characterization of perturbed regions caused due to mutation as a result that disrupts the normal interactions. The helical region was calculated for each residue at the angle between the helices formed in between 67th, 68th and 69th position and the results are shown in **Fig. 12**. The A30G mutant showed changes in bending angle with respect to a time series of 100ns. A maximum bending of was observed in A30G mutant.

Inter-molecular Hydrogen bond Analysis

Hydrogen bond refers to the stability of the protein-membrane complex. The average inter-molecular H-bond between the A30G mutant and lipid membrane was estimated to be 20. The interaction between lipid membrane as acceptor/donor and A30G mutant as receptor/donor was showed in **Fig. 13**. The number of inter-molecular hydrogen bonds are higher in membrane bound A30G mutant.

Secondary Structure Analysis

The secondary structural analysis of mutant A30G is calculated by Kabsch and Sander Algorithm using DSSP software as shown in Fig. 14. In the case of the A30G mutant (Table 2), however, the α-helical propensity was further decreased to be 5%. The combined analysis showed that the A30G mutation decreased locally resulting in decreased α-helical propensity. From the analysis, Mutant A30G showed rare α-helical peaks. The dssp plot in Fig. 14 showed secondary structure variation residue in A30G during simulation time period of 100 ns. The α-helical conformations were very rare in occurrence as very few α-helical peaks were observed in the A30G mutant chain. This decrease in α-helical content in A30G suggests unfavourablility on its binding to the membrane as well in formation α-helical formation, but not necessarily inhibit the interaction with lipid membrane. In A30G mutant, membrane curvature was observed during MD simulation of 100 ns due to changes in binding mechanism of A30G caused by decreasing α-helical as shown in Fig. 15.
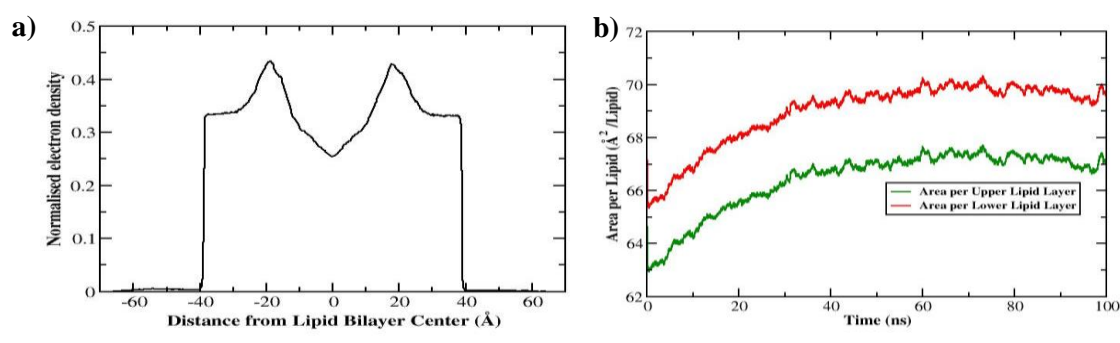
Fig. 12. a). Electron Density profile Analysis b). Area per Lipid Layer Analysis of membrane bound A30G mutant during a simulation time period of 100ns

a)   b)
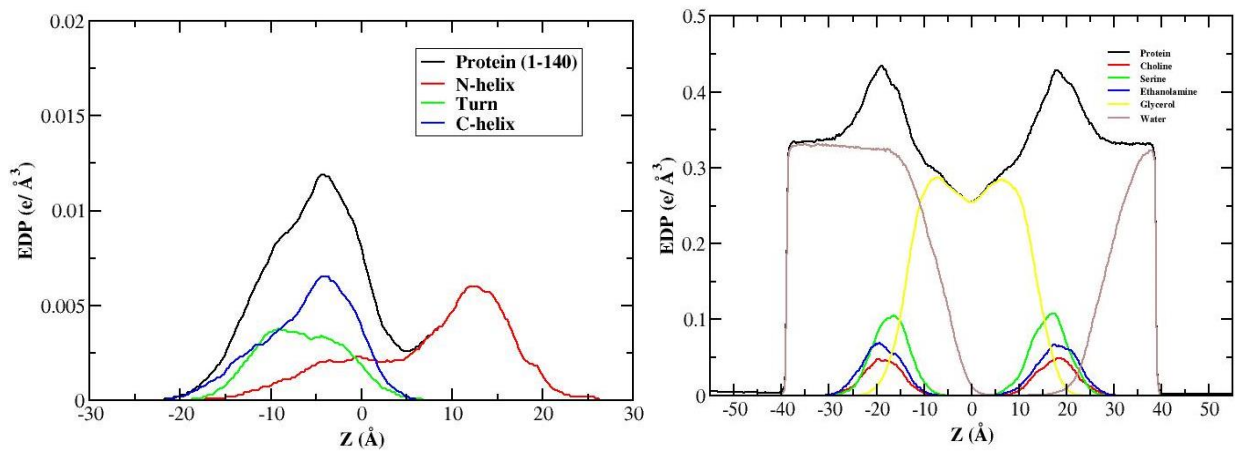
Fig. 13. a). Electron density profile of N helix, Turn and C helix of α-syn b). Electron density profile of different lipid profile of α-synuclein
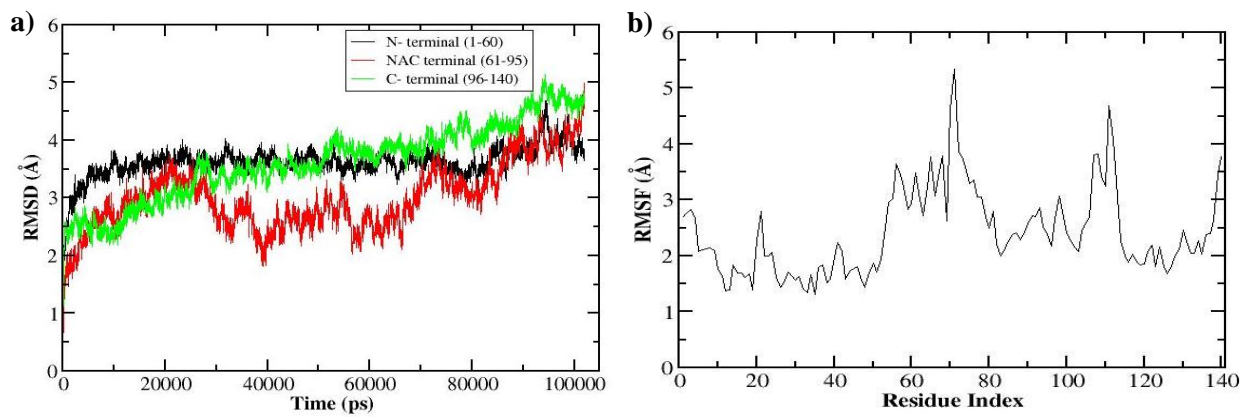
Fig. 14. a). Root Mean Square Deviation Analysis of membrane bound A30G mutant α- synuclein during simulation

period. Root Mean Square Fluctuation Analysis A30G mutant α-synuclein during simulation period of 100ns.
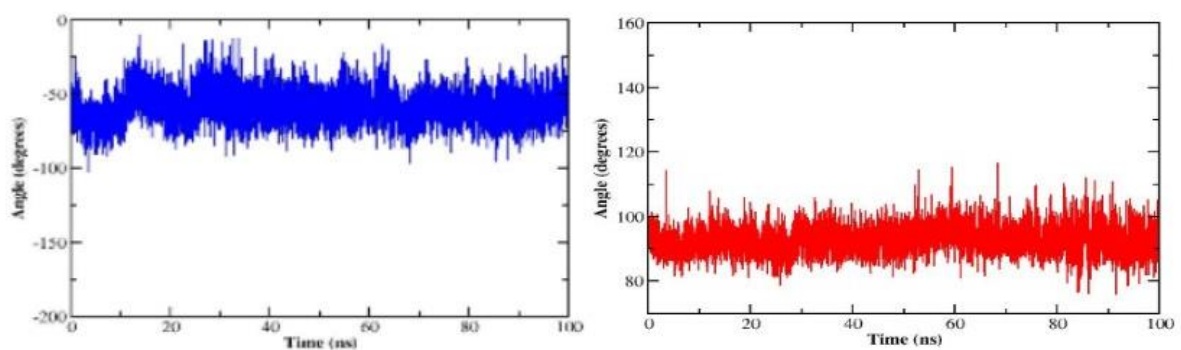
Fig. 15. a). Helical bending at position Glycine 68. The color scheme is as follows: A30G in lipid-bound state (blue) b). The conformations of each residues of the mutant chain in its bound state that demonstrate unfolding leading to unbinding at residue 26 of the A53T mutant chain.
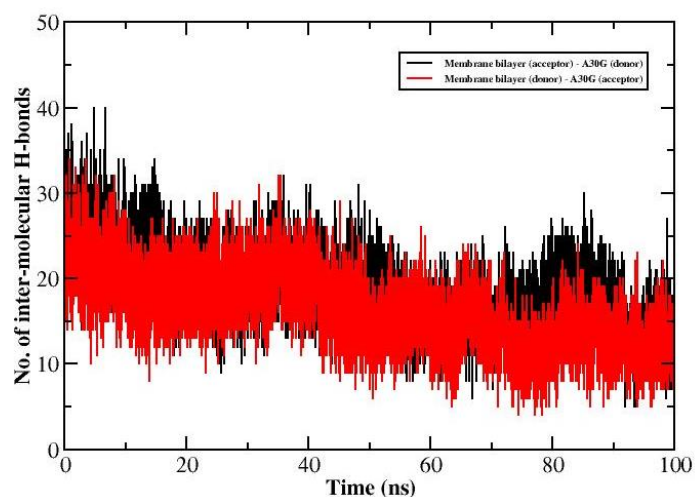
Fig. 16. The number of intermolecular hydrogen bonds between A30G α-synuclein in lipid bound state during MD simulation of 100 ns

No. of Frames
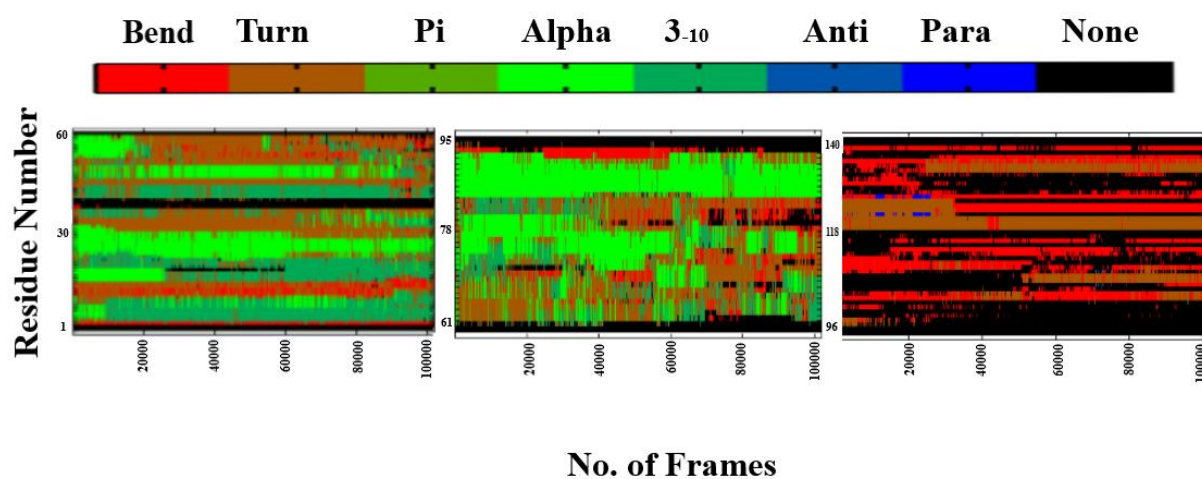
Fig. 17. Secondary structural analysis of membrane bound A30G mutant is calculated by Kabsch and Sander Algorithm using dssp software The color index depicts different conformational changes of each residue of A30G mutant α-synuclein during simulation period of 100ns

Table 7: Secondary Structural Analysis of A30G mutant during the simulation time period of 100 ns using YASARA software

A30G mutant	Turn	Sheet	Pi	Alpha	3-10	Coil
Percentage (%)	40	0	0	5	2.9	52.1
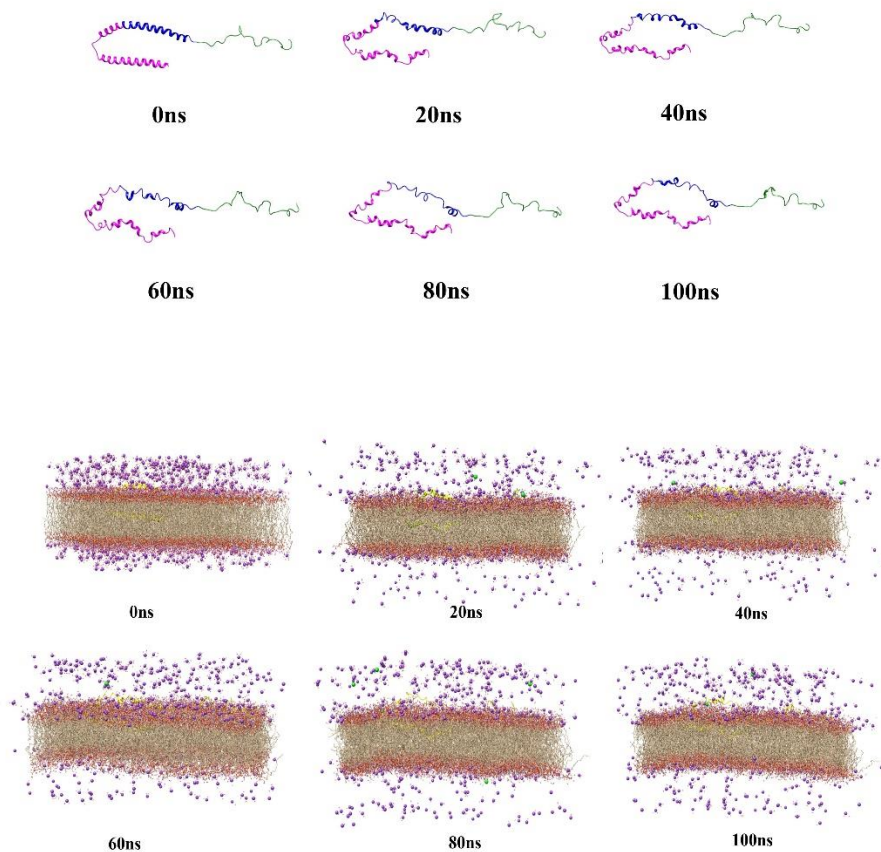
Fig. 18. Snapshots of Membrane bound A30G α- synuclein at different intervals of simulation time

1.2 Molecular Dynamic Analysis of A30P α- synuclein mutant bound to lipid membrane DOPE: DOPC: DOPS

An electron density corresponds to the probability of the electrons being present at a specific location. In this profile, it exhibits a global minimum in the middle of the bilayer (near the terminal CH3 groups of the acyl chains), two maxima corresponding to the positions of the head groups (phosphate groups) in each leaflet, and a local minimum reflecting the water layer outside the membrane. From the profile it can be inferred that the time-averaged positions of electrons (Fig 16). Area per Lipid analysis determines the degree of quality of a lipid Force field. Area per lipid analysis determines the degree of binding to other membrane properties, acyl chain ordering, compressibility, and molecular packaging. From the Area per lipid profile of mutant A30P α-synuclein, it showed an equilibrium of insertion of the protein into the lipid profile (Fig. 17.).

Snapshots of A30P mutant α-synuclein bound to lipid membrane (DOPE: DOPS: DOPC) during simulation time period of 100 ns (Fig. 22).

RMSD analysis

From the MD analysis of RMSD (root mean square deviation), DOPE:DOPS:DOPC lipid membrane bound A30P mutant showed oscillation in the range of (1-5 Å). Also, indicated higher fluctuation rates that inhibit the stability of the system. N-terminal and NAC region are stable during the simulation as compared to C terminal region as shown in Fig. 18.(a).

RMSF Analysis

The RMSF (root mean square fluctuation) plots demonstrate flexibility of individual residues during simulation period of 100ns. The observed RMSF values of A30P mutant in Fig. 18. (b) showed that residue fluctuations were less (1.25–4 Å) during simulation time period of 100 ns.

Helical bend Analysis

Helical bending can determine two factors i.e. the equiliberated fluctuations that causes the binding and shaping of the helices to a rigid membrane bilayer and the characterization of perturbed regions caused due to mutation as a result that disrupts the normal interactions. The helical region was calculated for each residue at the angle between the helices formed in between 67th, 68th and 69th position and the results are shown in **Fig. 19.** The A30P mutant showed changes in bending angle with respect to a time series of 100ns. A maximum bending of was observed in A30P mutant as shown in Fig. 22.

Inter-molecular Hydrogen bond Analysis

Hydrogen bond refers to the stability of the protein-membrane complex. The average inter-molecular H-bond between the A30P mutant and lipid membrane was estimated. The interaction between lipid membrane as acceptor/donor and A30P mutant as receptor/donor was showed in **Fig.**

20. The number of inter-molecular hydrogen bonds are higher in membrane layer (acceptor) and A30P mutant (donor).

Secondary Structure Analysis

The secondary structural analysis of mutant A30P is calculated by Kabsch and Sander Algorithm using DSSP software. In the case of the A30P mutant (Table 3), however, the α-helical propensity was further decreased to be 14.3% when compared to wild type α-synuclein to be 20.7% .The combined analysis showed that the A30P mutation decreased locally resulting in decreased α-helical propensity. The α-helical conformations were evident in case of A30P mutant chain. Turns and Coil conformation increases during simulation suggests decreased binding affinity to the membrane. In A30P mutant, membrane curvature was observed during MD simulation of 100ns due to changes in binding mechanism of A30P caused by decreasing α-helical content on the contrary wild type showed no events of membrane curvature.
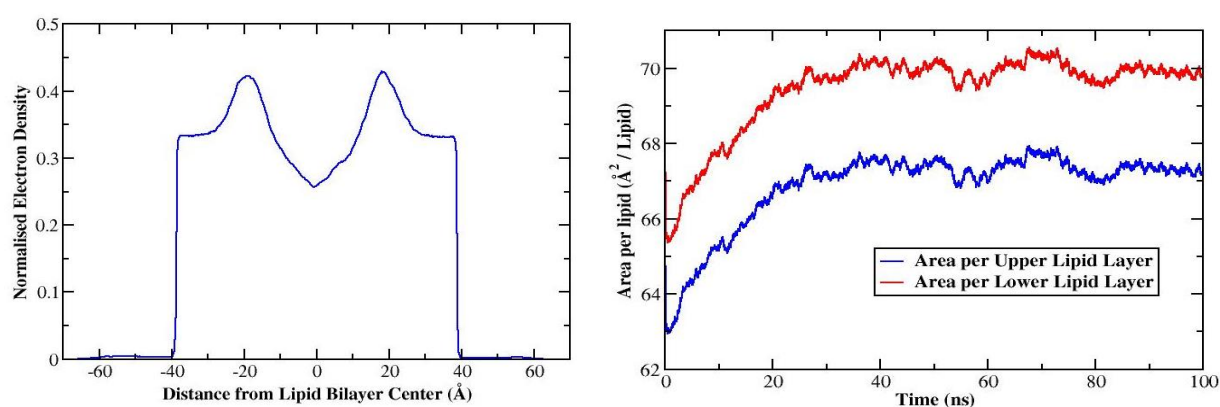
Fig. 19. a). Electron Density profile Analysis b). Area per Lipid Layer Analysis of membrane bound A30P mutant during a simulation time period of 100ns
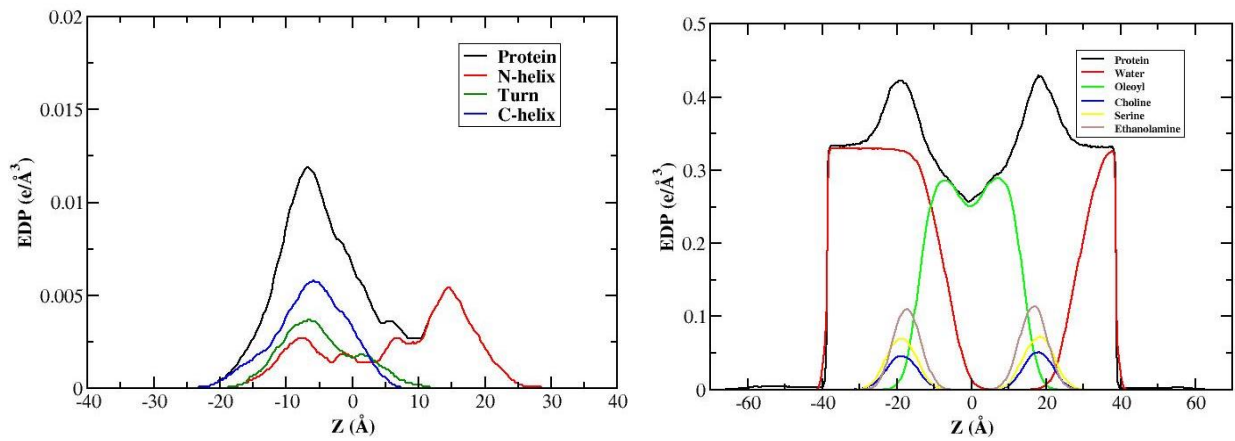
Fig. 20. a). Electron density profile of N helix, Turn and C helix of α-syn **b).** Electron density profile of different lipid profile of α-synuclein
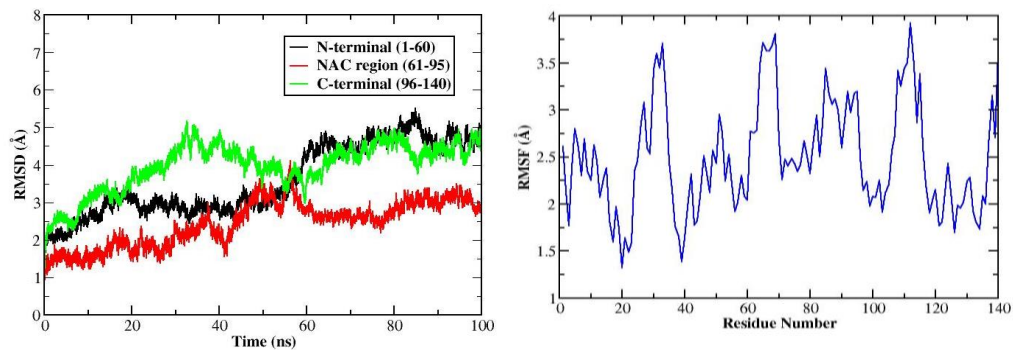
Fig. 21. a) Root Mean Square Deviation Analysis of membrane bound A30P mutant α- synuclein during simulation period.

b) Root Mean Square Fluctuation Analysis A30P mutant α-synuclein during simulation period of 100ns.
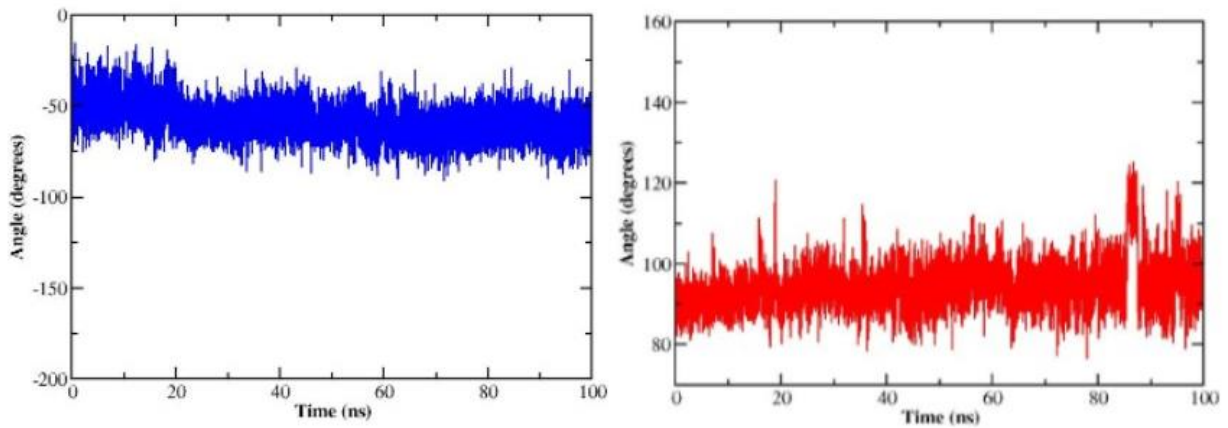
Fig. 22. a). Helical bending at position Glycine 68. The color scheme is as follows: A30P in lipid-bound state (blue) b). The conformations of each residues of the mutant chain in its bound state that demonstrate unfolding leading to unbinding at residue 26 of the A30P mutant chain.
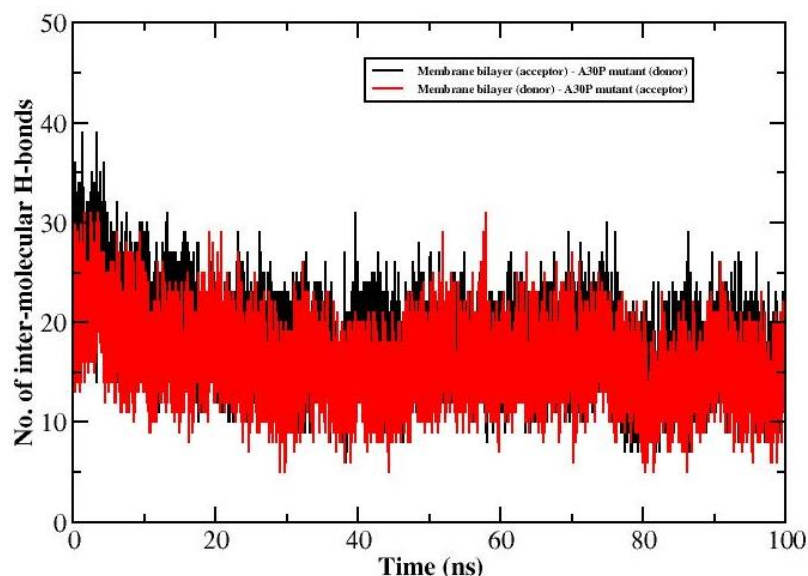
Fig. 23. The number of intermolecular hydrogen bonds between A30P α-synuclein in lipid bound state during MD simulation of 100 ns

No. of Frames
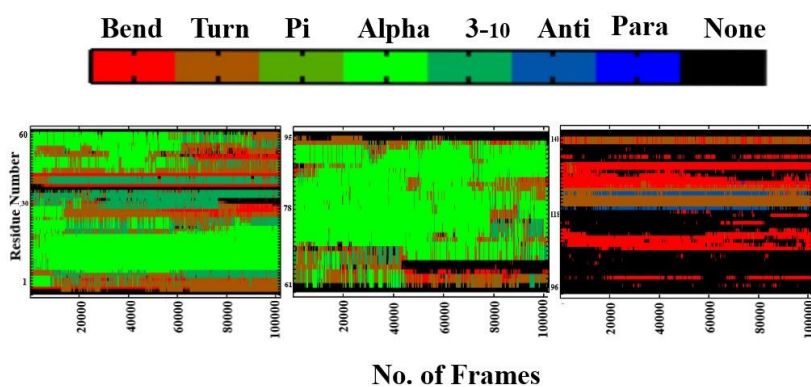
Fig. 24. Secondary structural analysis of membrane bound A30P mutant is calculated by Kabsch and Sander Algorithm using dssp software The color index depicts different conformational changes of each residue of A30P mutant α-synuclein during simulation period of 100ns

Table 8: Secondary Structural Analysis of A30P mutant during the simulation time period of 100 ns using YASARA software

A30P mutant	Turn	Sheet	Pi	Alpha	3-10	Coil
Percentage (%)	30	0	0	14.3	1.4	54.3
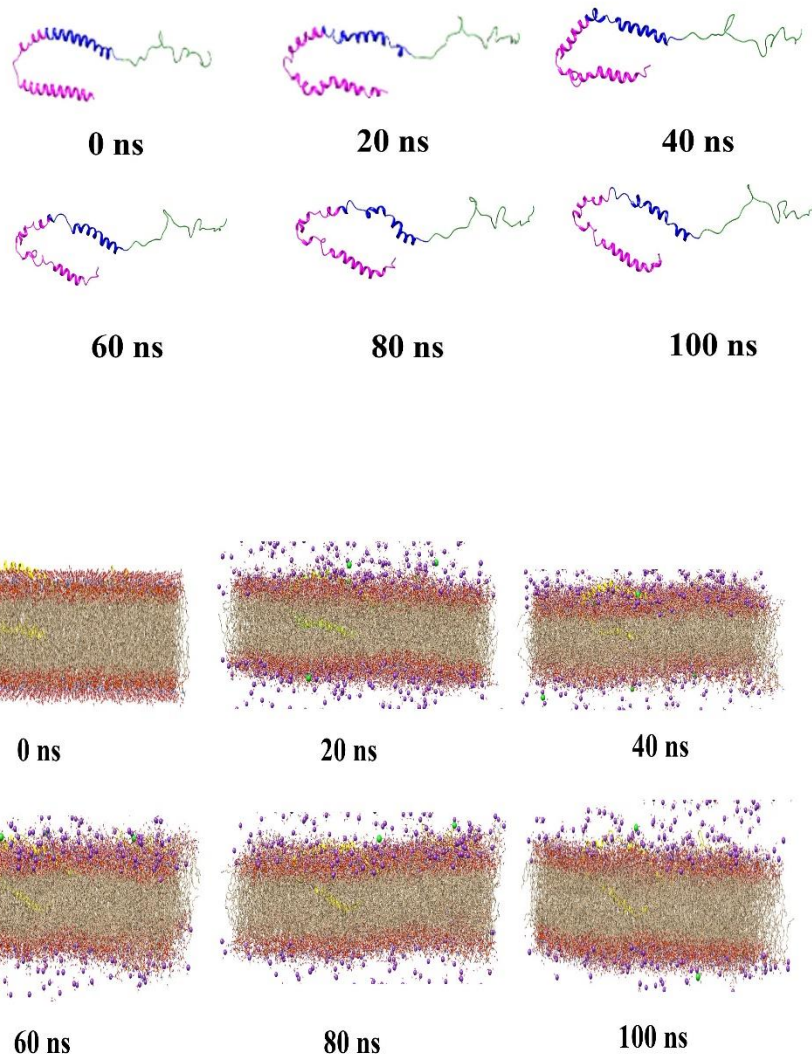
Fig. 25. Snapshots of Membrane bound A30P α- synuclein at different intervals of simulation time

1.3 Molecular Dynamic Analysis of A53E α- synuclein mutant bound to lipid membrane DOPE: DOPC: DOPS

An electron density corresponds to the probability of the electrons being present at a specific location. In this profile, it exhibits a global minimum in the middle of the bilayer (near the terminal CH3 groups of the acyl chains), two maxima corresponding to the positions of the head groups (phosphate groups) in each leaflet, and a local minimum reflecting the water layer outside the membrane. From the profile it can be inferred that the time-averaged positions of electrons (**Fig 23. a) and 24**. Area per Lipid analysis determines the degree of quality of a lipid Force field. Area

per lipid analysis determines the degree of binding to other membrane properties, acyl chain ordering, compressibility, and molecular packaging. From the Area per lipid profile of mutant A53E α-synuclein and wild type α-synuclein, it showed an equilibrium of insertion of the protein into the lipid profile as shown in **Fig. 23.(b)**. Snapshots of A53E mutant α-synuclein bound to lipid membrane (DOPE: DOPS: DOPC) during simulation time period of 100ns as shown in **Fig. 29.**

RMSD analysis

From the MD analysis of RMSD (root mean square deviation), DOPE:DOPS:DOPC lipid membrane bound A53E mutant showed higher oscillation (1-6 Å) **Fig. 25. a)**. Also, indicated higher fluctuation rates in C terminal that inhibit the stability of the system. N- helix and helix 2 region showed lower fluctuation rate indicating stability of the system.

RMSF Analysis

The RMSF (root mean square fluctuation) plots demonstrate flexibility of individual residues during simulation period of 100 ns is shown in **Fig. 25. b)**. The observed RMSF plot showed that residue 40-60 and 78-90 exhibited higher fluctuations.

Helical bend Analysis

Helical bending can determine two factors i.e. the equilibrated fluctuations that causes the binding and shaping of the helices to a rigid membrane bilayer and the characterization of perturbed regions caused due to mutation as a result that disrupts the normal interactions. The helical region was calculated for each residue at the angle between the helices formed in between 67th, 68th and 69th position and the results are shown in **Fig. 26**. The A53E mutant showed changes in bending angle with respect to a time series of 100 ns. A maximum bending of was observed in A53E mutant.

Inter-molecular Hydrogen bond Analysis

Hydrogen bond refers to the stability of the protein-membrane complex. The average inter-molecular H-bond between the A53E mutant and lipid membrane was estimated. The interaction between lipid membrane as acceptor/donor and A53E as receptor/donor was observed in **Fig**. **27**. The number of inter-molecular hydrogen bonds are higher in membrane bilayer as acceptor and A30G mutant as receptor.

Secondary Structure Analysis

The secondary structural analysis of mutant A53E is calculated by Kabsch and Sander Algorithm using DSSP software as shown in **Fig. 28**. In the case of the A53E mutant (**Table 4**), however, the α-helical propensity was further decreased to be 14.5% when compared to wild type α-synuclein to be 20.7%. The combined analysis showed that the A53E mutation decreased locally resulting in decreased α-helical propensity. From the analysis, the wild type showed higher α-helical peaks in contrast to Mutant A53E that assumed decreased α-helical peaks.The α-helical conformations were evident in of α-helical peaks were observed to be reduced in the A53E mutant chain. This increase in turns and coil content in A53E suggests increased binding to the membrane and inhibits the formation α-helical content, but not necessarily inhibit the interaction with lipid membrane. In A53E mutant, membrane curvature was observed during MD simulation of 100ns due to changes in binding mechanism of A53E caused by decreasing α-helical content in **Fig. 28**.
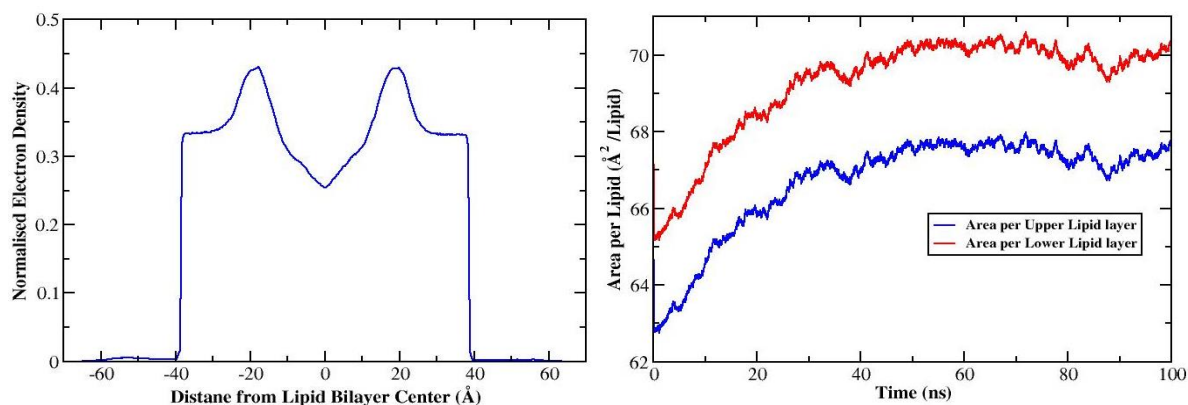
Fig. 26. a). Electron Density profile Analysis b). Area per Lipid Layer Analysis of membrane bound A53E mutant during a simulation time period of 100ns
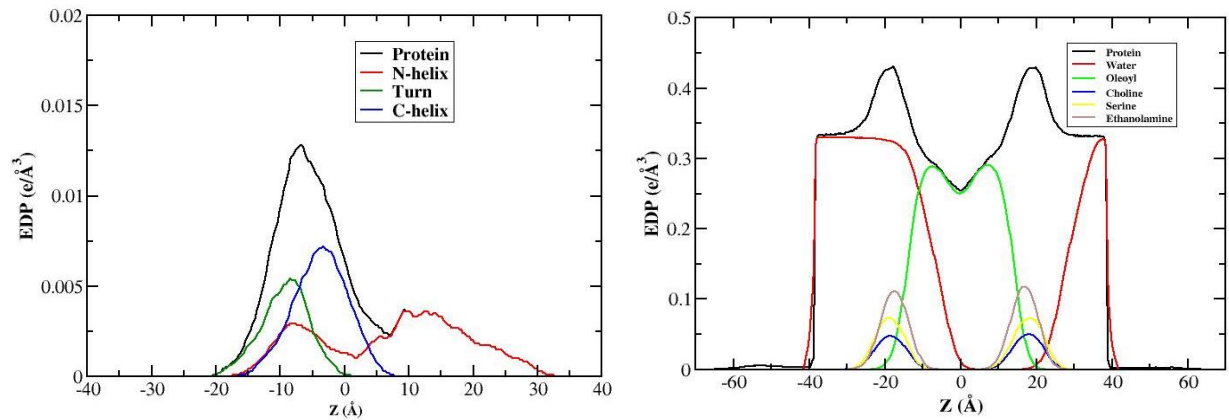
Fig. 27. a). Electron density profile of N helix, Turn and C helix of α-syn **b).** Electron density profile of different lipid profile of α-synuclein
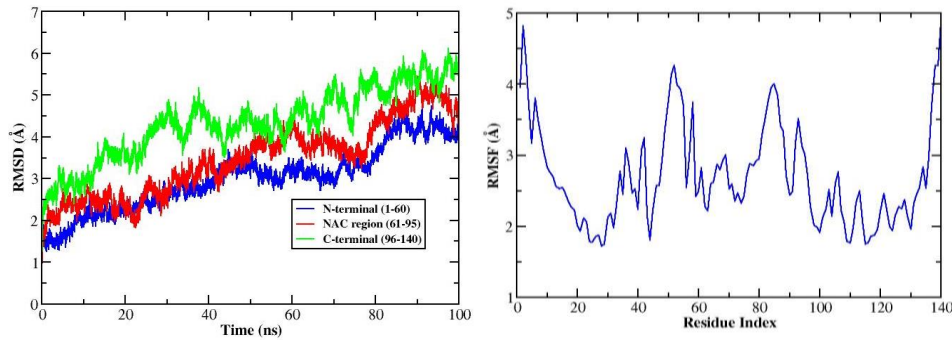
Fig. 28. a) Root Mean Square Deviation Analysis of membrane bound A53E mutant α- synuclein during simulation period.b) Root Mean Square Fluctuation Analysis A53E mutant α-synuclein during simulation period of 100ns
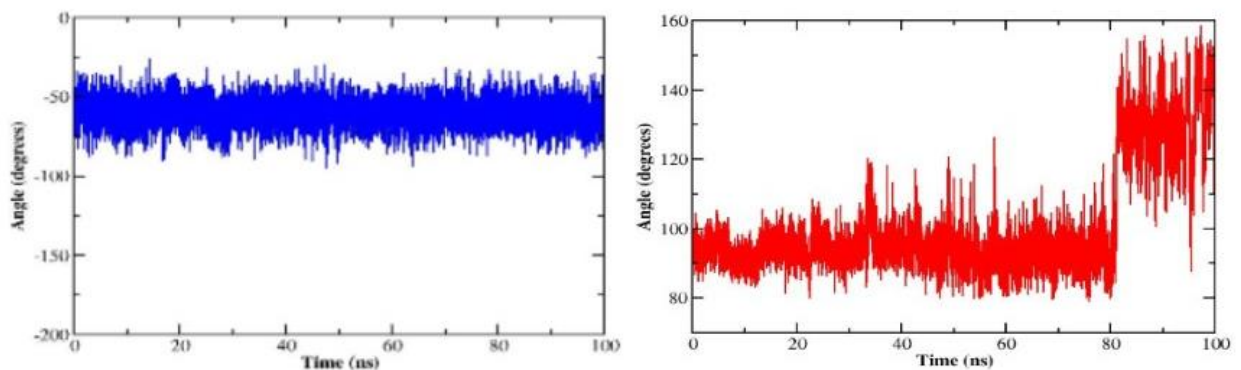
Fig. 29. a). Helical bending at position Glycine 68. The color scheme is as follows: A53E in lipid-bound state (blue) b). The conformations of each residues of the mutant chain in its bound state that demonstrate unfolding leading to unbinding at residue 26 of the A53E mutant chain.
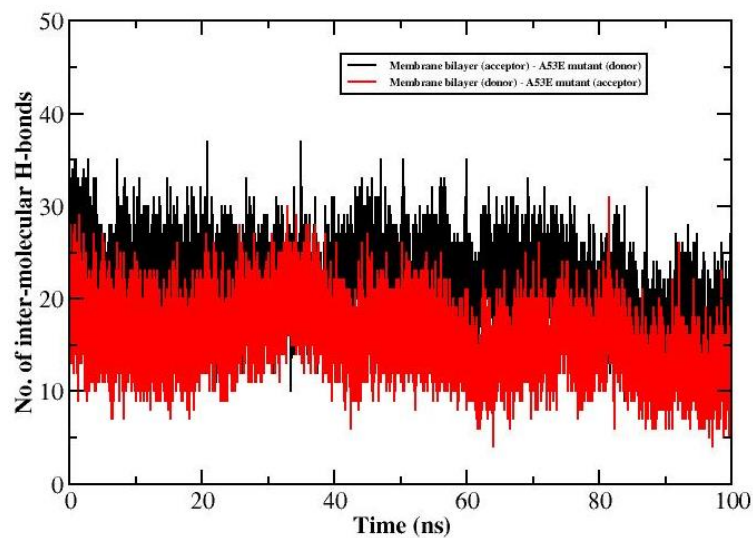
Fig. 30. The number of intermolecular hydrogen bonds between A53E α-synuclein in lipid bound state during MD simulation of 100 ns
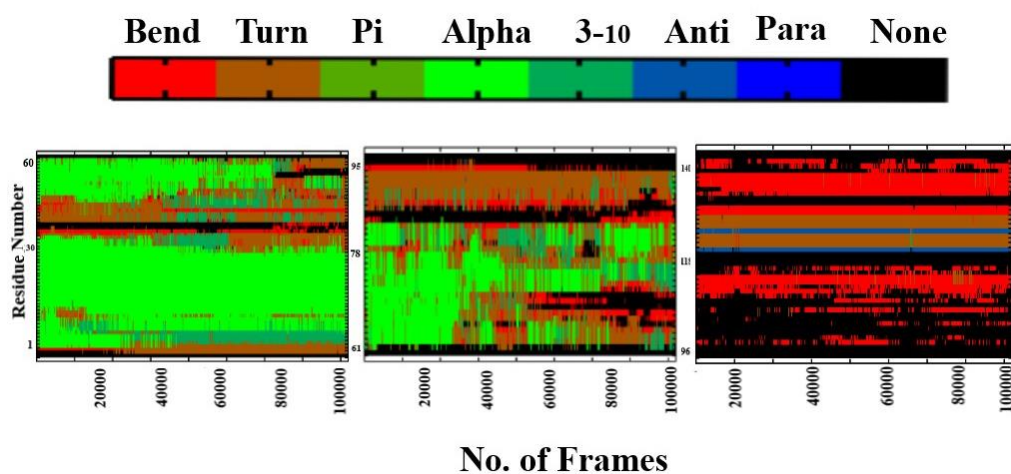
Fig. 31. Secondary structural analysis of membrane bound A53E mutant is calculated by Kabsch and Sander Algorithm using dssp software. The color index depicts different conformational changes of each residue of A53E mutant α-synuclein during simulation period of 100ns

Table 9: Secondary Structural Analysis of A53E mutant during the simulation time period of 100 ns using YASARA software

A53E mutant	Turn	Sheet	Pi	Alpha	3-10	Coil
Percentage (%)	29.5	0	0	14.5	1.9	54
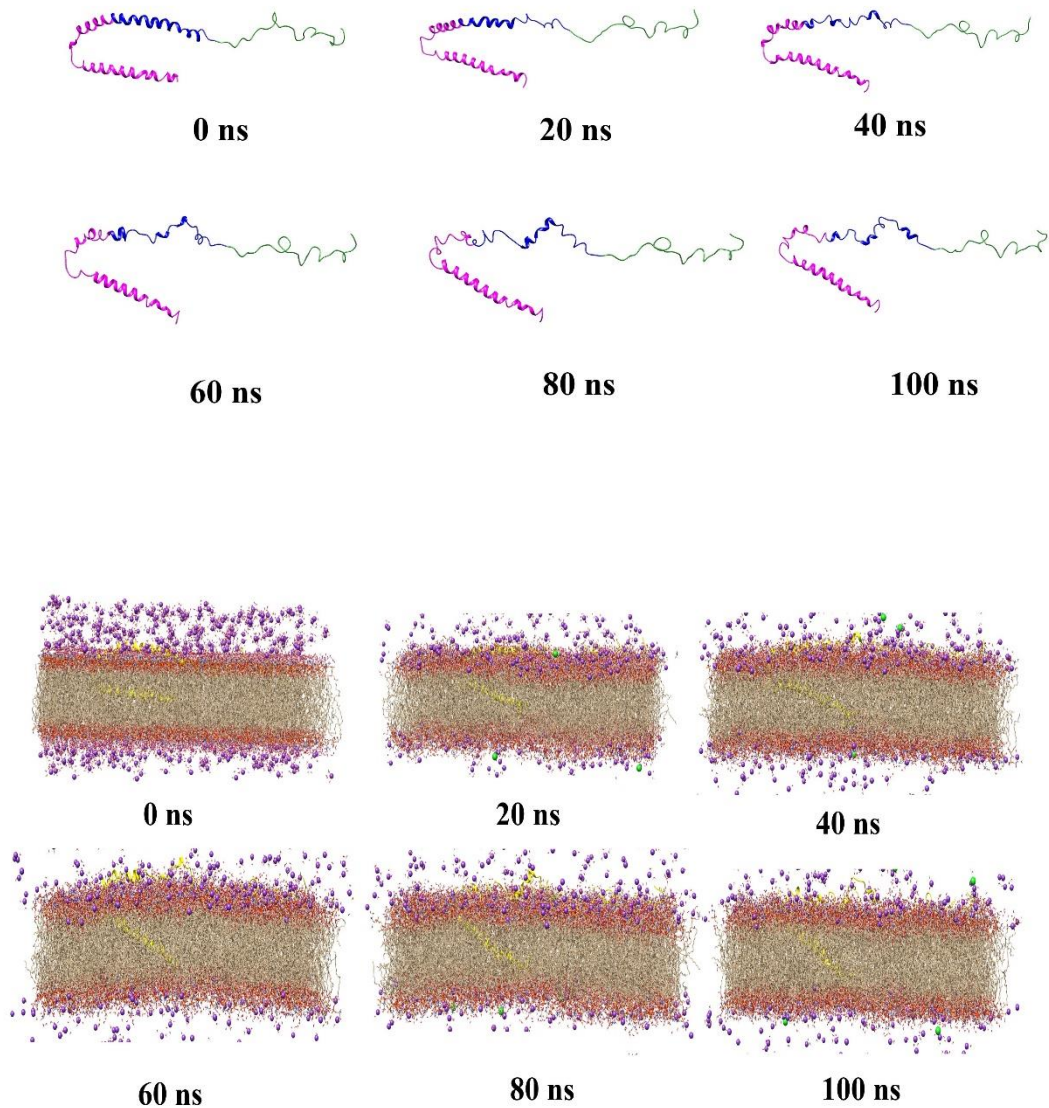
Fig. 32. Snapshots of Membrane bound A53E α- synuclein at different intervals of simulation time

1.4. Molecular Dynamic Analysis of A53T α- synuclein mutant bound to lipid membrane DOPE: DOPC: DOPS

An electron density corresponds to the probability of the electrons being present at a specific location. In this profile, it exhibits a global minimum in the middle of the bilayer (near the terminal CH3 groups of the acyl chains), two maxima corresponding to the positions of the head groups (phosphate groups) in each leaflet, and a local minimum reflecting the water layer outside the membrane. From the profile it can be inferred that the time-averaged positions of electrons (**Fig 30. a) and 31**. Area per Lipid analysis determines the degree of quality of a lipid Force field. Area per lipid analysis determines the degree of binding to other membrane properties, acyl chain

ordering, compressibility, and molecular packaging. From the Area per lipid profile of mutant A53T α-synuclein, it showed an equilibrium of insertion of the protein into the lipid profile as shown in **Fig. 30.(b)**. Snapshots of A53E mutant α-synuclein bound to lipid membrane (DOPE: DOPS: DOPC) during simulation time period of 100ns as shown in **Fig. 36.**

RMSD analysis

From the MD analysis of RMSD (root mean square deviation), DOPE:DOPS:DOPC lipid membrane bound A53T mutant showed higher oscillation (1-6.5 Å) **Fig. 32. a)**. Also, indicated higher fluctuation rates in C terminal that inhibit the stability of the system. N- helix and helix 2 region showed lower fluctuation rate indicating stability of the system. But after 60 ns of MD simulation, NAC region also fluctuated that exhibits structural flexibility.

RMSF Analysis

The RMSF (root mean square fluctuation) plots demonstrate flexibility of individual residues during simulation period of 100 ns is shown in **Fig. 32. b)**. The observed RMSF plot showed that residue 50-75 exhibited higher fluctuations that indicates the A53T mutation in αS reduces the propensity of αS to aggregate.

Helical bend Analysis

Helical bending can determine two factors i.e. the equilibrated fluctuations that causes the binding and shaping of the helices to a rigid membrane bilayer and the characterization of perturbed regions caused due to mutation as a result that disrupts the normal interactions. The helical region was calculated for each residue at the angle between the helices formed in between 67th, 68th and 69th position and the results are shown in **Fig. 33**. The A53T mutant showed changes in bending angle with respect to a time series of 100 ns. A maximum bending of was observed in A53E mutant.

Inter-molecular Hydrogen bond Analysis

Hydrogen bond refers to the stability of the protein-membrane complex. The average inter-molecular H-bond between the A53T mutant and lipid membrane was estimated. The interaction between lipid membrane as acceptor/donor and A53T as receptor/donor was observed in **Fig**. **34**. The number of inter-molecular hydrogen bonds are higher in membrane bilayer as acceptor and A53T mutant as receptor.

Secondary Structure Analysis

The secondary structural analysis of mutant A53T is calculated by Kabsch and Sander Algorithm using DSSP software as shown in **Fig. 35**. In the case of the A53T mutant (**Table 6**), however, the α-helical propensity was further decreased to be 16.1% when compared to wild type α-synuclein to be 20.7%. The combined analysis showed that the A53T mutation decreased locally resulting in decreased α-helical propensity. From the analysis, the wild type showed higher α-helical peaks in contrast to Mutant A53T that assumed decreased α-helical peaks. The α-helical conformations were evident in of α-helical peaks were observed to be reduced in the A53T mutant chain. This increase in turns (30.7%) and coil (51.8%) content in A53T suggests increased binding to the membrane and inhibits the formation α-helical content, but not necessarily inhibit the interaction with lipid membrane. In A53T mutant, membrane curvature was observed during MD simulation of 100ns due to changes in binding mechanism of A53T caused by decreasing α-helical content in **Fig. 36**.
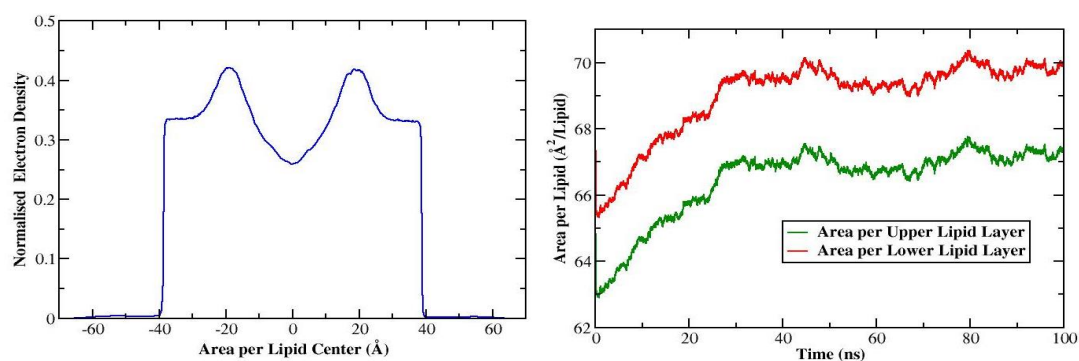
Fig. 33. a). Electron Density profile Analysis b). Area per Lipid Layer Analysis of membrane bound A53T mutant during a simulation time period of 100ns
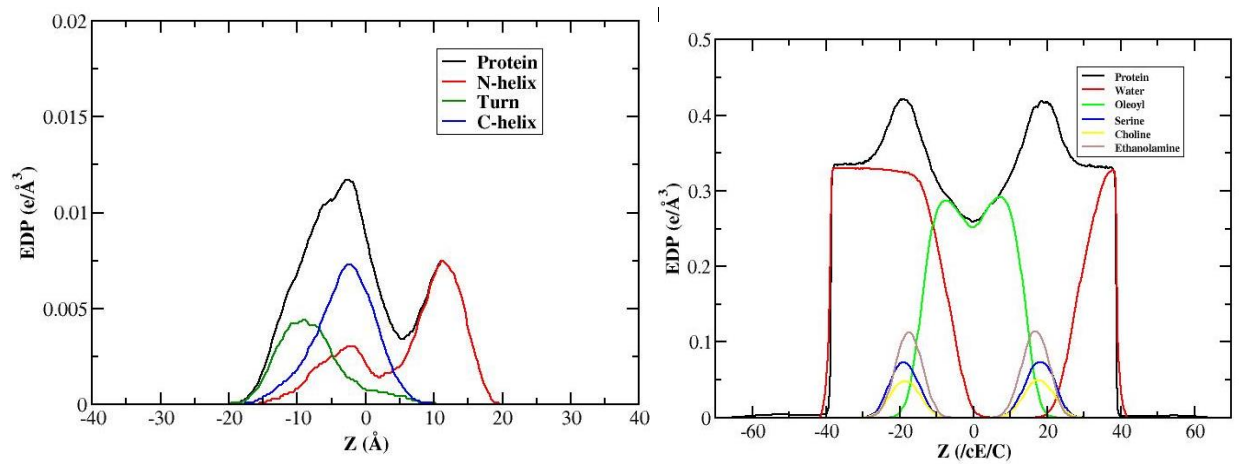
Fig. 34. a). Electron density profile of N helix, Turn and C helix of α-syn **b).** Electron density profile of different lipid profile of α-synuclein
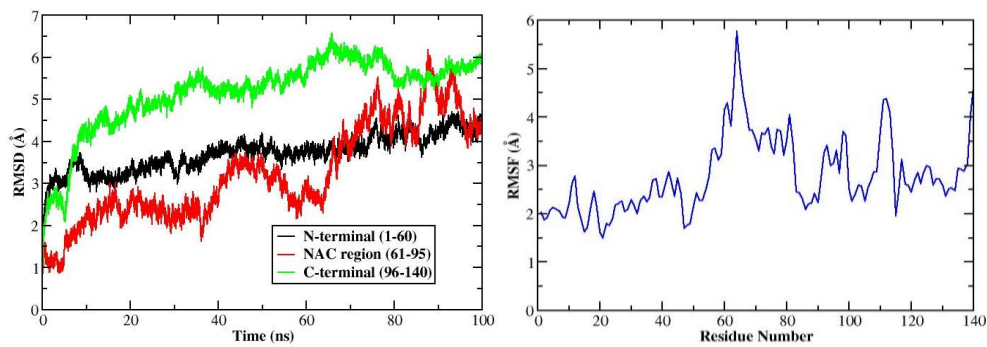
Fig. 35. a) Root Mean Square Deviation Analysis of membrane bound A53T mutant α- synuclein during simulation period. b) Root Mean Square Fluctuation Analysis A53T mutant α-synuclein during simulation period of 100ns.
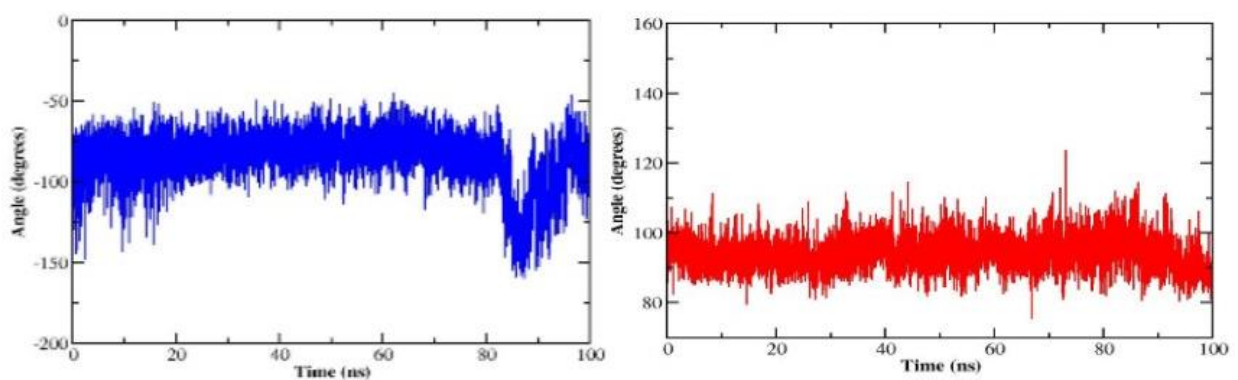
Fig. 36. a). Helical bending at position Glycine 68. The color scheme is as follows: A53T in free monomer state (red) and lipid-bound state (blue). b). The conformations of each residues of the mutant chain in its bound state that demonstrate unfolding leading to unbinding at residue 26 of the A53T mutant chain
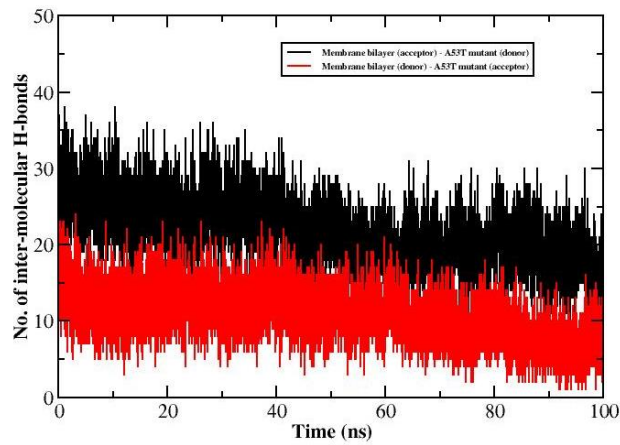
Fig. 37. The number of intermolecular hydrogen bonds between A53T α-synuclein in lipid bound state during MD simulation of 100 ns
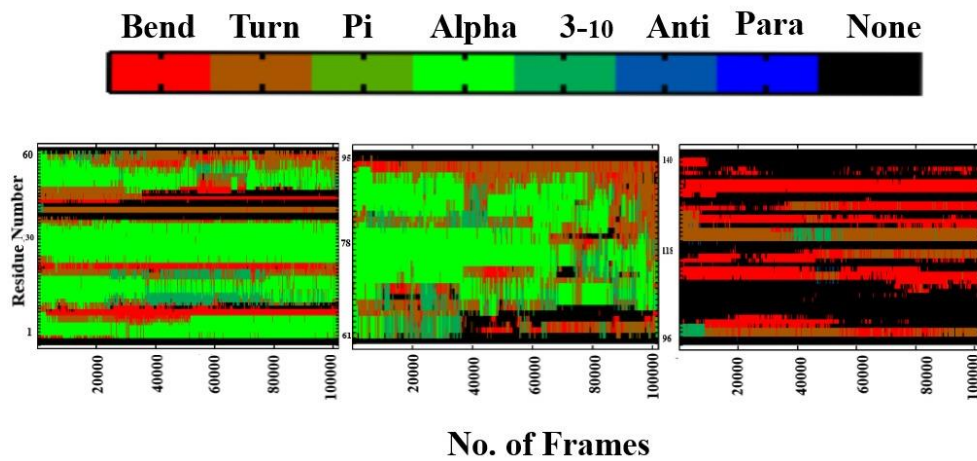
Fig. 38. Secondary structural analysis of membrane bound A53T mutant is calculated by Kabsch and Sander Algorithm using dssp software. The color index depicts different conformational changes of each residue of A30G mutant α-synuclein during simulation period of 100ns

Table 10. Secondary Structural Analysis of A53T mutant during the simulation time period of 100 ns using YASARA software

A53T mutant	Turn	Sheet	Pi	Alpha	3-10	Coil
Percentage (%)	30.7	0	0	16.1	1.4	51.8
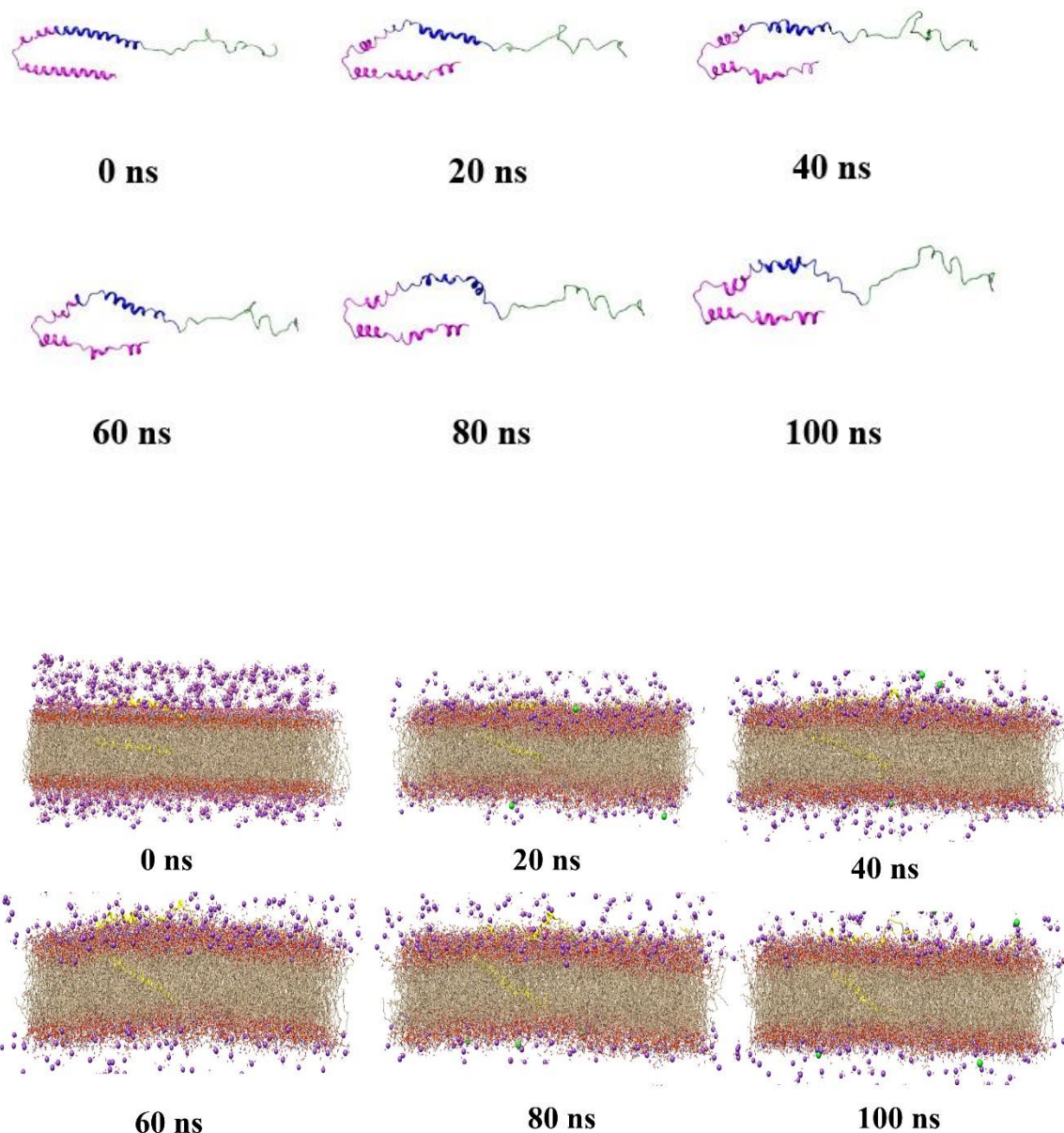
Fig. 39. Snapshots of Membrane bound A53E α- synuclein at different intervals of simulation time

1.5. Molecular Dynamic Analysis of E46K mutant bound to lipid membrane DOPE: DOPC: DOPS

An electron density corresponds to the probability of the electrons being present at a specific location. In this profile, it exhibits a global minimum in the middle of the bilayer (near the terminal CH3 groups of the acyl chains), two maxima corresponding to the positions of the head groups (phosphate groups) in each leaflet, and a local minimum reflecting the water layer outside the membrane. From the profile it can be inferred that the time-averaged positions of electrons (**Fig**

37. a) and 38. Area per Lipid analysis determines the degree of quality of a lipid Force field. Area per lipid analysis determines the degree of binding to other membrane properties, acyl chain ordering, compressibility, and molecular packaging. From the Area per lipid profile of mutant E46K α-synuclein, it showed an equilibrium of insertion of the protein into the lipid profile as shown in **Fig. 37.(b)**. Snapshots of E46K mutant α-synuclein bound to lipid membrane (DOPE: DOPS: DOPC) during simulation time period of 100ns as shown in **Fig. 43.**

RMSD analysis

From the MD analysis of RMSD (root mean square deviation), DOPE:DOPS:DOPC lipid membrane bound E46K mutant showed higher oscillation (1-5.5 Å) **Fig. 39. a)**. Also, indicated higher fluctuation rates in C terminal that inhibit the stability of the system. N-helix showed flexibility in the range (2.5-4.2Å) throughout the simulation time period. But, helix 2 region showed lower fluctuation rate indicating stability of the system.

RMSF Analysis

The RMSF (root mean square fluctuation) plots demonstrate flexibility of individual residues during simulation period of 100 ns is shown in **Fig. 39. b)**. The observed RMSF plot showed that residue 98-110 exhibited higher fluctuations that indicates the E46K mutation in αS reduces the propensity of αS to aggregate.

Helical bend Analysis

Helical bending can determine two factors i.e. the equilibrated fluctuations that causes the binding and shaping of the helices to a rigid membrane bilayer and the characterization of perturbed regions caused due to mutation as a result that disrupts the normal interactions. The helical region was calculated for each residue at the angle between the helices formed in between 67th, 68th and 69th position and the results are shown in **Fig. 40**. The E46K mutant showed changes in bending angle with respect to a time series of 100 ns.

Inter-molecular Hydrogen bond Analysis

Hydrogen bond refers to the stability of the protein-membrane complex. The average inter-molecular H-bond between the E46K mutant and lipid membrane was estimated. The interaction between lipid membrane as acceptor/donor and E46K as receptor/donor was observed in **Fig**. **41**. The number of inter-molecular hydrogen bonds are higher in membrane bilayer as acceptor and E46K mutant as receptor.

Secondary Structure Analysis

The secondary structural analysis of mutant A53E is calculated by Kabsch and Sander Algorithm using DSSP software as shown in **Fig. 42**. In the case of the A53E mutant (**Table 7**), however, the α-helical propensity was further decreased to be 19.3% when compared to wild type α-synuclein to be 20.7%. The combined analysis showed that the E46K mutation decreased locally resulting in decreased α-helical propensity. From the analysis, the wild type showed higher α-helical peaks in contrast to Mutant E46K that assumed decreased α-helical peaks. The α-helical conformations were evident in α-helical peaks. This increase in turns (28%) and coil (51%) content in E46K suggests increased binding to the membrane and inhibits the formation α-helical content, but not necessarily inhibit the interaction with lipid membrane.
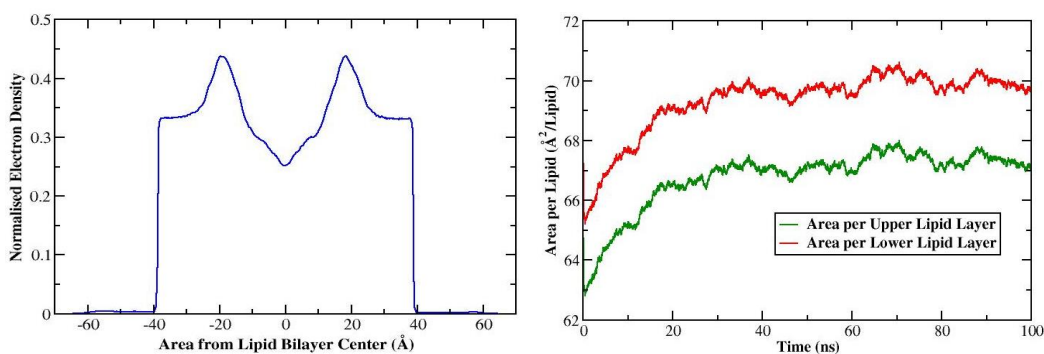
Fig. 40. a). Electron Density profile Analysis b). Area per Lipid Layer Analysis of membrane bound E46K mutant during a simulation time period of 100 ns
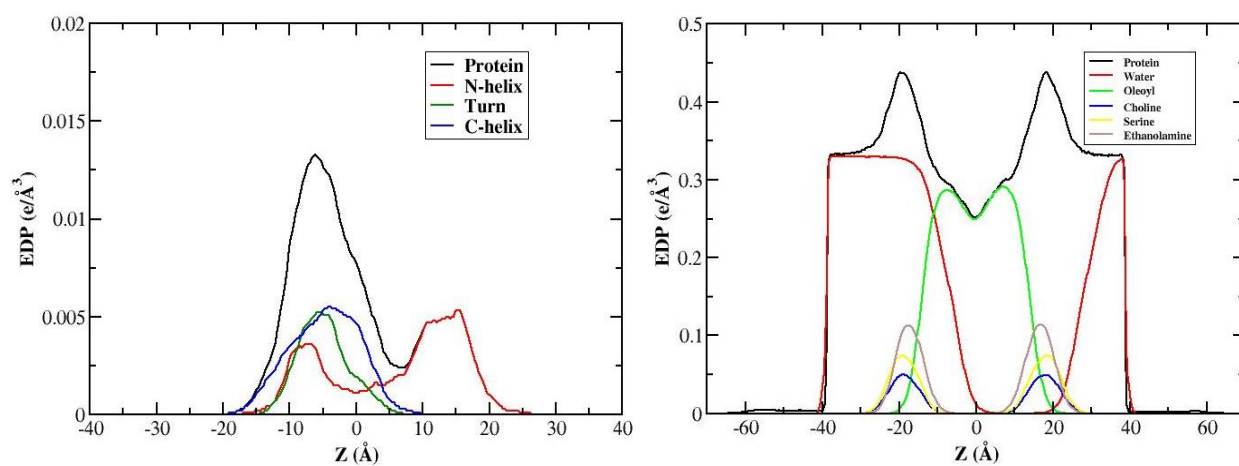
Fig. 41. a). Electron density profile of N helix, Turn and C helix of α-syn **b).** Electron density profile of different lipid profile of α-synuclein
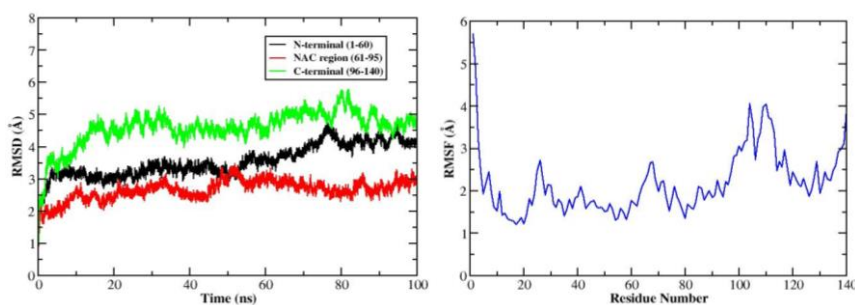
Fig. 42. Root Mean Square Deviation Analysis of membrane bound E46K mutant α- synuclein during simulation period. Root Mean Square Fluctuation Analysis E46K mutant α-synuclein during simulation period of 100ns.
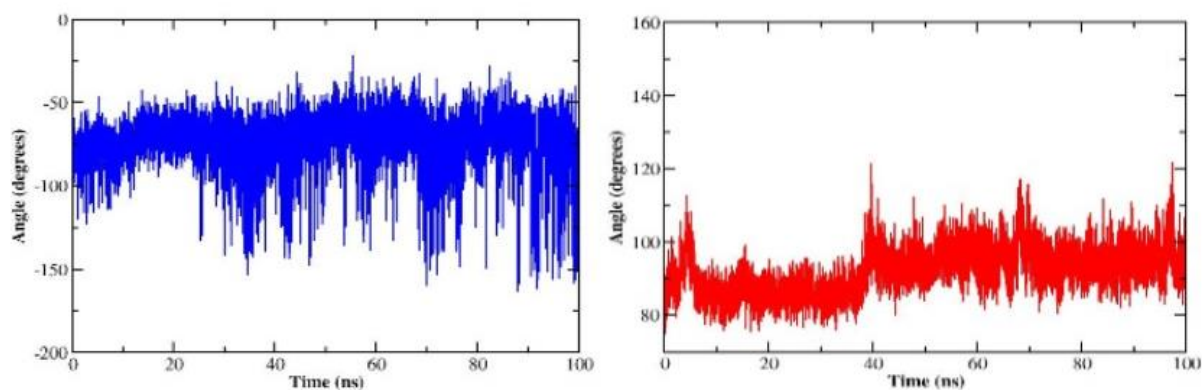
Fig. 43. Helical bending at position Glycine 68. The color scheme is as follows: E46K in free monomer state (red) and lipid-bound state (blue).The conformations of each residues of the mutant chain in its bound state that demonstrate unfolding leading to unbinding at residue 26 of the E46K mutant chain.
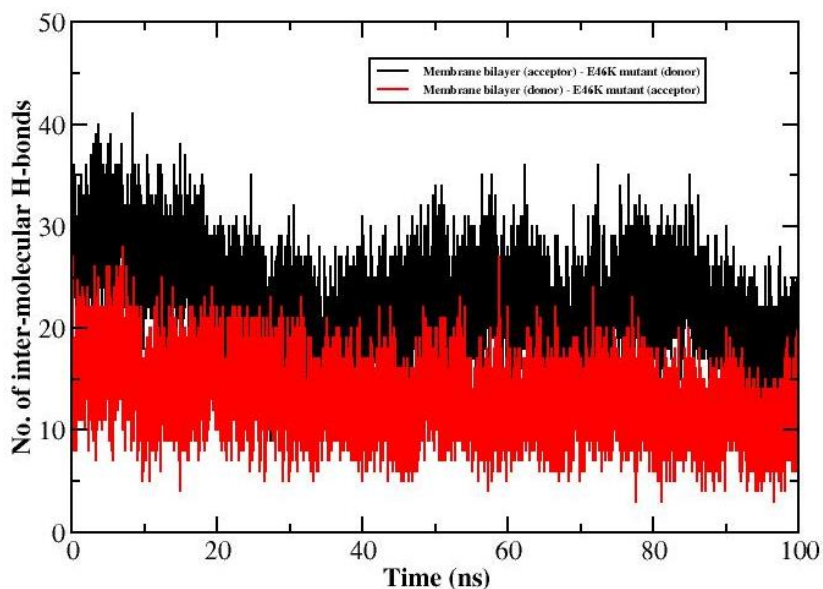
Fig. 44. The number of intermolecular hydrogen bonds between E46K α-synuclein in lipid bound state during MD simulation of 100 ns

No. of Frames
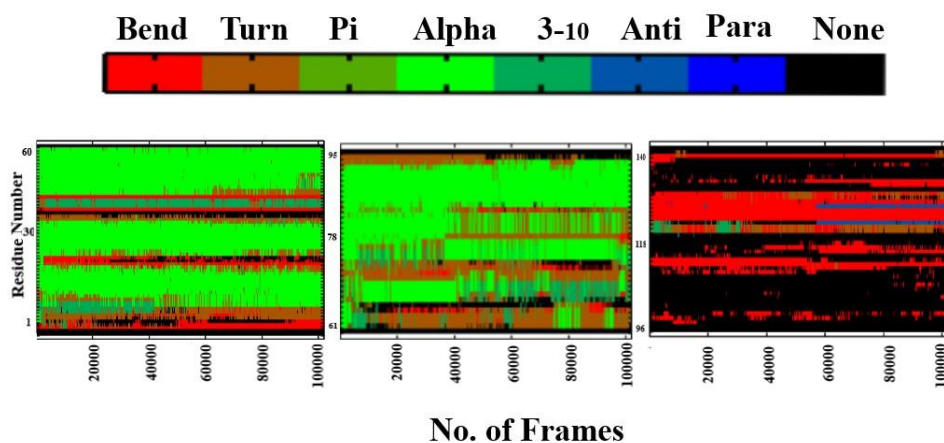
Fig. 45. Secondary structural analysis of membrane bound E46K mutant is calculated by Kabsch and Sander Algorithm using dssp software The color index depicts different conformational changes of each residue of E46K mutant α-synuclein during simulation period of 100ns

Table 11. Secondary Structural Analysis of E46K mutant during the simulation time period of 100 ns using YASARA software

E46K mutant	Turn	Sheet	Pi	Alpha	3-10	Coil
Percentage (%)	28	0	0	19.3	1.7	51

0 ns   20 ns   40 ns

60 ns   80 ns   100 ns

0 ns   20 ns   40 ns

60 ns   80 ns   100 ns
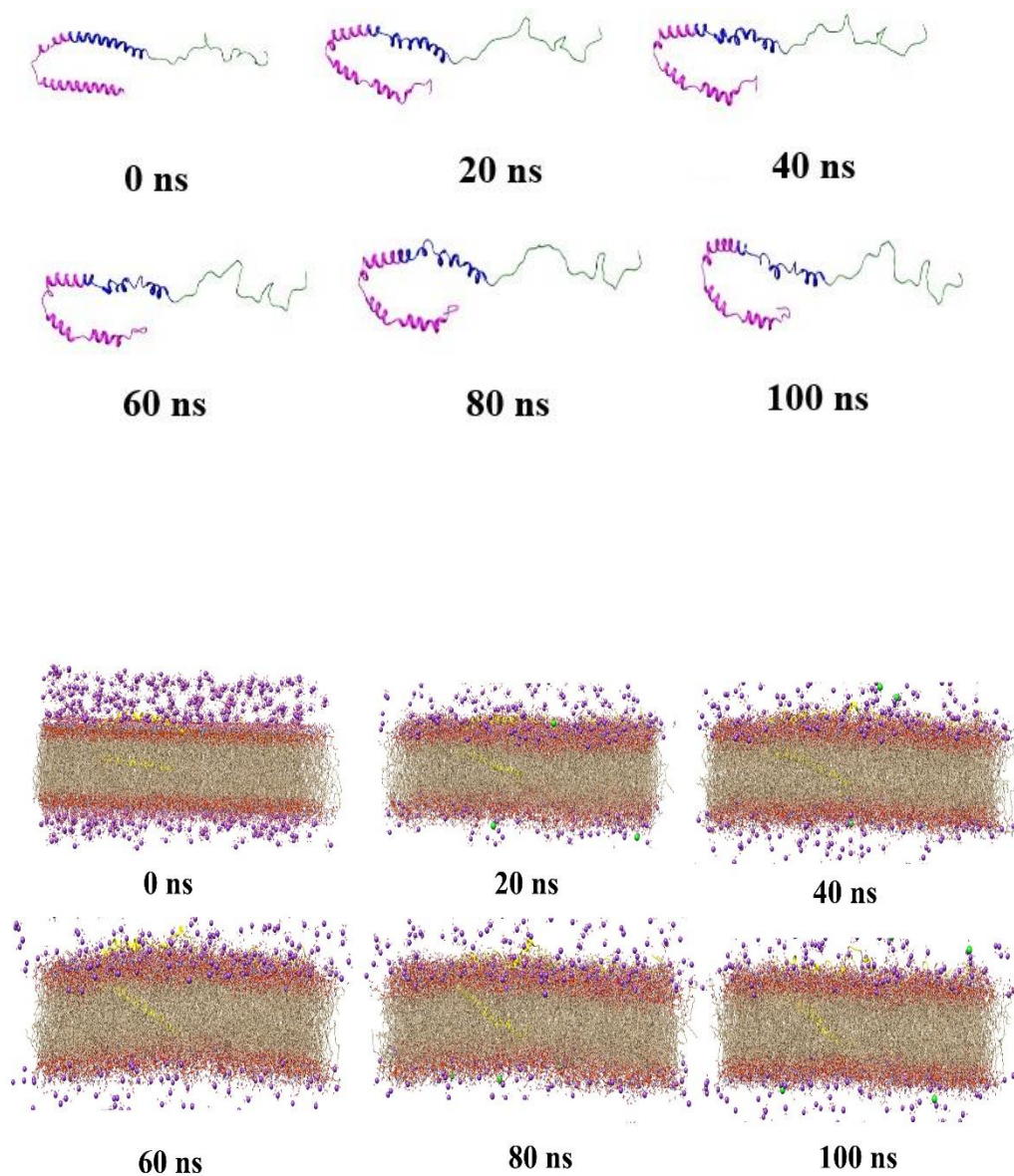
Fig. 46. Snapshots of Membrane bound E46K α- synuclein at different intervals of simulation time

1.6. Molecular Dynamic Analysis of G51D mutant bound to lipid membrane DOPE: DOPC: DOPS

An electron density corresponds to the probability of the electrons being present at a specific location. In this profile, it exhibits a global minimum in the middle of the bilayer (near the terminal CH3 groups of the acyl chains), two maxima corresponding to the positions of the head groups (phosphate groups) in each leaflet, and a local minimum reflecting the water layer outside the membrane. From the profile it can be inferred that the time-averaged positions of electrons (**Fig**

44. a) and 45. Area per Lipid analysis determines the degree of quality of a lipid Force field. Area per lipid analysis determines the degree of binding to other membrane properties, acyl chain ordering, compressibility, and molecular packaging. From the Area per lipid profile of mutant G51D α-synuclein, it showed an equilibrium of insertion of the protein into the lipid profile as shown in **Fig. 44(b)**. Snapshots of G51D mutant α-synuclein bound to lipid membrane (DOPE: DOPS: DOPC) during simulation time period of 100ns as shown in **Fig. 50.**

RMSD analysis

From the MD analysis of RMSD (root mean square deviation), DOPE:DOPS:DOPC lipid membrane bound E46K mutant showed higher oscillation (1-6 Å) **Fig. 45. a)**. Also, indicated higher fluctuation rates in NAC region and C terminal that inhibit the stability of the system. After 50 ns simulation, N-helix showed flexibility in the range (3-6Å) throughout the simulation time period.

RMSF Analysis

The RMSF (root mean square fluctuation) plots demonstrate flexibility of individual residues during simulation period of 100 ns is shown in **Fig. 45. b)**. The observed RMSF plot showed that residue 60-78 exhibited higher fluctuations that indicates the G51D mutation in αS reduces the propensity of αS to aggregate.

Helical bend Analysis

Helical bending can determine two factors i.e. the equilibrated fluctuations that causes the binding and shaping of the helices to a rigid membrane bilayer and the characterization of perturbed regions caused due to mutation as a result that disrupts the normal interactions. The helical region was calculated for each residue at the angle between the helices formed in between 67th, 68th and 69th position and the results are shown in **Fig. 46**. The G51D mutant showed changes in bending angle with respect to a time series of 100 ns.

Inter-molecular Hydrogen bond Analysis

Hydrogen bond refers to the stability of the protein-membrane complex. The average inter-molecular H-bond between the G51D mutant and lipid membrane was estimated. The interaction between lipid membrane as acceptor/donor and E46K as receptor/donor was observed in **Fig**. **47**. The number of inter-molecular hydrogen bonds are higher in membrane bilayer as acceptor and G51D mutant as receptor.

Secondary Structure Analysis

The secondary structural analysis of mutant A53E is calculated by Kabsch and Sander Algorithm using DSSP software as shown in **Fig. 48**. In the case of the A53E mutant (**Table 8**), however, the α-helical propensity was further decreased to be 20.1% when compared to wild type α-synuclein to be 20.7%. The combined analysis showed that the G51D mutation decreased locally resulting in decreased α-helical propensity. From the analysis, the wild type and G51D showed similar α-helical content. The α-helical conformations were evident in α-helical peaks. This increase in turns (25.4%) and coil (52%) content in G51D suggests reduced formation α-helical content, but not necessarily inhibit the interaction with lipid membrane.
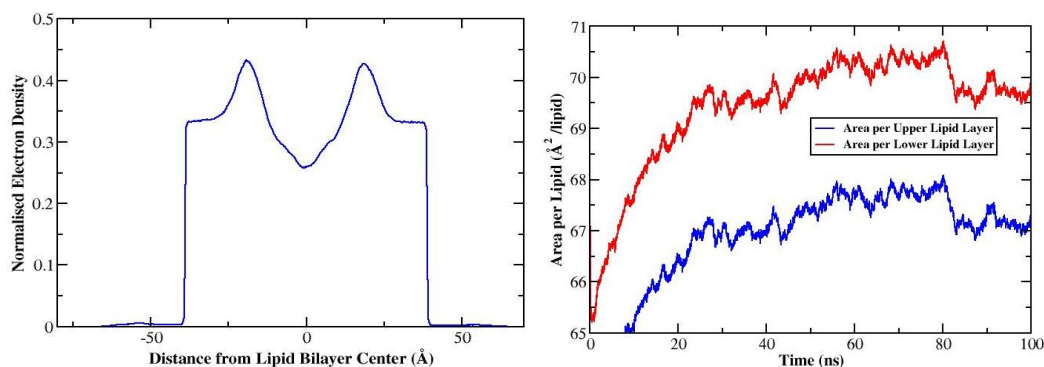
Fig. 47. a). Electron Density profile Analysis b). Area per Lipid Layer Analysis of membrane bound G51D mutant during a simulation time period of 100 ns
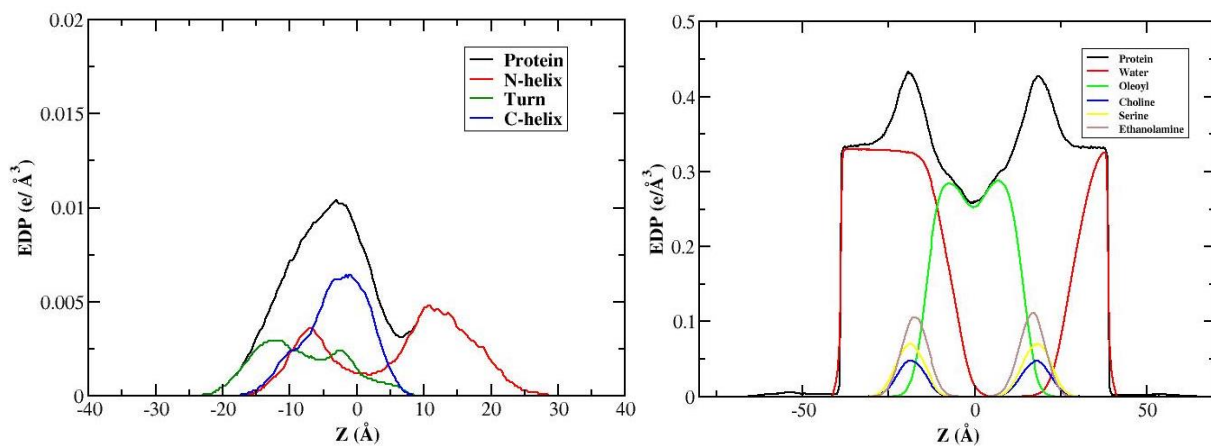
Fig. 48. a). Electron density profile of N helix, Turn and C helix of α-syn **b).** Electron density profile of different lipid profile of α-synuclein
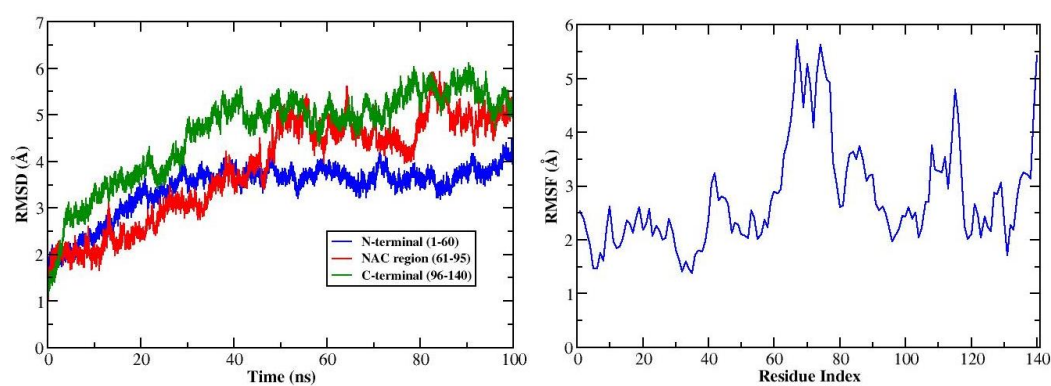
Fig. 49. Root Mean Square Deviation Analysis of membrane bound G51D mutant α- synuclein during simulation period. Root Mean Square Fluctuation Analysis G51D mutant α-synuclein during simulation period of 100 ns.
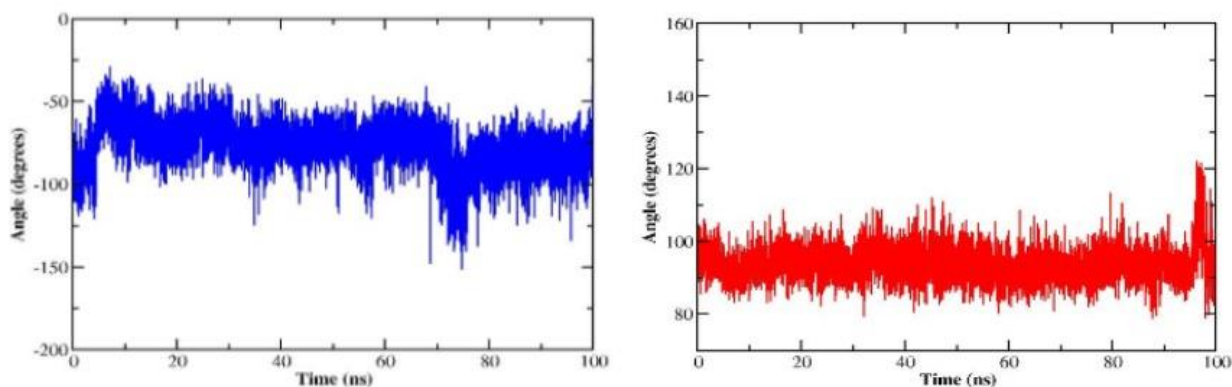
Fig. 50. Helical bending at position Glycine 68. The color scheme is as follows: G51D in lipid-bound state (blue).The conformations of each residues of the mutant chain in its bound state that demonstrate unfolding leading to unbinding at residue 26 of the G51D mutant chain.
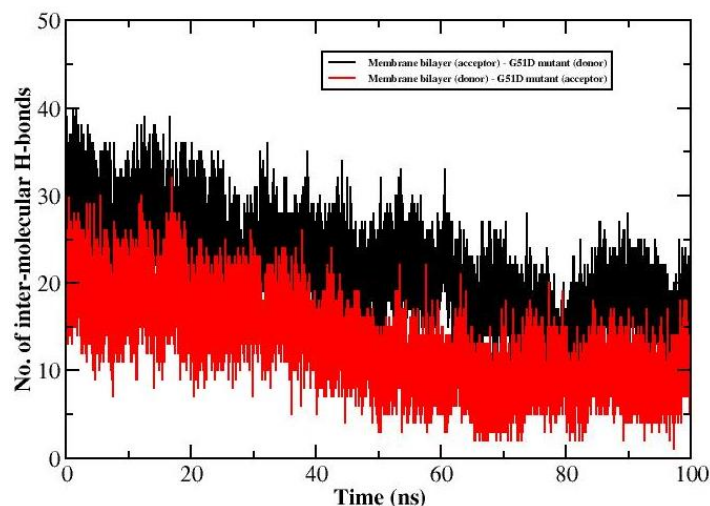
Fig. 51. The number of intermolecular hydrogen bonds between G51D α-synuclein in lipid bound state during MD simulation of 100 ns

No. of Frames
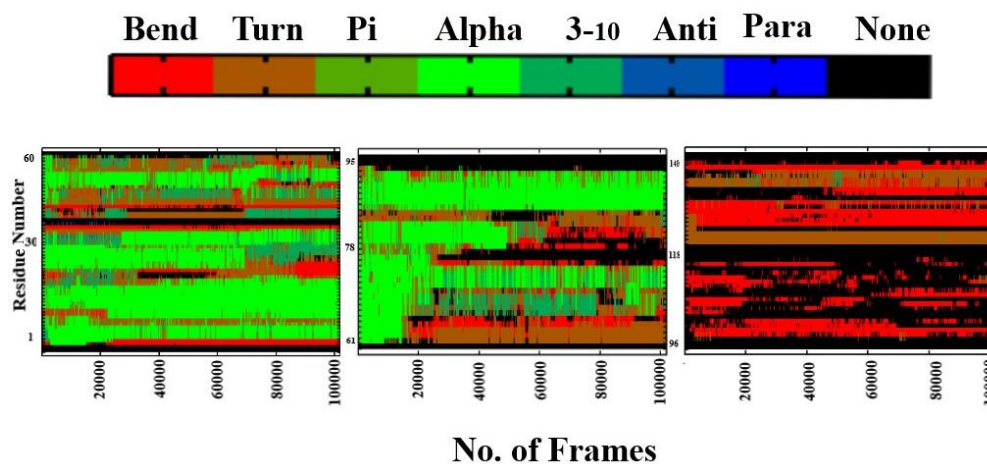
Fig. 52. Secondary structural analysis of membrane bound G51D mutant is calculated by Kabsch and Sander Algorithm using dssp software The color index depicts different conformational changes of each residue of G51D mutant α-synuclein during simulation period of 100 ns

Table 12. Secondary Structural Analysis of G51D mutant during the simulation time period of 100 ns using YASARA software

G51D mutant	Turn	Sheet	Pi	Alpha	3-10	Coil
Percentage (%)	25.4	0	0	20.1	2.5	52
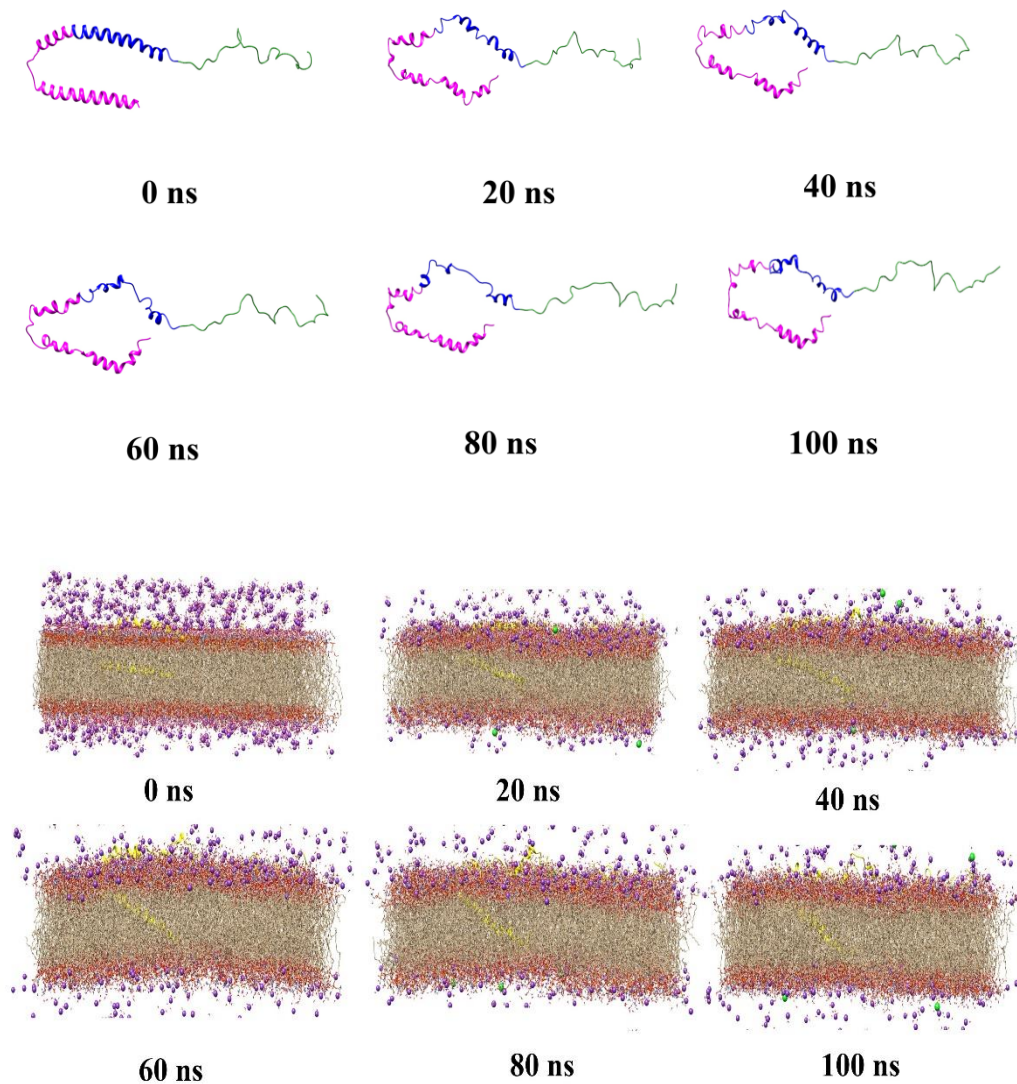
Fig. 53. Snapshots of Membrane bound G51D α- synuclein at different intervals of simulation time

1.7. Molecular Dynamic Analysis of H50Q mutant bound to lipid membrane DOPE: DOPC: DOPS

An electron density corresponds to the probability of the electrons being present at a specific location. In this profile, it exhibits a global minimum in the middle of the bilayer (near the terminal CH3 groups of the acyl chains), two maxima corresponding to the positions of the head groups (phosphate groups) in each leaflet, and a local minimum reflecting the water layer outside the membrane. From the profile it can be inferred that the time-averaged positions of electrons (**Fig 51. a) and 52**. Area per Lipid analysis determines the degree of quality of a lipid Force field. Area

per lipid analysis determines the degree of binding to other membrane properties, acyl chain ordering, compressibility, and molecular packaging. From the Area per lipid profile of mutant H50Q α-synuclein, it showed an equilibrium of insertion of the protein into the lipid profile as shown in **Fig. 51(b)**. Snapshots of H50Q mutant α-synuclein bound to lipid membrane (DOPE: DOPS: DOPC) during simulation time period of 100ns as shown in **Fig. 57.**

RMSD analysis

From the MD analysis of RMSD (root mean square deviation), DOPE:DOPS:DOPC lipid membrane bound H50Q mutant showed higher oscillation (1-7 Å) **Fig. 53. a)**. Also, indicated higher fluctuation rates in NAC region and C terminal that inhibit the stability of the system. After 60 ns simulation, N-helix showed flexibility in the range (3-4.2Å) throughout the simulation time period.

RMSF Analysis

The RMSF (root mean square fluctuation) plots demonstrate flexibility of individual residues during simulation period of 100 ns is shown in **Fig. 53. b)**. The observed RMSF plot showed that residue 60-70 exhibited higher fluctuations that indicates the H50Q mutation in αS reduces the propensity of αS to aggregate.

Helical bend Analysis

Helical bending can determine two factors i.e. the equilibrated fluctuations that causes the binding and shaping of the helices to a rigid membrane bilayer and the characterization of perturbed regions caused due to mutation as a result that disrupts the normal interactions. The helical region was calculated for each residue at the angle between the helices formed in between 67th, 68th and 69th position and the results are shown in **Fig. 54**. The H50Q mutant showed changes in bending angle with respect to a time series of 100 ns.

Inter-molecular Hydrogen bond Analysis

Hydrogen bond refers to the stability of the protein-membrane complex. The average inter-molecular H-bond between the H50Q mutant and lipid membrane was estimated. The interaction between lipid membrane as acceptor/donor and H50Q as receptor/donor was observed in **Fig**. **55**. The number of inter-molecular hydrogen bonds are higher in membrane bilayer as acceptor and H50Q mutant as receptor.

Secondary Structure Analysis

The secondary structural analysis of mutant H50Q is calculated by Kabsch and Sander Algorithm using DSSP software as shown in **Fig. 56**. In the case of the A53E mutant (**Table 9**), however, the α-helical propensity was further increased to be 21.1% when compared to wild type α-synuclein to be 20.7%. The combined analysis showed that the G51D mutation increased locally resulting in increased α-helical propensity. From the analysis, the wild type and G51D showed similar α-helical content. The α-helical conformations were evident in α-helical peaks. This increase in turns (24.9%) and coil (51.4%) content in G51D suggests reduced formation α-helical content, but not necessarily inhibit the interaction with lipid membrane.
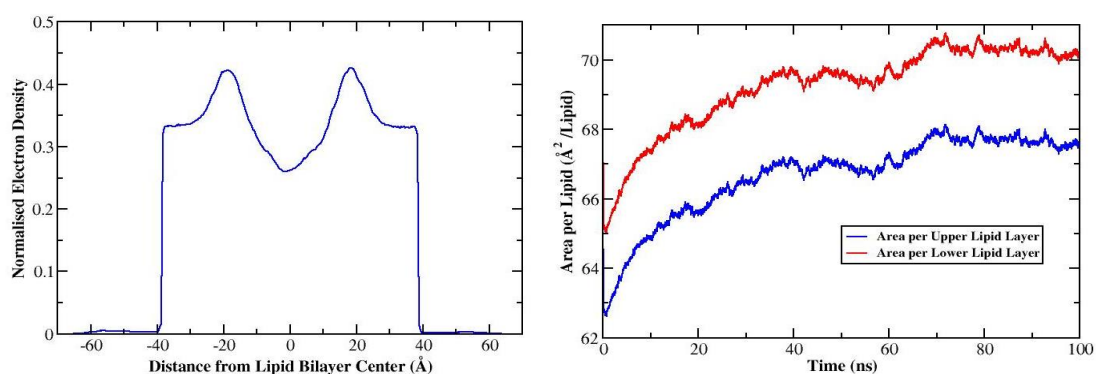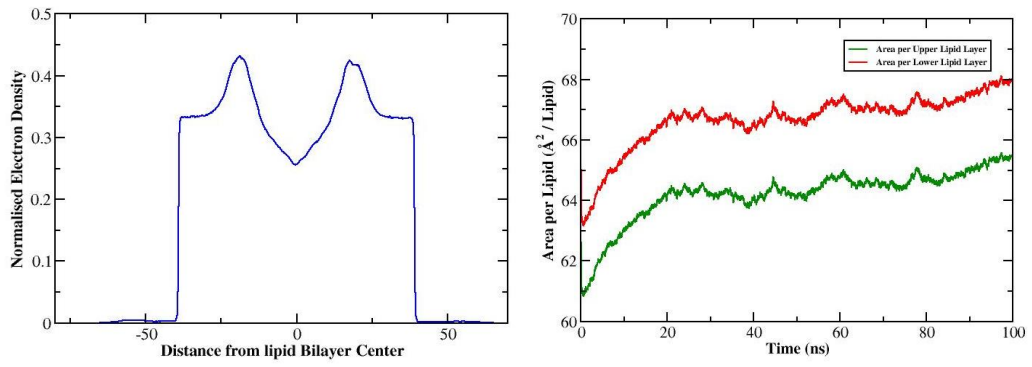

Fig. 54. a). Electron Density profile Analysis (b). Area per Lipid Layer Analysis of membrane bound H50Q mutant during a simulation time period of 100 ns
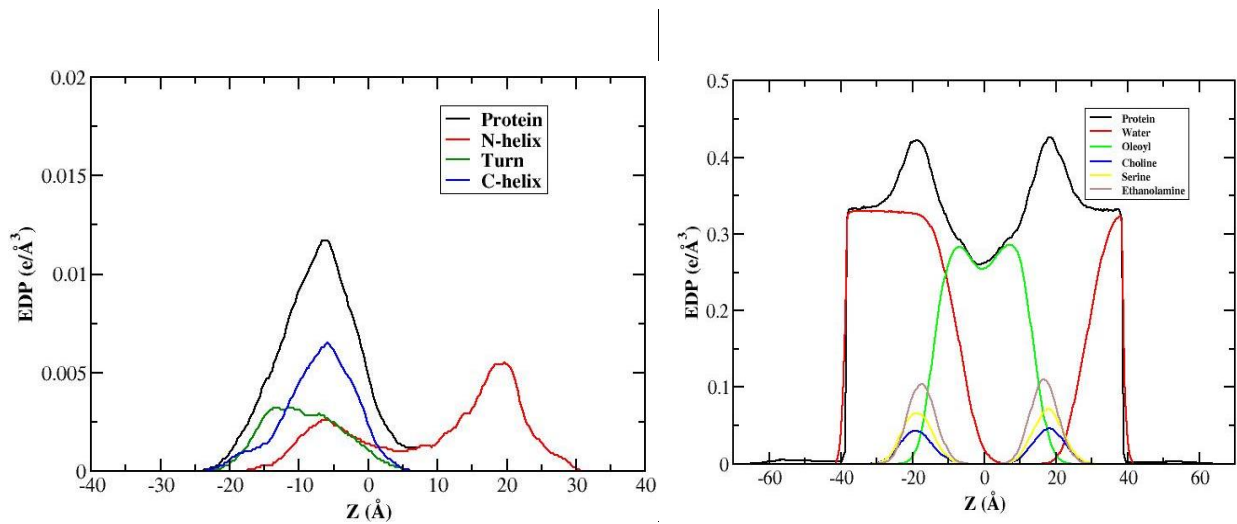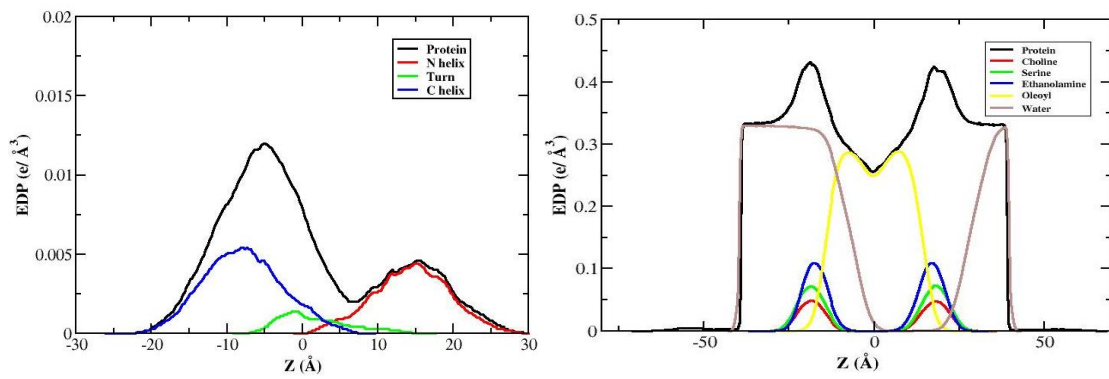
Fig. 55. a). Electron density profile of N helix, Turn and C helix of α-syn **b).** Electron density profile of different lipid profile of H50Q α-synuclein
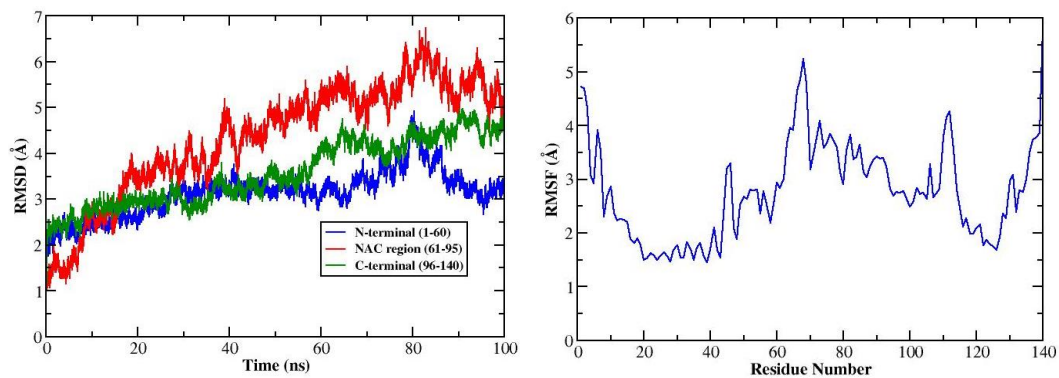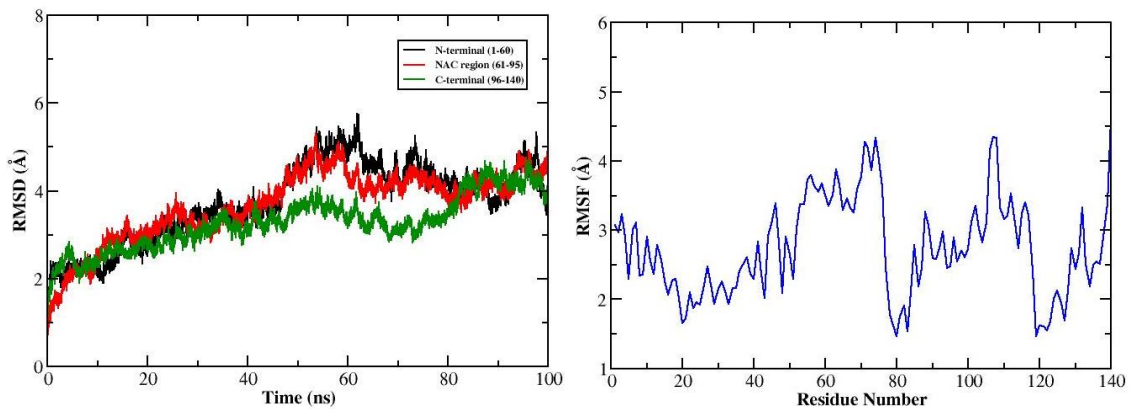

Fig. 56. Root Mean Square Deviation Analysis of membrane bound H50Q mutant α- synuclein during simulation period. Root Mean Square Fluctuation Analysis H50Q mutant α-synuclein during simulation period of 100ns.
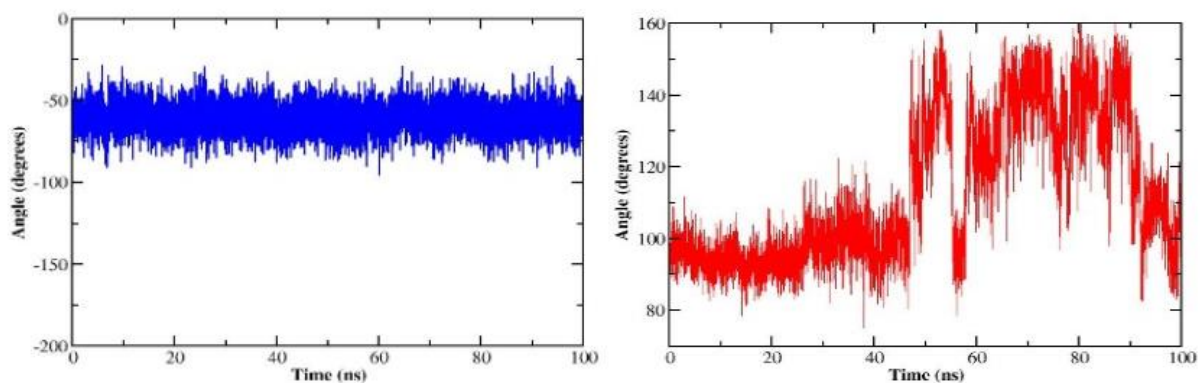
Fig. 57. Helical bending at position Glycine 68. The color scheme is as follows: H50Q in lipid-bound state.The conformations of each residues of the mutant chain in its bound state that demonstrate unfolding leading to unbinding at residue 26 of the H50Q mutant chain.
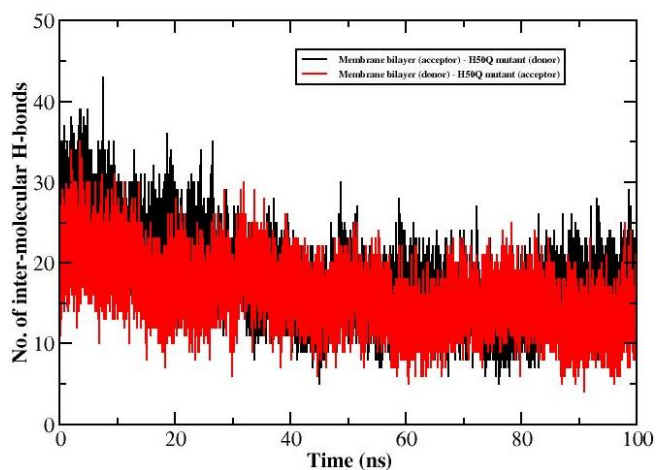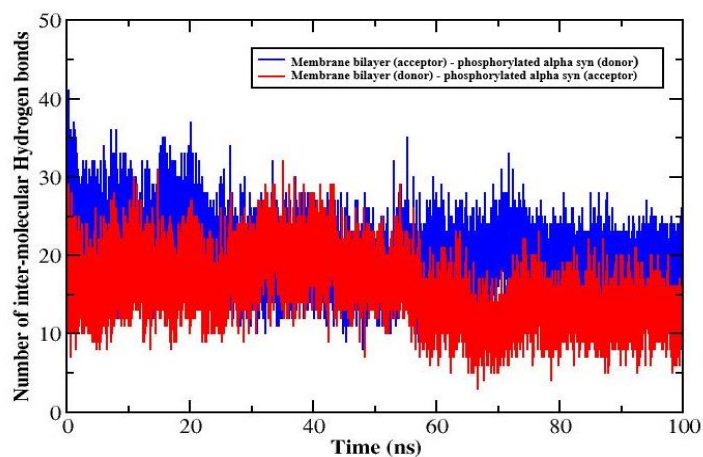
Fig. 58. The number of intermolecular hydrogen bonds between H50Q α-synuclein in lipid bound state during MD simulation of 100 ns

No. of Frames
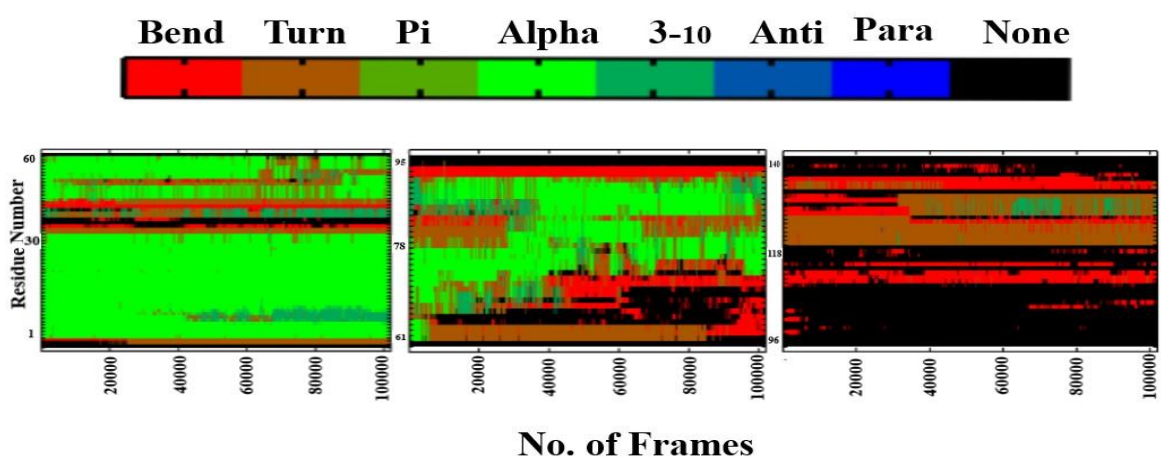
Fig. 59. Secondary structural analysis of membrane bound H50Q mutant is calculated by Kabsch and Sander Algorithm using dssp software The color index depicts different conformational changes of each residue of A30G mutant α-synuclein during simulation period of 100ns

Table 12: Secondary Structural Analysis of H50Q mutant during the simulation time period of 100 ns using YASARA software

H50Q mutant	Turn	Sheet	Pi	Alpha	3-10	Coil
Percentage (%)	24.9	0	0	21.1	2.5	51.4

0 ns   **20 ns**   **40 ns**

60 ns   **80 ns**   **100 ns**

0 ns   **20 ns**   **40 ns**

60 ns   **80 ns**   **100 ns**
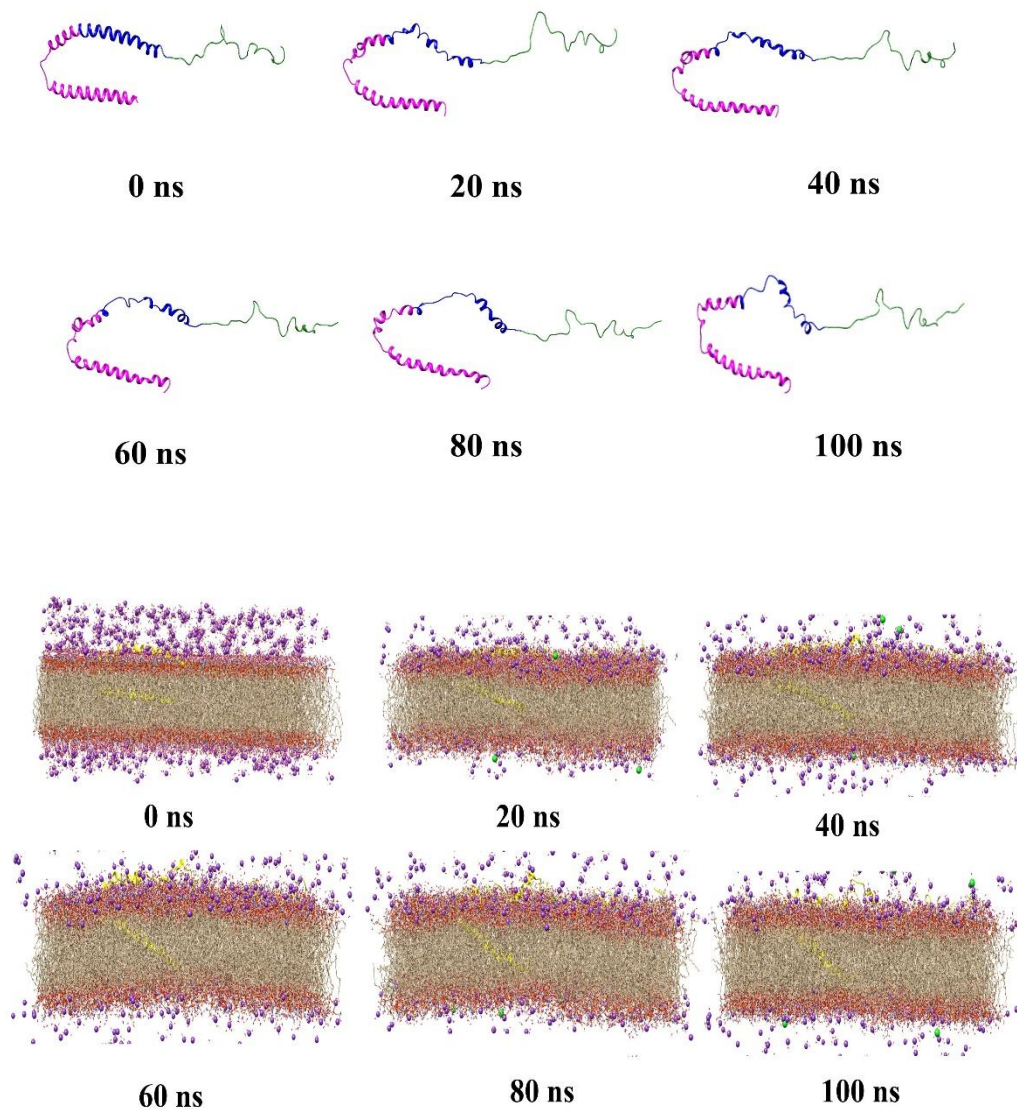
Fig. 60. Snapshots of Membrane bound G51D α- synuclein at different intervals of simulation time

Objective 3: To develop therapeutic strategies that disrupts the α-synuclein protein-lipid interactions

1. <u>Effect of post-translational modification on lipid membrane bound α-synuclein</u>
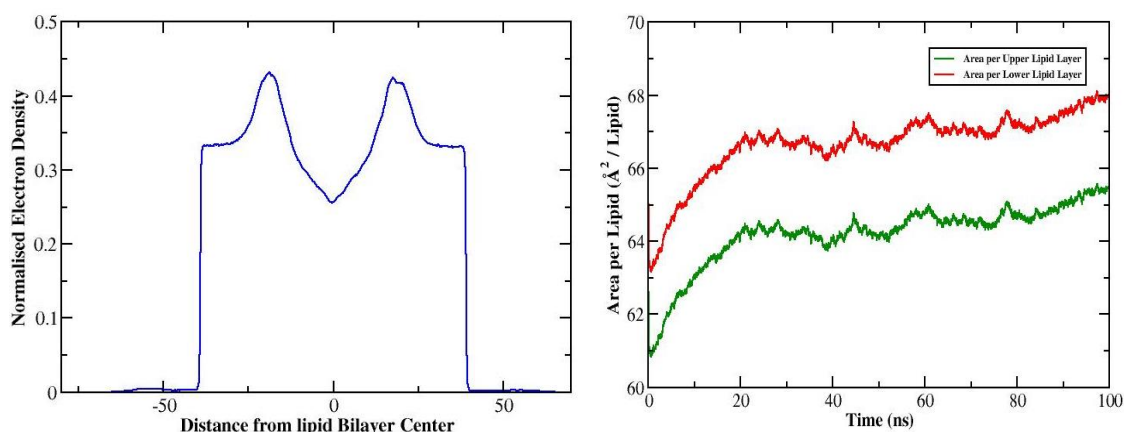
1.1 Phosphorylation of p39Y on lipid bound α-synuclein

Fig. 61. a). Electron Density profile Analysis (b). Area per Lipid Layer Analysis of membrane bound pY39 during a simulation time period of 100ns
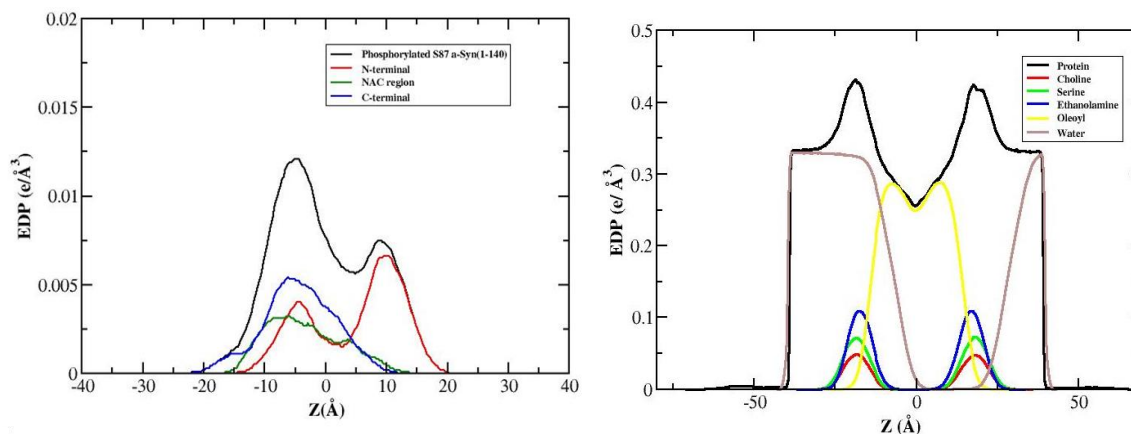

Fig. 62. a). Electron density profile of N helix, Turn and C helix of α-syn **b).** Electron density profile of different lipid profile of pY39 α-synuclein

Fig. 63: Root Mean Square Deviation Analysis of membrane bound pY39 α- synuclein during simulation period. Root Mean Square Fluctuation Analysis pY39 α- synuclein α-synuclein during simulation period of 100ns.

Fig. 64. a) The number of intermolecular hydrogen bonds between b pY39 α- synuclein in lipid bound state during MD simulation of 100ns
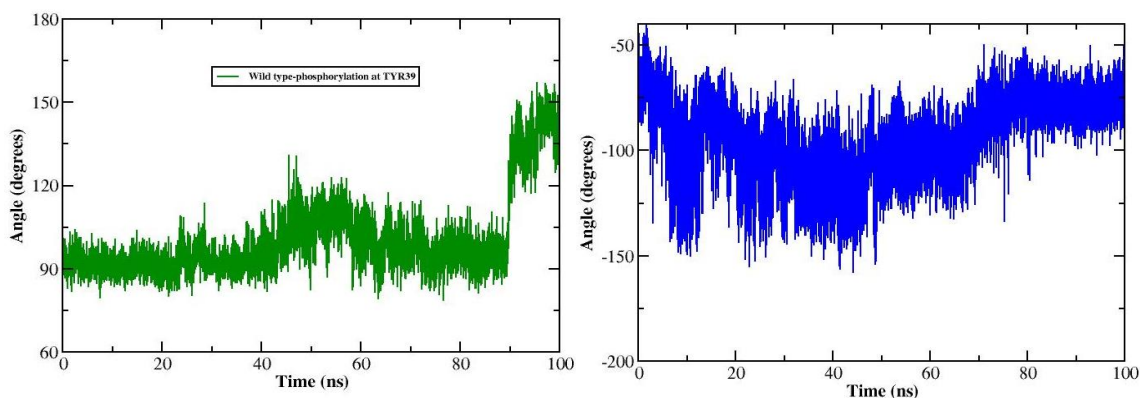
Fig. 65. Helical bending at position Glycine 68. The color scheme is as follows: **pY39 α- synuclein** lipid-bound state.The conformations of each residues of the mutant chain in its bound state that demonstrate unfolding leading to unbinding at residue 26 of the H50Q mutant chain.

No. of Frames
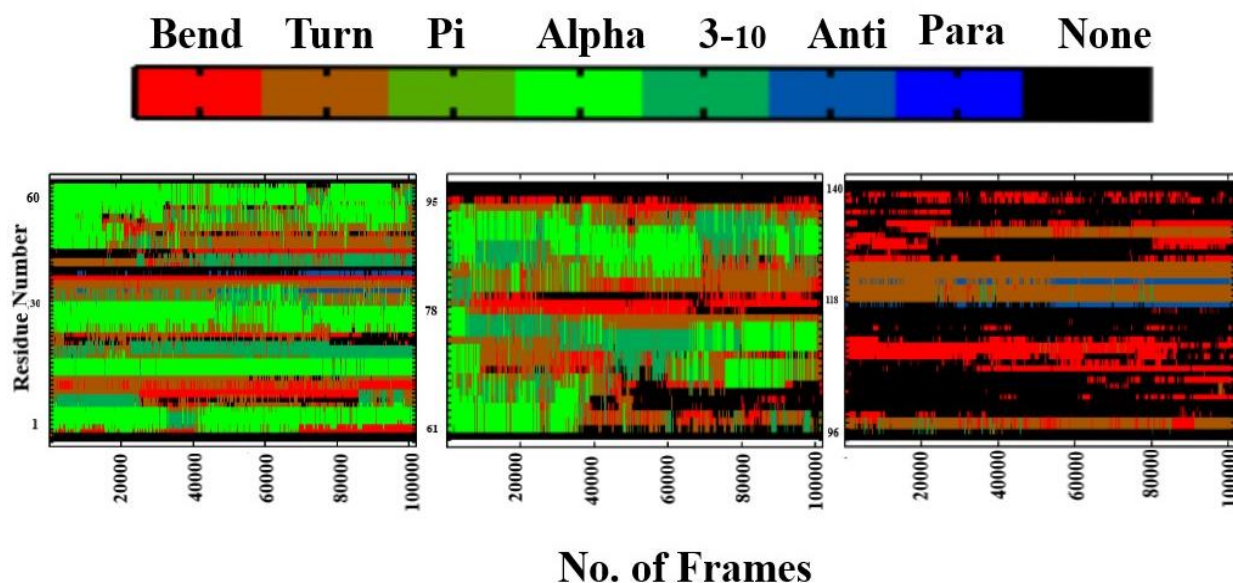
Fig. 66. Secondary structural analysis of membrane bound p39Y α-synuclein is calculated by Kabsch and Sander Algorithm using dssp software The color index depicts different conformational changes of each residue of p39Y α-synuclein during simulation period of 100ns

Table 13: Secondary Structural Analysis of p39Y α-synuclein during the simulation time period of 100 ns using YASARA software

p39Y α-synuclein	Turn	Sheet	Pi	Alpha	3-10	Coil
Percentage (%)	34.3	1.4	0	11.4	2.9	50

1.2 Phosphorylation of Serine 87 on lipid bound α-synuclein

Fig. 67 a). Electron Density profile Analysis (b). Area per Lipid Layer Analysis of membrane bound H50Q mutant during a simulation time period of 100ns

Fig. 68. a).Electron density profile of N helix, Turn and C helix of α-syn b). Electron density profile of different lipid profile of S87 α-synuclein
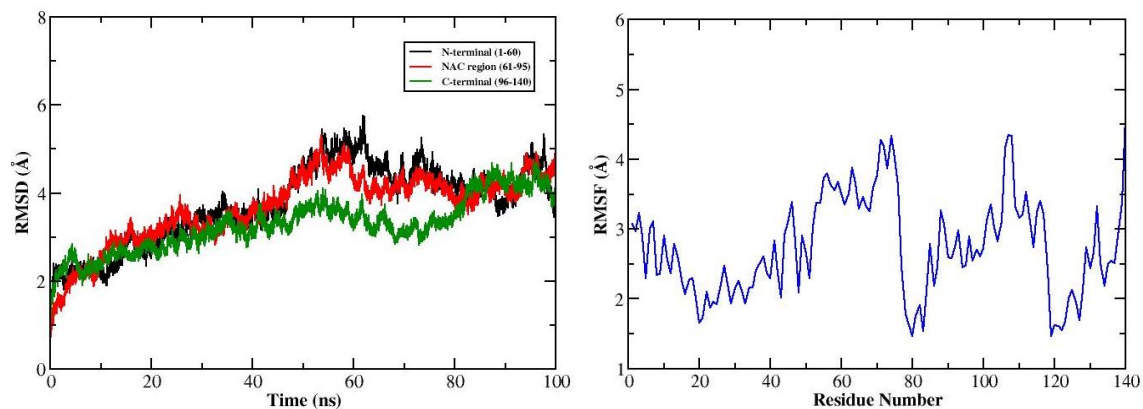
Fig. 69. Root Mean Square Deviation Analysis of membrane bound S87 α-Syn during simulation period. Root Mean Square Fluctuation Analysis S87 α-Syn during simulation period of 100ns.
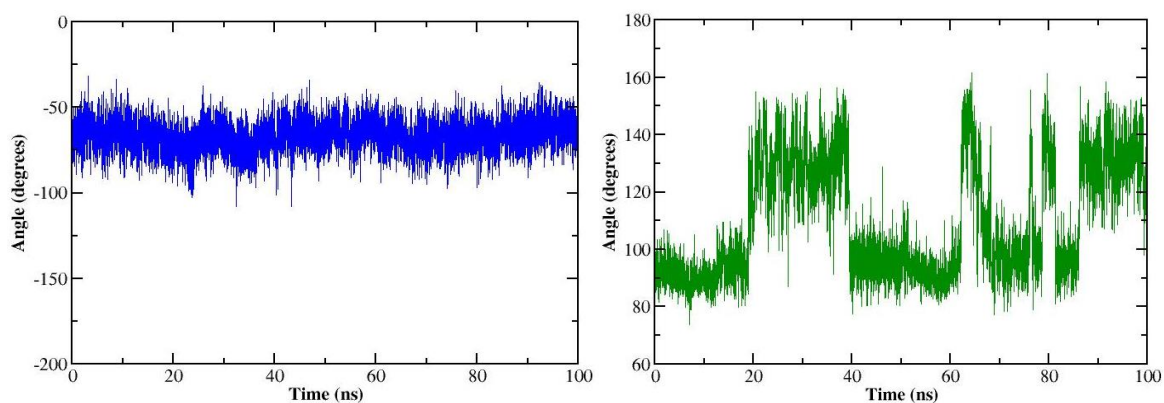

Fig. 70. Helical bending at position Glycine 68. The color scheme is as follows: S87 α-Syn in lipid-bound state.The conformations of each residues of the mutant chain in its bound state that demonstrate unfolding leading to unbinding at residue 26 of the S87 α-Syn chain.
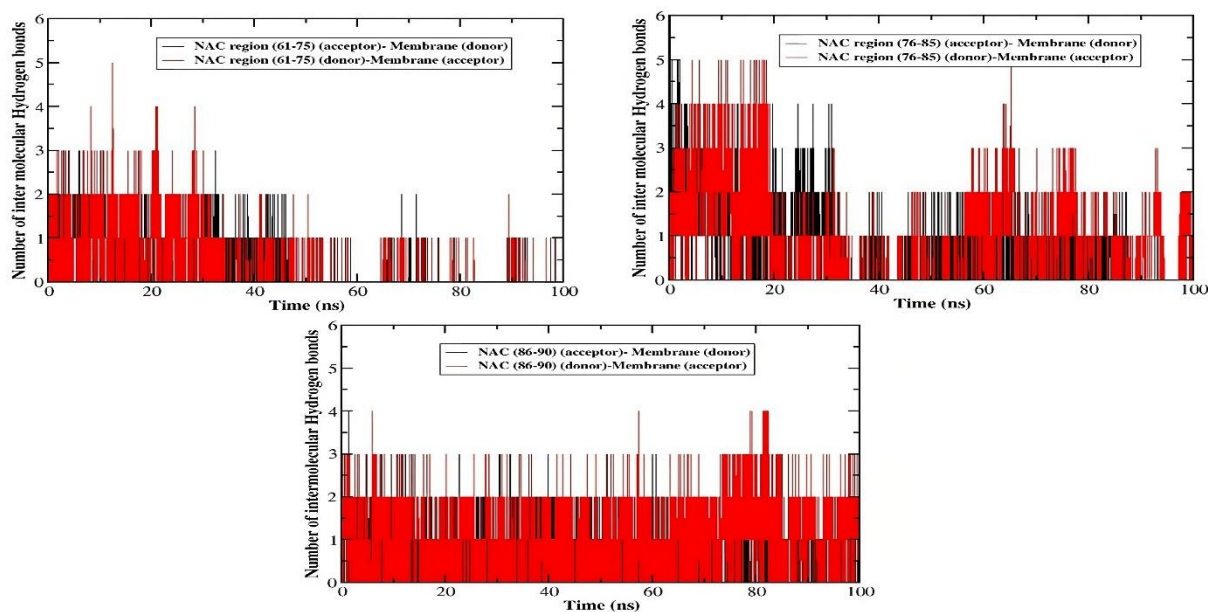
Fig. 71. The number of intermolecular hydrogen bonds between b) S87 α-Syn in lipid bound state during MD simulation of 100ns
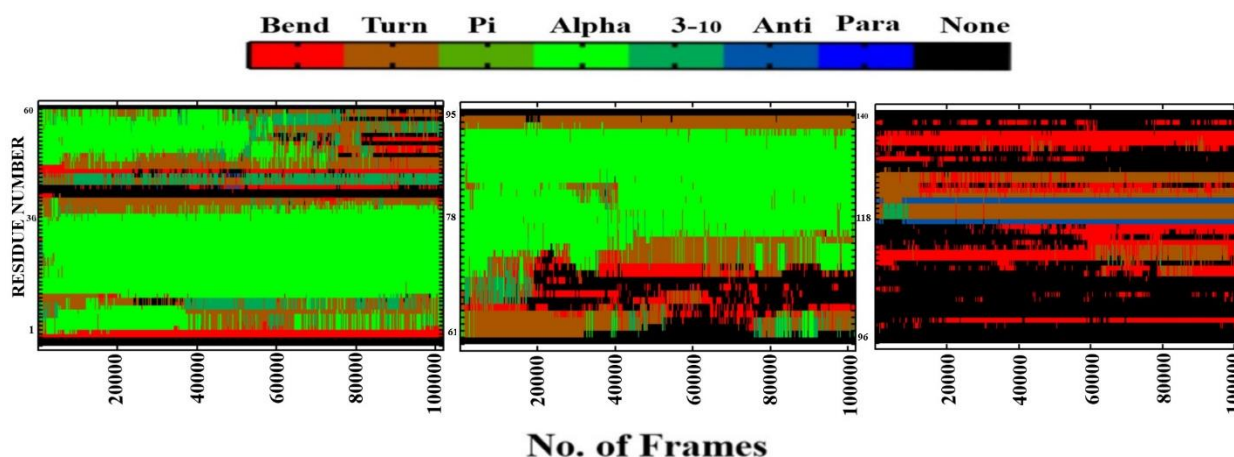

Fig. 72. Secondary structural analysis of membrane bound phosphorylated at 87 residue of α-synuclein is calculated by Kabsch and Sander Algorithm using dssp software. The color index depicts different conformational changes of each residue of S87 α-synuclein during simulation period of 100ns

Table 14: Secondary Structural Analysis of S87 α-synuclein during the simulation time period of 100 ns using YASARA software

S87 α-synuclein	Turn	Sheet	Pi	Alpha	3-10	Coil
Percentage (%)	24.6	0.1	0	22.5	2.4	50.4

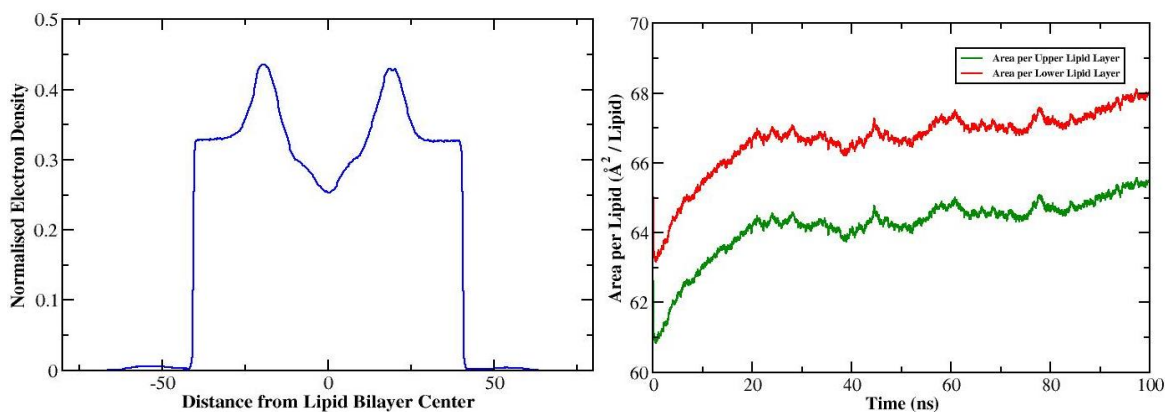## *2. Truncation of C-terminal of lipid bound α-synuclein*

Fig. 73. (a). Electron Density profile Analysis (b). Area per Lipid Layer Analysis of membrane bound C-terminal truncated α-Syn during a simulation time period of 100ns
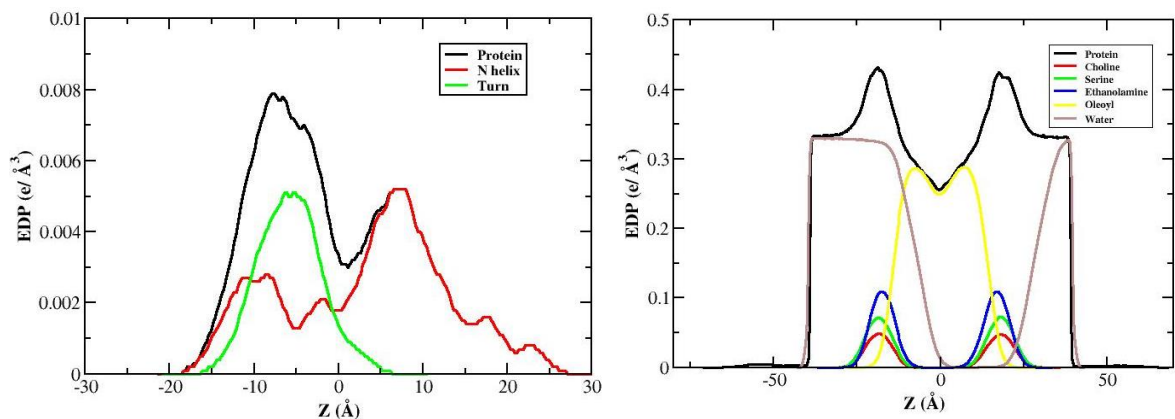
Fig. 74. a). Electron density profile of N helix, Turn and C helix of α-syn b). Electron density profile of different lipid profile of C-terminal truncated α-Syn
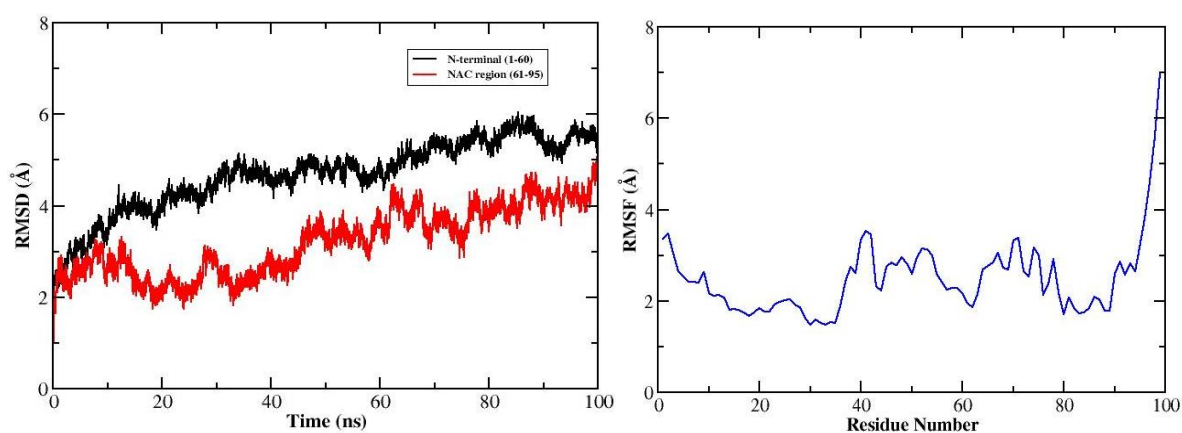

Fig. 75. Root Mean Square Deviation Analysis of membrane bound C-terminal truncated α-Syn during simulation period. Root Mean Square Fluctuation Analysis C-terminal truncated α-Syn during simulation period of 100ns.
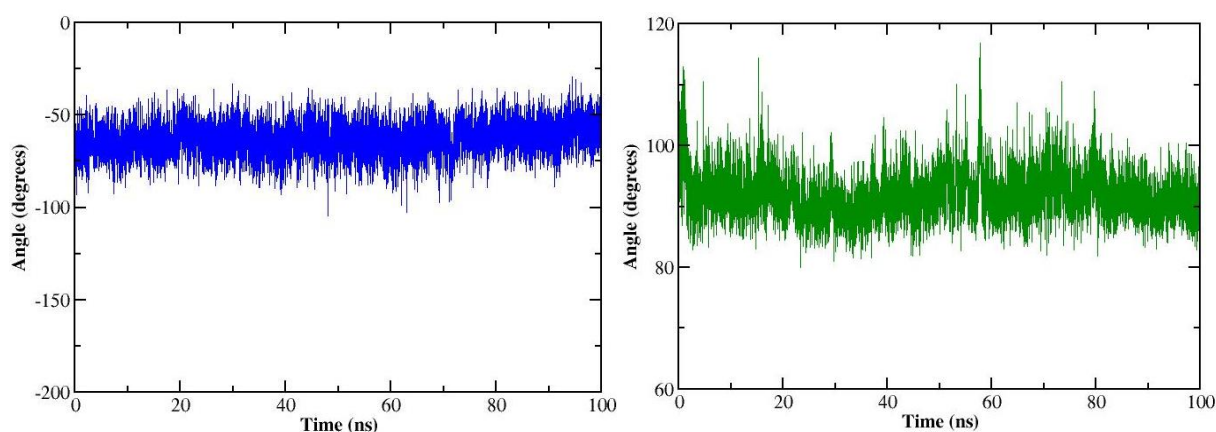

Fig. 76. Helical bending at position Glycine 68. The color scheme is as follows: C-terminal truncated α-Syn in lipid-bound state.The conformations of each residues of the mutant chain in its bound state that demonstrate unfolding leading to unbinding at residue 26 of the C-terminal truncated α-Syn mutant chain.
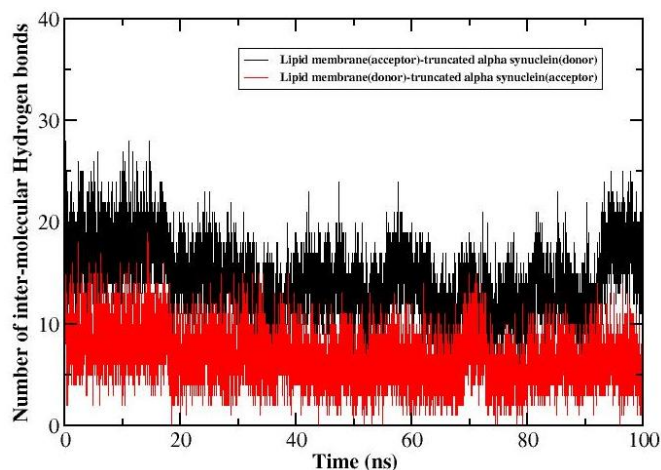
Fig. 77. The number of intermolecular hydrogen bonds between C terminal truncated α-synuclein α-synuclein in lipid bound state during MD simulation of 100ns
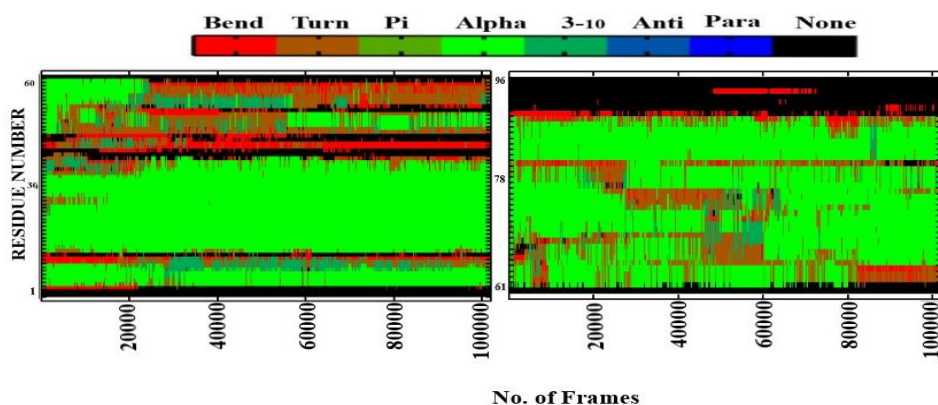

Fig. 78. Secondary structural analysis of membrane bound C terminal truncated α-synuclein is calculated by Kabsch and Sander Algorithm using dssp software.The color index depicts different conformational changes of each residue of C terminal truncated α-synuclein during simulation period of 100ns

Table 15: Secondary Structural Analysis of C-terminal truncated α-synuclein during the simulation time period of 100 ns using YASARA software

C-terminal truncated α-synuclein	Turn	Sheet	Pi	Alpha	3-10	Coil
Percentage (%)	24.6	0.1	0	23.8	2.4	49.1

3. Effect of peptidomimetic inhibitors on disrupting α-synuclein and membrane interaction

The pathophysiology of synucleopathies such as Parkinson's disease (PD), dementia with lewy bodies (DLB), and multiple system atrophy (MSA) has been hypothesised to be caused by abnormal accumulation on propagation of the neuronal protein α-Synuclein. One of the most crucial therapeutic approaches for synucleopathies now involves focusing on the

interaction between α-Syn and membrane. Recently, two small molecule inhibitors (NPT100-18A and NPT200-11) of α-Syn misfolding aggregation were identified. These inhibitors have been shown to change how α-Syn interacts with the membrane and offer a practical therapeutic approach for the development of new disease-modifying medicines for Parkinson's disease and other synucleopathies. In this study, we have demonstrated the effect of two pepditomimetic inhibitors on the interaction between α-Syn and membrane using all atom Molecular Dynamics (MD) simulation. From MD analyses, the membrane bound α-Syn in presence of inhibitor NPT200-11 showed higher compactness and less flexibility. Membrane bound α-Syn in presence of small molecule inhibitor NPT200-11 showed higher helicity at the region (45-57) that causes a tightening effect on the conformational intermediates due to stabilization of the structure. α-Syn+NPT200-11 complex exhibited higher helical content suggesting a significant inhibitory role for the secondary structure formation required for aggregation mechanism. The C-terminal is the binding domain for the inhibitors and it is was found that the distance between N-terminal and C-terminal was the highest in case of NPT200-11, thereby preventing the misfolding of α-Syn. Therefore, inhibitor NPT200-11 has reduced the rate of aggregation by targeting the membrane interacting with the α-Syn protein.

Optimization of the initial structure of Inhibitors

NPT100-18A   NPT200-11

Fig. 79. B3LYP+D3/def2-TZVP (/CPCM) calculated optimized structure of inhibitors (NPT100-18A and NPT200-11) considered in this study.

The α-Syn protein retrieved from Protein Data Bank was then docked to the two peptidomimetic molecules (NPT100-18A and NPT200-11) using the CB-Dock2, an online docking server. **Figure 30** provides a diagrammatic illustration of the process of preparing the docked complex of the receptor molecule and the pepditomimetic molecules. The CB-dock2 server (Liu, et al., 2022) has provided us with many model complex structures. Among the model structures, the initial complex structure were chosen based on the number of binding pockets and docking score for further investigation.
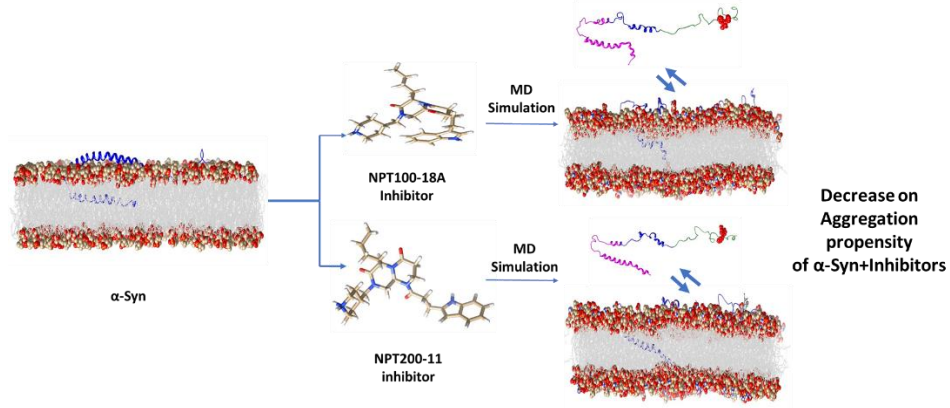
Fig. 80. Schematic representation for the formation of docked complexes (α-Synuclein+NPT100-18A and α-Synuclein+NPT200-11)
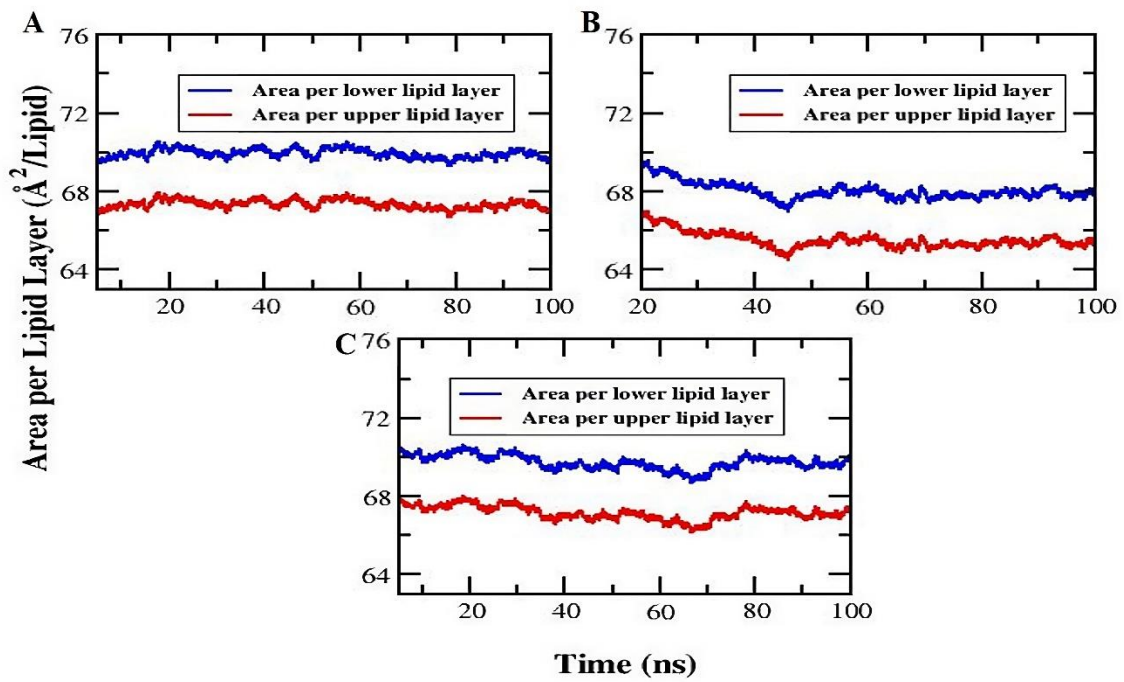

Fig. 81. Area per lipid analysis for (A) membrane bound α-Syn, (B) NPT100-18A associated membrane bound α-Syn and (C) NPT200-11 associated membrane bound α-Syn
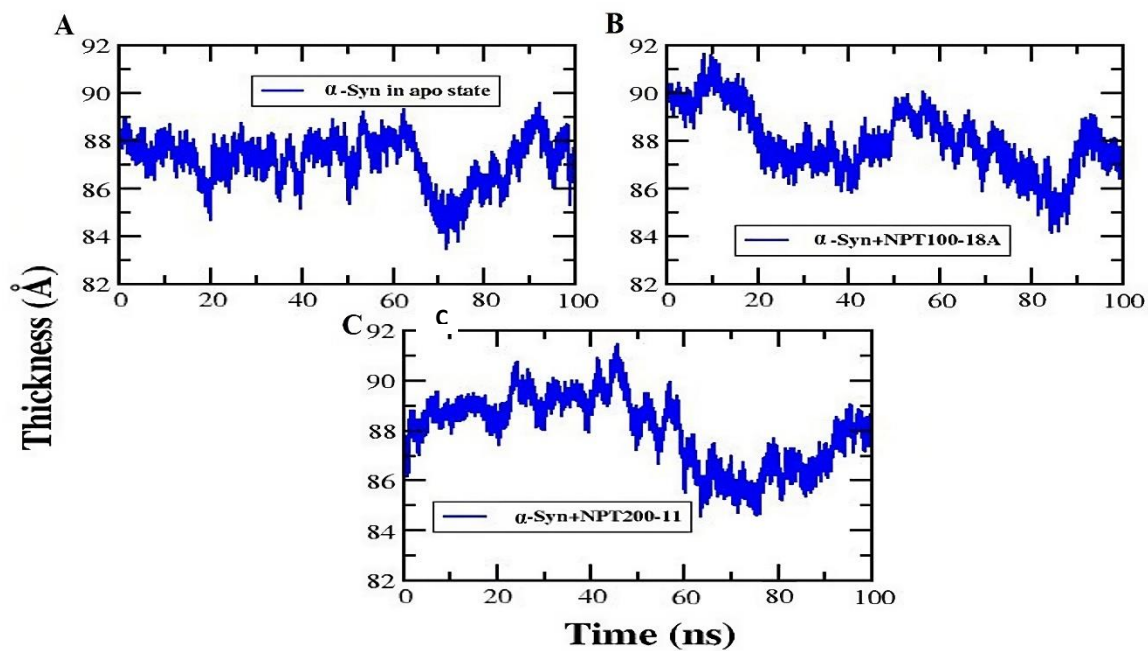
Fig. 82. Membrane thickness analysis of for (A) membrane bound α-Syn, (B) NPT100-18A associated membrane bound α-Syn and (C) NPT200-11 associated membrane bound α-Syn during MD simulation
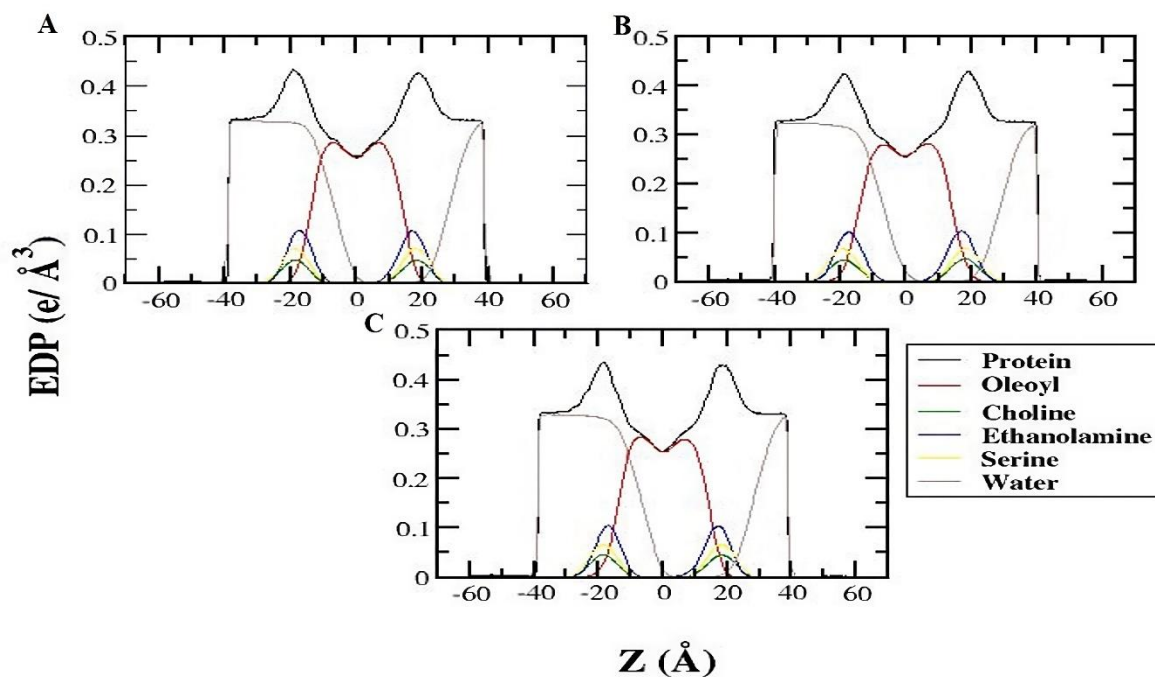

Fig. 83. Electron density profile of (a) α-Syn , inhibitors (b) NPT100-18 and (c) NPT200-11 attached to the α-Syn after the simulation of 100 ns
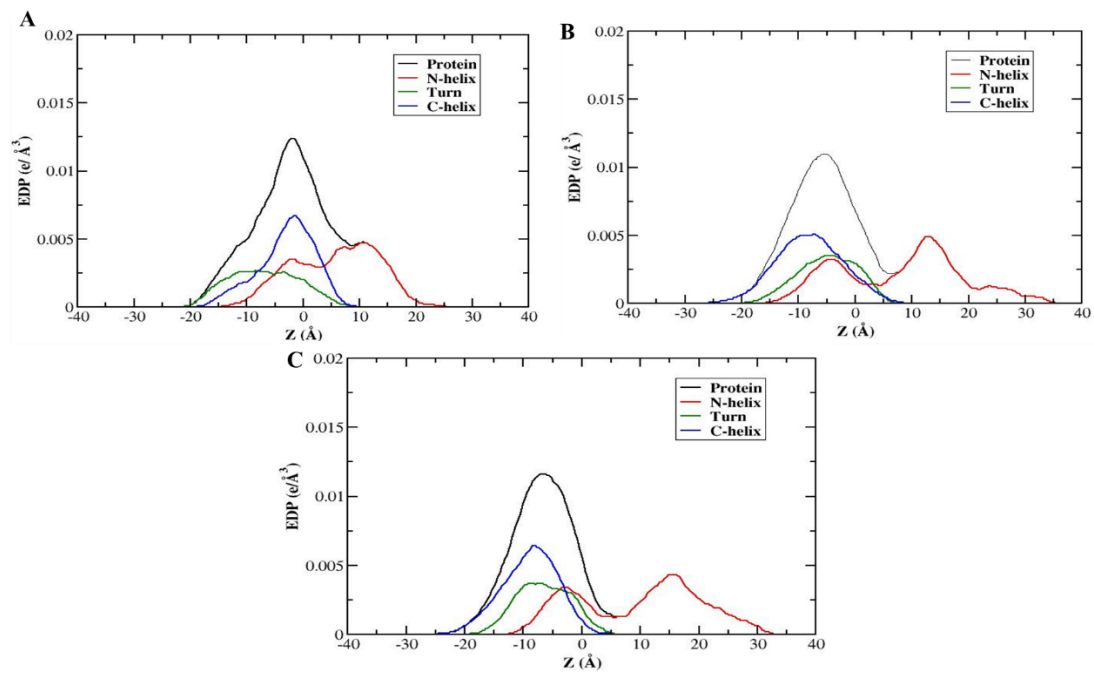
Fig. 84. Electron density profile of (a) α-Syn , inhibitors (b) NPT100-18 and (c) NPT200-11 attached to the α-Syn after the simulation of 100 ns.

Conformational snapshots

0 ns

20 ns

40 ns

60 ns

80 ns

100 ns

0 ns **20 ns** **40 ns**

60 ns **80 ns** **100 ns**
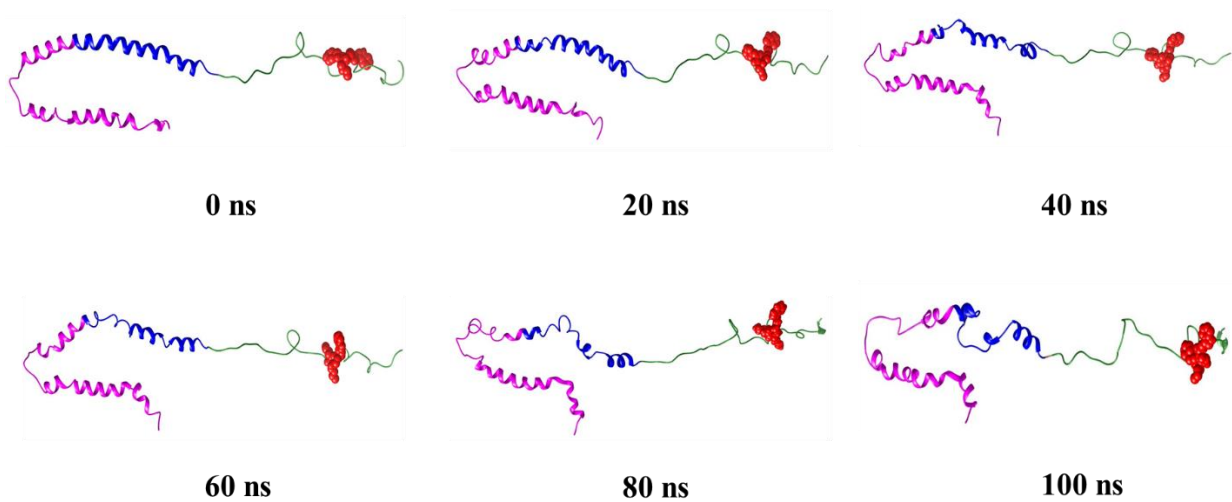
Fig. 85. Snapshots of conformational changes observed in membrane bound α-Syn in presence NPT100-18A inhibitor

0 ns **20 ns** **40 ns**

60 ns **80 ns** **100 ns**

0 ns **20 ns** **40 ns**

60 ns **80 ns** **100 ns**
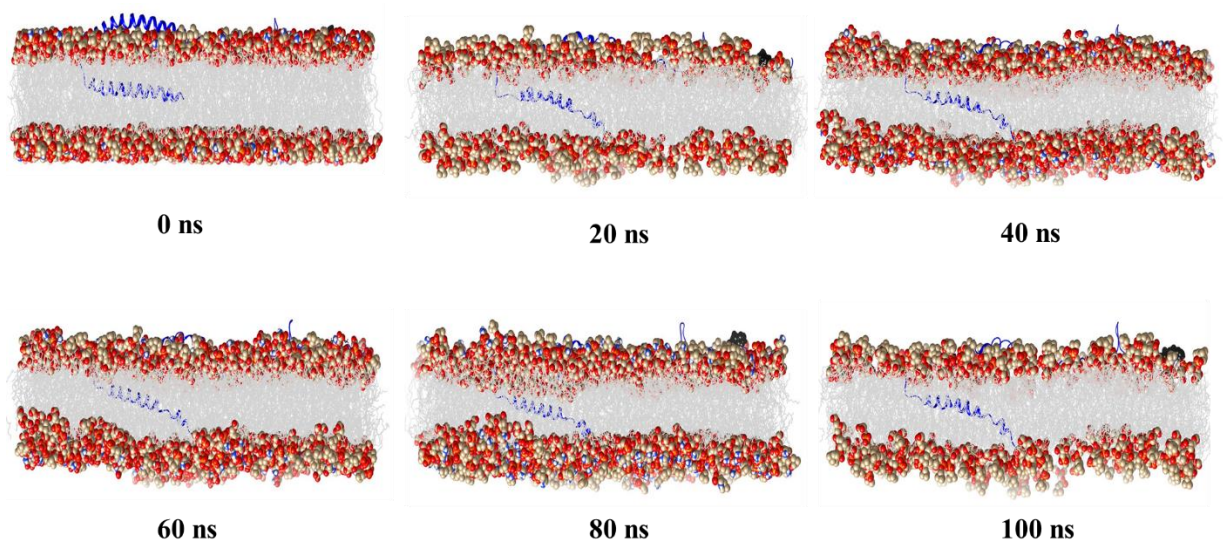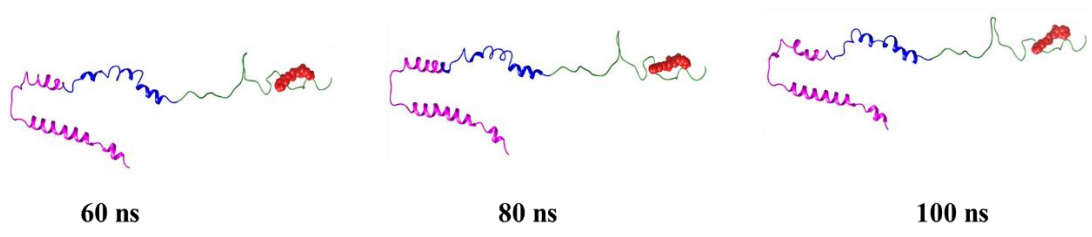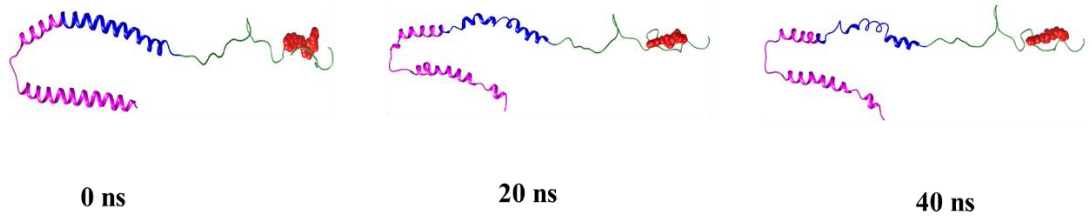
Fig. 86. Snapshots of conformational changes observed in membrane bound α-Syn in presence NPT200-11 inhibitor
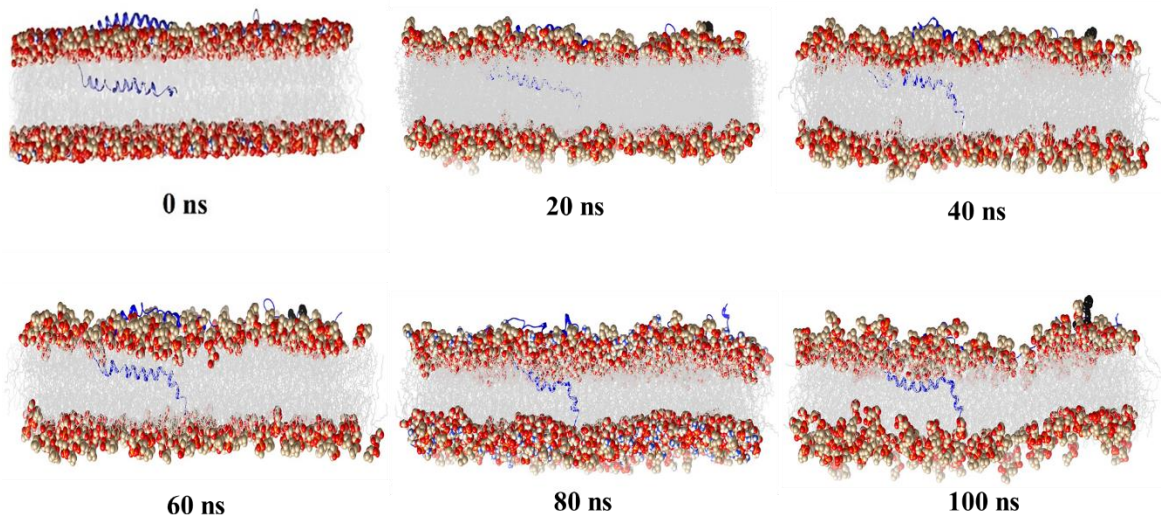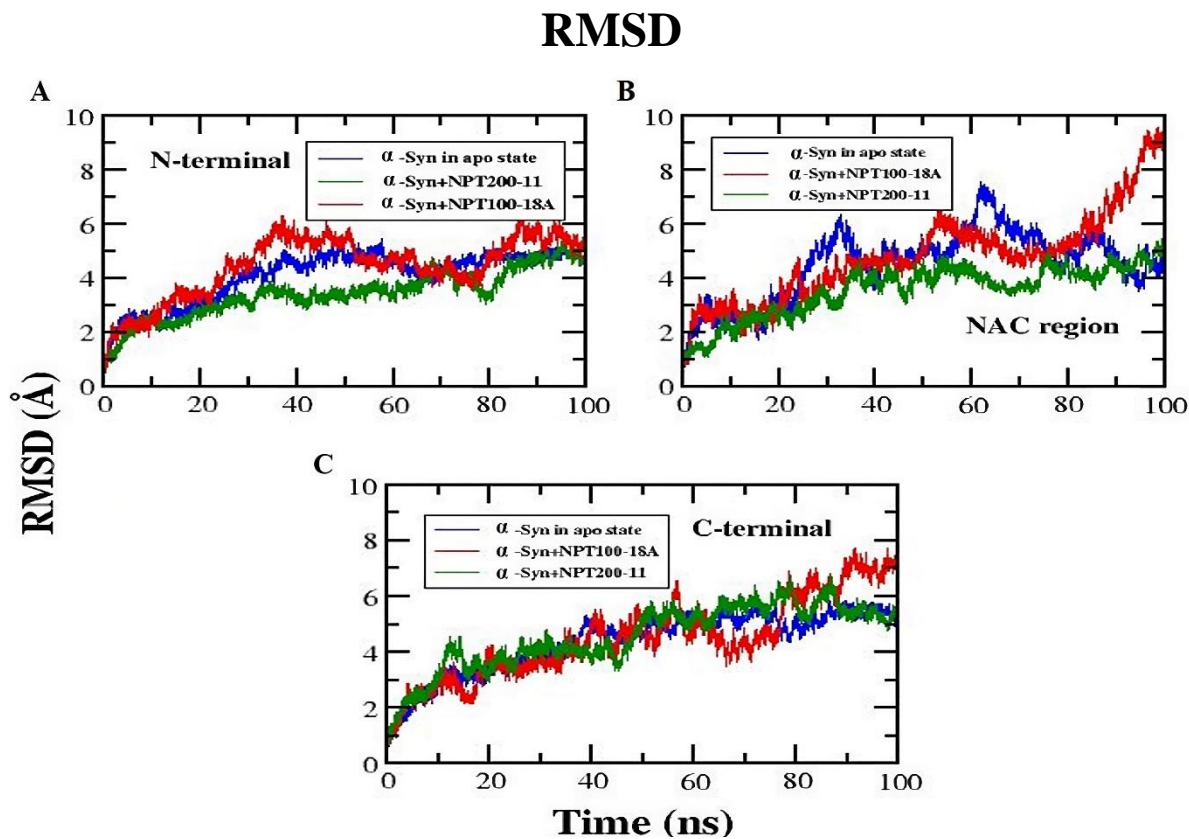
RMSD

Fig. 87. RMSD analysis of inhibitors (NPT100-18 and NPT200-11) after the simulation of 100 ns
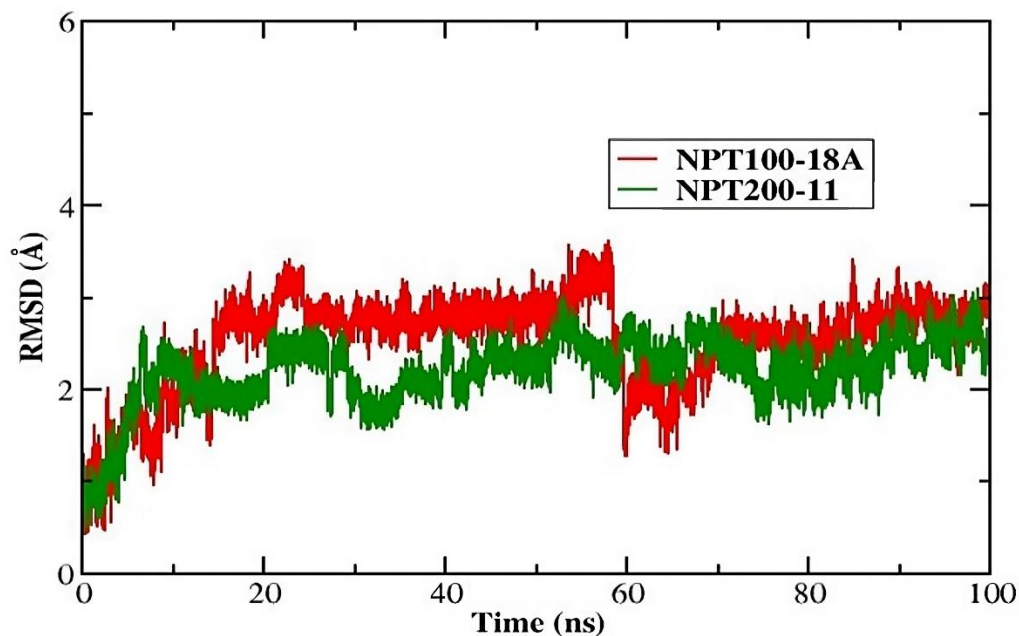
Fig 88. RMSD analysis of inhibitors (NPT100-18 and NPT200-11) after the simulation of 100 ns

RMSF
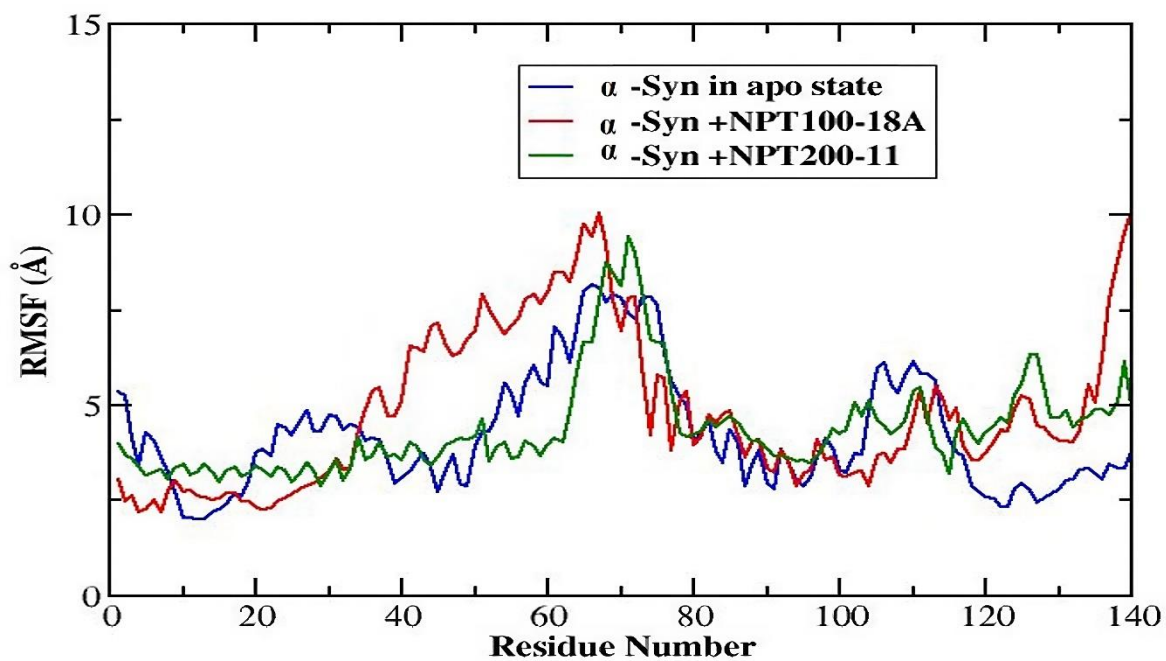
Fig. 89. RMSF analysis of membrane bound α-Synuclein and inhibitors (NPT100-18 and NPT200-11) - α-Syn complexes after the simulation of 100 ns

Secondary Structural Analysis
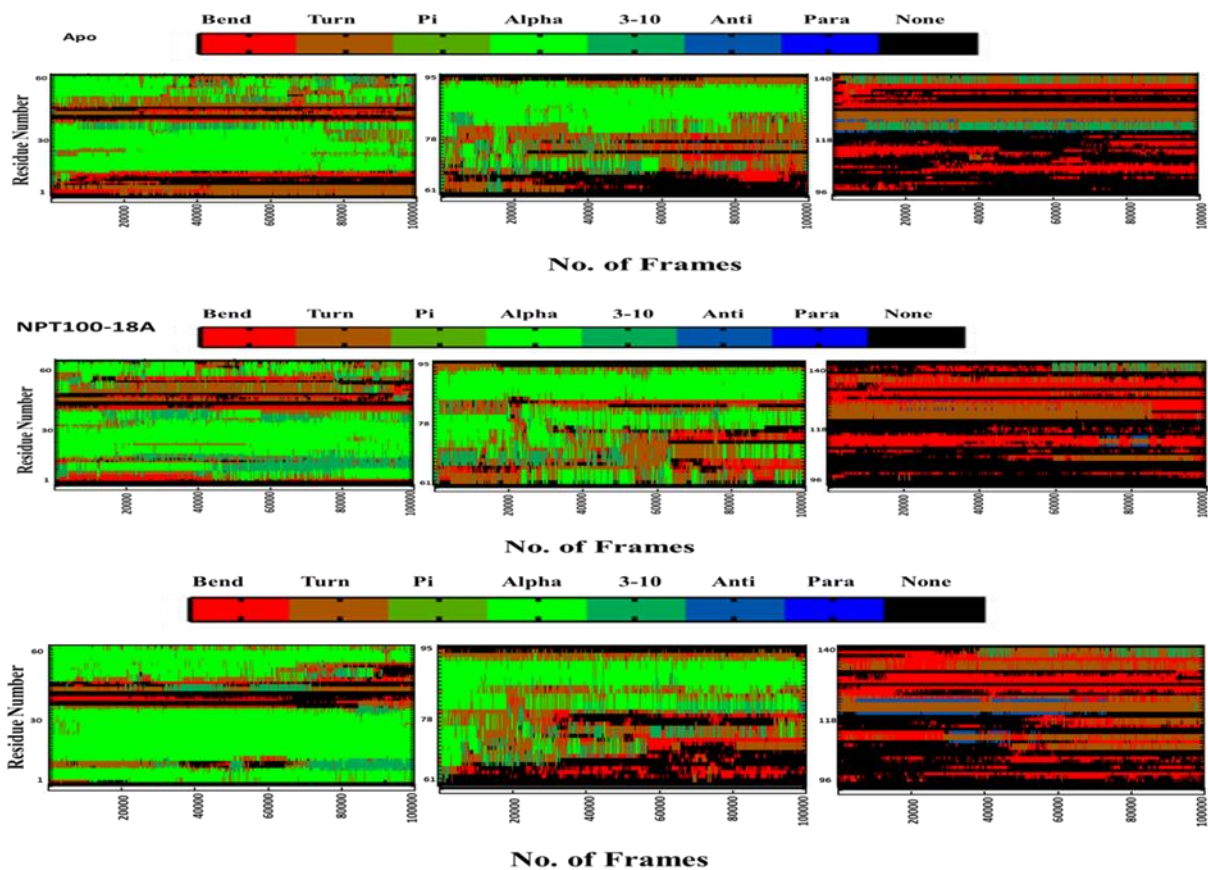
Fig. 90. DSSP plot of secondary Structural content of α-Syn in apo state and α-Syn in presence of inhibitor (B) NPT100-18A and (C) NPT200-11 complex during MD simulation obtained from Kabsch and Sander algorithm

Table 17: Secondary structural content of all the complexes during simulation time period of 100 ns

COMPLEX	TURN %	SHEET %	Pi %	ALPHA %	3-10 %	COIL %
NPT100-18A-α-Syn	20	2.9	0	20	5	55
NPT200-11-α-Syn	28.6	0	0	28.6	0	42.9
α-Syn	19.3	2.5	0	20.7	0	57.5

Inter-molecular Hydrogen bond analysis
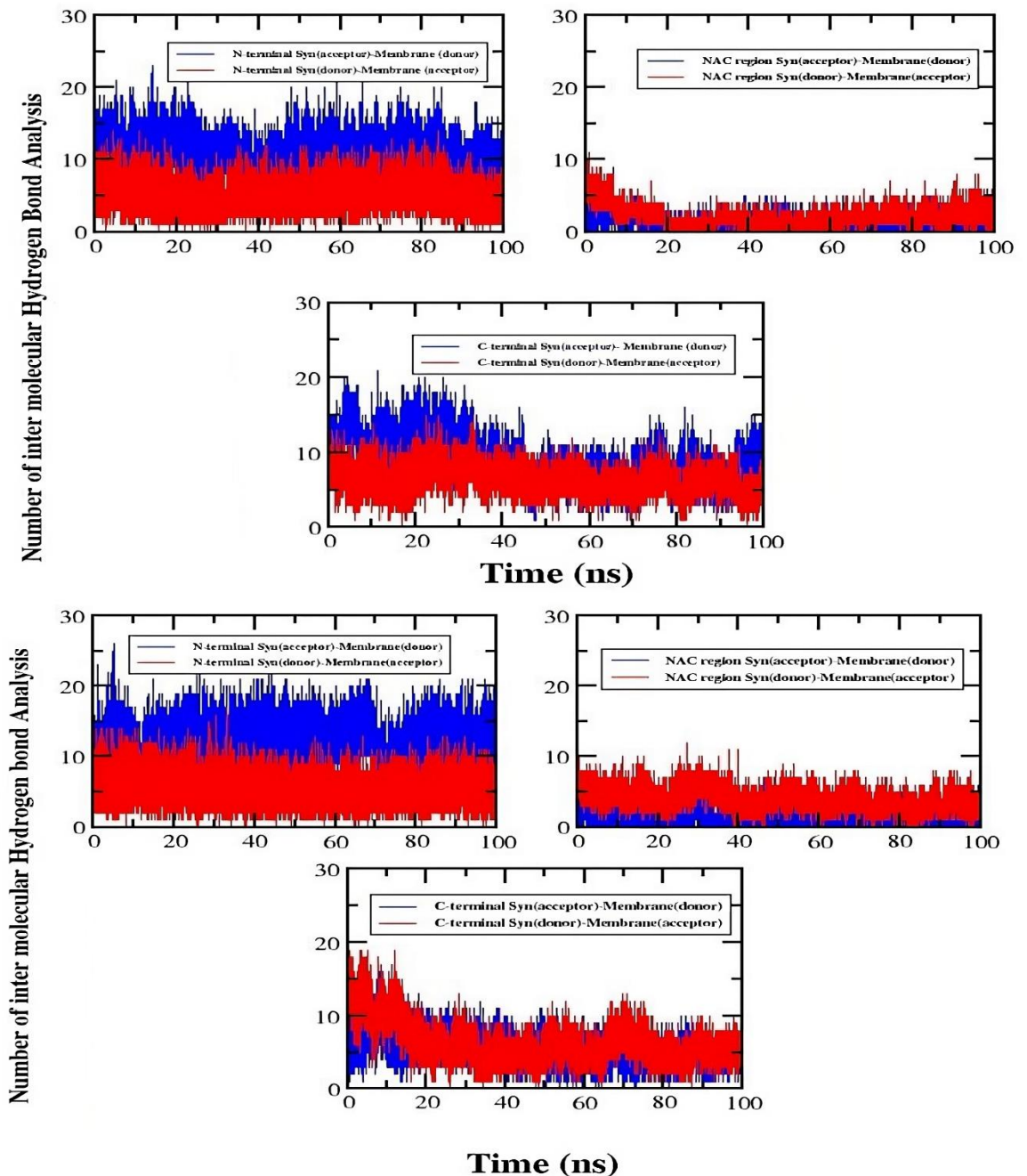
Fig. 91. The number of intermolecular Hydrogen bond analysis between membrane bilayer and all the regions (N-terminal, NAC region and C-terminal) of α-Syn in presence of (A) NPT100-18A and (B) NPT200-11 α-Syn complexes during MD simulation

Conclusions

(a)We found the α-synuclein conformers with lower solvent accessible surface area and higher secondary structure content of α-helical to have well defined and suitable binding pockets for druggability.

(b) We observed the α-synuclein protein to experience stronger crowding effects with an increase in concentration of ethanol, the crowding agent. The findings that we obtained from this simulation study would serve as valuable guides for expected crowding effects on conformational dynamics of α- synuclein.

(c) From the MD trajectory analysis, the structure of Wild type and variants (A30P, A30G, A53E, A53T, E46K, G51D and H50Q) of α-Syn were noticed to undergo rapid change in conformations and to have higher backbone flexibility near the site of mutation.

(d) In particular, the helicity of membrane-bound A30G α-Syn was found to be more pronounced in the N-helix (3–37) and turn (38–44) regions, but helicity was shown to be significantly disrupted in the elevated regions above the lipid bilayer surface.

(e)   We found that the different regions (N-terminal, NAC and C-terminal regions) of α-Syn demonstrated diverse interaction modes rather than attaching evenly to membranes as a single entity.

(f) The post translational modification of α-Syn such as phosphorylation at pY39 plays an important role in enhancing aggregation propensity of α-Syn but Ser87 and Ser129 PTMs decreased aggregation of α-Syn. Phosphorylation of α-Syn impacts membrane protein interaction.

(g) The number of long range interactions between the N-terminal and C-terminal domains of α-Syn were noticed to decrease by the C-terminal truncation.

(h) The peptidomimetic inhibitors (NPT100-18A and NPT200-11) on binding to C-terminal region of membrane bound α-Syn showed decreasing effect on aggregation propensity by disrupting protein-lipid interactions.

Scope of future work

In this study, the conformational dynamics of wild type and variants of α-Syn protein bound to membrane were studied along with the methods to disrupt the protein-membrane interactions. Also methods to inhibit α-Syn self-assembly and aggregation have been discussed. But the interaction of membrane bound α-Syn with the unbound free monomer of α-Syn protein needs to be studied in future to understand the self-assembly mechanism.

GFR 12-A
[(See Rule 238 (1))]
UTILIZATION CERTIFICATE (UC) FOR THE YEAR 2021-2022
in respect of *NON-RECURRING*
as on 31st March 2022 to be submitted to SERB
Is the UC (*Provisional/Audited*)

1. Name of the grant receiving Organization : Tezpur University

2. Name of Principal Investigator(PI): Dr. Venkata Satish Kumar Mattaparthi

3. SERB Sanction order no. & date: EMR/2017/005383, 04-Dec-2018

4. Title of the project : Computational Investigation on the membrane-induced self-assembly and aggregation of α-Synuclein

5. Name of the SERB Scheme: CRG (Formerly known as EMR) (CRG/NPDF/ECR......etc.)

6. Whether recurring or non-recurring grants: *NON-RECURRING*

7. Grants position at the beginning of the Financial year

   (i)   Carry forward from previous financial year : Rs. 160787

   (ii)   Others, if any : NIL

   (iii)   Total   : Rs. 160787

8. Details of grants received, expenditure incurred and closing balances: (Actuals)

Unspent Balance of Grants received previous years [figure as at Sl.No.7(iii)]	Interest Earned thereon	Interest Deposited Back to the SERB	Grants received during the year (2021-2022)			Total available Funds (1+2+3+4)	Expenditure incurred	Closing Balances (5-6)
1	2	3	4			5	6	7
Rs.			Sanction No. (i)	Date (ii)	Amount (iii)	(Rs.)		(Rs.)
160787	NIL	NIL	NIL	NIL	NIL	160787	NIL	160787

Component wise utilization of grants:

Grants-in-aid- General	Grants-in-aid-creation for Capital assets	Total
NIL	NIL	NIL

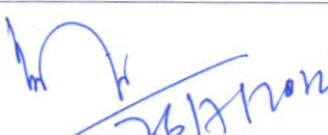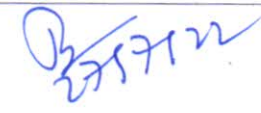Details of grants position at the end of the year

   (i)   Balance available at end of financial year   : Rs. 160787

   (ii)   Unspent balance refunded to SERB (if any): Rs. 160787 (7th October, 2021)

   (iii)   Balance (Carried forward to next financial year) if applicable: NIL

Certified that I have satisfied that the conditions on which grants were sanctioned have been duly fulfilled/are being fulfilled and that I have exercised following checks to see that the money has been actually utilized for the purpose for which it was sanctioned:

(i) The main accounts and other subsidiary accounts and registers (including assets registers) are maintained as prescribed in the relevant Act/Rules/Standing instructions (mention the Act/Rules) and have been duly audited by designated auditors. The figures depicted above tally with the audited figures mentioned in financial statements/accounts.

(ii) There exist internal controls for safeguarding public funds/assets, watching outcomes and achievements of physical targets against the financial inputs, ensuring quality in asset creation etc. & the periodic evaluation of internal controls is exercised to ensure their effectiveness.

(iii) To the best of our knowledge and belief, no transactions have been entered that are in violation of relevant Act/Rules/standing instructions and scheme guidelines.

(iv) The responsibilities among the key functionaries for execution of the scheme have been assigned in clear terms and are not general in nature.

(v) The benefits were extended to the intended beneficiaries and only such areas/districts were covered where the scheme was intended to operate.

(vi) The expenditure on various components of the scheme was in the proportions authorized as per the scheme guidelines and terms and conditions of the grants-in-aid.

(vii) It has been ensured that the physical and financial performance under **CRG** (CRG/NPDF/ECR.....etc.) (Name of the scheme has been according to the requirements, as prescribed in the guidelines issued by Govt. of India and the performance/targets achieved statement for the year to which the utilization of the fund resulted in outcomes given at Annexure – I duly enclosed).

(viii) The utilization of the fund resulted in outcomes given at Annexure – II duly enclosed (to be formulated by the Ministry / Department concerned as per their requirements/specifications)

(ix) Details of various schemes executed by the agency through grants-in-aid received from the same Ministry or from other Ministries is enclosed at Annexure- II (to be formulated by the Ministry/Department concerned as per their requirements/specifications).

Date: 18/07/22

Place: TEZPUR

Signature of PI:	**Finance Officer** Tezpur University Signature with seal: .... Name: .... **Chief Finance Officer** **(Head of Finance)**	**Registrar** Tezpur University Signature with Seal: .... Name: .... **Head of Organisation**

(Strike out inapplicable terms)

GFR 12-A
[(See Rule 238 (1))]
UTILIZATION CERTIFICATE (UC) FOR THE YEAR 2021-2022
in respect of *RECURRING*
as on 31ˢᵗ March 2022 to be submitted to SERB
Is the UC (*Provisional/Audited*)

1. Name of the grant receiving Organization : Tezpur University

2. Name of Principal Investigator(PI): Dr. Venkata Satish Kumar Mattaparthi

3. SERB Sanction order no. & date: EMR/2017/005383, 04-Dec-2018

4. Title of the project : Computational Investigation on the membrane-induced self-assembly and aggregation of α-Synuclein

5. Name of the SERB Scheme: CRG (Formerly known as EMR) (CRG/NPDF/ECR......etc)

6. Whether recurring or non-recurring grants: *RECURRING*

7. Grants position at the beginning of the Financial year

      (i) Carry forward from previous financial year : Rs. 194126

      (ii) Others, if any : NIL

      (iii) **Total**   : Rs. 194126

8. Details of grants received, expenditure incurred and closing balances: (Actuals)

Unspent Balance of Grants received previous years [figure as at Sl.No.7(iii)]	Interest Earned thereon	Interest Deposited Back to the SERB	Grants received during the year (2021-2022)			Total available Funds (1+2+3+4)	Expenditure incurred	Closing Balances (5-6)
1	2	3	4			5	6	7
(Rs.)			Sanction No. (i)	Date (ii)	Amount (iii) (Rs.)	(Rs.)	(Rs.)	(Rs.)
194126	NIL	NIL	SERB/F/3977 /2021-2022	26/10 /21	300000	494126	489807	4319

Component wise utilization of grants:

Grants-in-aid- General (Rs.)	Grants-in-aid-creation for Capital assets	Total (Rs.)
489807	NIL	489807

Details of grants position at the end of the year
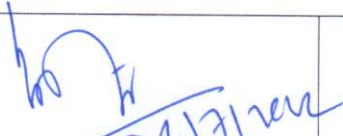
    (i)   Balance available at end of financial year : Rs. 4319

    (ii)   Unspent balance refunded to SERB (if any): NIL

    (iii)   Balance (Carried forward to next financial year) if applicable: Rs. 4319

GFR 12-A
[(See Rule 238 (1))]
UTILIZATION CERTIFICATE (UC) FOR THE YEAR 2021-2022
in respect of *RECURRING*
as on 31st March 2022 to be submitted to SERB
Is the UC (*Provisional/Audited*)

Certified that I have satisfied that the conditions on which grants were sanctioned have been duly fulfilled/are being fulfilled and that I have exercised following checks to see that the money has been actually utilized for the purpose for which it was sanctioned:

(i) The main accounts and other subsidiary accounts and registers (including assets registers) are maintained as prescribed in the relevant Act/Rules/Standing instructions (mention the Act/Rules) and have been duly audited by designated auditors. The figures depicted above tally with the audited figures mentioned in financial statements/accounts.

(ii) There exist internal controls for safeguarding public funds/assets, watching outcomes and achievements of physical targets against the financial inputs, ensuring quality in asset creation etc. & the periodic evaluation of internal controls is exercised to ensure their effectiveness.

(iii) To the best of our knowledge and belief, no transactions have been entered that are in violation of relevant Act/Rules/standing instructions and scheme guidelines.

(iv) The responsibilities among the key functionaries for execution of the scheme have been assigned in clear terms and are not general in nature.

(v) The benefits were extended to the intended beneficiaries and only such areas/districts were covered where the scheme was intended to operate.

(vi) The expenditure on various components of the scheme was in the proportions authorized as per the scheme guidelines and terms and conditions of the grants-in-aid.

(vii) It has been ensured that the physical and financial performance under **CRG(CRG/NPDF/ECR.....etc.)** (Name of the scheme has been according to the requirements, as prescribed in the guidelines issued by Govt. of India and the performance/targets achieved statement for the year to which the utilization of the fund resulted in outcomes given at Annexure – I duly enclosed).

(viii) The utilization of the fund resulted in outcomes given at Annexure – II duly enclosed (to be formulated by the Ministry / Department concerned as per their requirements/specifications)

(ix) Details of various schemes executed by the agency through grants-in-aid received from the same Ministry or from other Ministries is enclosed at Annexure- II (to be formulated by the Ministry/Department concerned as per their requirements/specifications).

Date: 18|08|22

Place: Tezpur

Signature of PI:	**Finance Officer** Tezpur University Signature with seal: .... Name: .... **Chief Finance Officer** (Head of Finance)	**Registrar** Tezpur University Signature with Seal: .... Name: .... **Head of Organisation**

(Strike out inapplicable terms)

Annexure-II

REQUEST FOR ANNUAL INSTALMENT WITH UP-TO-DATE STATEMENT OF EXPENDITURE

1. SERB Sanction Order No and date : EMR/2017/005383, 04-Dec-2018

2. Name of the PI: Dr. Venkata Satish Kumar Mattaparthi

3. Total Project Cost :Rs.4478375

4. Revised Project Cost: NA
(if applicable)

5. Date of Commencement: 04-Dec-2018

6. Statement of Expenditure:
(Month wise expenditure incurred during financial year)

Month & year	Expenditure incurred/ committed (Rs.)
07-Oct-2021	160787 (Refunded amount to SERB)
02-Dec-2021	248000 (Fellowship)
02-Dec-2021	83334 (50% of 3rd yr. overhead transferred to corpus fund and 12.5% to DG set share)
02-Dec-2021	108592 (PI share of overhead transferred to corpus fund)
02-Dec-2021	35581 (Contingency bought stationery items)
02-Dec-2021	14300 (Contingency bought stationery items)

1. Grant received in each year

a. 1st Year   : Rs.3260000

b. 2nd Year   : Rs. 600000

c. 3rd Year   :Rs. 300000

d. Interest. if any   : Rs.6956 (FY 2018-19) + Rs.86734 (FY 2019-20)+ Rs. 2204 (FY 2020-21) + Rs. 0.00 (FY 2021-22)= Rs. 95894

e. Total (a+b+c+d).   :Rs.4255894

Statement of Expenditure
(to be submitted financial year 01.04.2021 to 31.03.2022)

Sr No (I)	Sanctioned Heads (II)	Total Funds Allocated (indicate Sanctioned or revised) (Rs.) (III)	Released amount (2018-2020) (Rs.) (IV)	Released amount (2020-21) (Rs.) (V)	Released Amount (2021-22) (Rs.) (VI)	1sr Year (04.12.2018 to 31.03.2019) (Rs.) (VII)	2nd Year (01.04.2019 to 31.03.2020) (VIII)	3rd (01.04.2020 to 31.03.2021) (IX)	4th year (01.04.2021 to 03.12.2021) (X)	Total Expenditure Till 03.12.2021 (Rs.) (XI= VII+VIII +IX+X)	Balance as on (03.12.2021) (Rs.) (XII= IV+V+VI--XI)	Remarks (if any) (XIII)
1.	Manpower Cost	1029600	380000	500000	130000	0	181500	403000	248000	832500	-2238	
2.	Consumables	0				0	0	0	0	0		
3.	Travel	100000				0	31259	0	0	31259		
4.	Contingencies	150000				4873	43990	49735	49881	148479		
5.	Others, if any	0	0	0		0	0	0	0	0	0	
6.	Equipment	2798775	2750000	0		0	0	2678550	0	2678550	71450	
7.	Over head expenses	400000	130000	100000	170000	0	107241	100833	191926	400000	0	
8	Interest Accrued (if any)	0	0	0	0	0	0	0	0	0	95894	Rs.6956 (FY 2018-19) + Rs.86734 (FY 2019-20) + Rs.2204 (FY 2020-21+ Rs.0.00 (FY 2021-22) =Rs.95894
9	Unspent Balance Refunded to SERB, if any										-160787	160787 Balance Non-recurring amount Refunded to SERB on 7th Oct, 2021
10.	Total	4478375	3260000	600000	300000	4873	363990	3232118	489807	4090788	4319	

Name and Signature of Principal Investigator:

Dr. M. V. SATISHKUMAR

Signature of Competent financial authority: (with seal)

Finance Officer
Tezpur University

Date: 28/08/2023

Date: _____

***

*DOS – Date of Start of project

Note:

1. Expenditure under the sanctioned heads, at any point of time, should not exceed funds allocated under that head, without prior approval of SERB i.e. Figures in Column (VIII) should not exceed corresponding figures in Column (III)

2. Utilization Certificate (Annexure III) for each financial year ending 31st March has to be enclosed along with request for carry-forward permission to the next financial year.